INVESTIGATION INTO SOME ASPECTS OF THE SPARK EROSION PROCESS AND ITS EFFECT ON SOME MECHANICAL PROPERTIES OF THE WORKPIECE

THESIS

SUBMITTED AS PART OF THE REQUIREMENTS FOR

THE DEGREE OF DOCTOR OF PHILOSOPHY

IN THE VICTORIA UNIVERSITY OF MANCHESTER

BY

Moshe Maksymilian Barash, B.Sc., Dipl.Ing.

Faculty of Technology,

Manchester

October - 1958.

ProQuest LLC.
789 East Eisenhower Parkway
P.O. Box 1346
Ann Arbor, MI 48106 – 1346

The author studied Mechanical and Electrical Engineering in Technion, The Israeli Institute of Technology, Haifa. He graduated in 1947 and was awarded the Degree of B.Sc. and the Diploma of Ingenieur.

In the period 1948 - 1953 he was with the Department of Research, Israeli Ministry of Defence, at first as Scientific Officer, later as Section Leader, in the military rank of a major.

In 1953 - 1955 he was a mechanical engineer with ATA Textile Company, near Haifa. In the Academic Session of 1954 - 1955 he was also a guest lecturer in Mechanical Engineering in the Technion.

The author came to Manchester in September, 1955, for research work towards a higher degree.

In 1956 he was appointed Lecturer in Mechanical Engineering in The Manchester College of Science and Technology and in the University of Manchester.

C O N T E N T S

A C K N O W L E D G M E N T S

The author wishes to express his gratitude to Professor H. Wright Baker, D.Sc., M.I.Mech.E., M.I.Prod.E., for his kindness and constant interest; to Dr. F. Koenigsberger, D.Sc., M.I.Mech.E., M.I.Prod.E., for all his help, encouragement and valuable guidance throughout the entire investigation, and to all the author's colleagues in The Manchester College of Science and Technology who have been helpful during this work.

The author's thanks are also due to Impregnated Diamonds Limited, Gloucester, who kindly lent the Sparcatron Machine used in this investigation, and last but not least to Miss Jeanne Vigurs who typed the manuscript of this thesis.

SUMMARY

The application of spark erosion to the machining of metals is very recent, and although this method is gaining everincreasing popularity, neither the physical fundamentals of the process nor its influence on the properties of the workpiece are known sufficiently well.

The present work, which was started towards the end of 1955, aimed at obtaining more information on certain aspects of the process than was available at that time.

As the result of the investigations, which were carried out in electrical as well as in mechanical fields, the following conclusions could be drawn:

1. In cases when the erosion has to be caused by sparks only and the formation of arcs has to be prevented, the minimum permissible ballast resistance in a relaxation circuit is a definite function of the capacity used. The knowledge of the relationship between these two parameters makes it possible to calculate and to design a relaxation circuit and to estimate the power requirements, once the voltage and the maximum capacity are chosen. The cathode ray oscilloscope is a convenient means for indicating the limit of non-arcing operation.

2. Conditions were established for the successful application of a relaxation circuit for spark turning and the reasons for unsuitable voltage causing out-of-roundness of the workpiece were found.

3. The typical forms of spark voltage and currents were found. Both in the case of single sparks and in the case of continuous sparking the reverse half-wave may be either present or absent. Its presence must be due to the swarf in the process, because the dielectric used (paraffin) was shown to be capable of very fast deionization. Values of inductance and current amplitudes were both calculated and measured, and the results were found to be in reasonable agreement. Skin effect, parasitic oscillations and other secondary phenomena were noted.

4. The theoretically predictable relationship between the centre line average value of a spark eroded surface and the energy of a single spark is very close to the actual one if the voltage is kept constant. When different voltages are applied the surface finish relationship indicates that the energy losses are growing with increasing gap length. The surface finish can be measured by means of the usual methods and with existing equipment, and the consistency of the results is comparable to that obtained on surfaces produced by machining.

5. Residual stresses arise as a result of spark erosion. They are tensile and of a high magnitude. The depth of the affected layer is small and is approximately proportional to the surface finish value. There are good reasons to attribute the creation of the residual stresses to the thermal effect of the spark.

6. Spark erosion reduces the endurance limit of mild steel. The effect of the residual stresses on this phenomenon could be demonstrated by considerable improvement in the endurance limit of

specimens which were stress relieved after being spark eroded. There was, however, also indication of some permanent damage attributable to microcracks.

Suggestions were made as to possible continuation of research into the different aspects of spark erosion process and technology.

NOTATION

r_1	-	Radius vector inside the heat source.
r_o	-	Radius of the heat source.
t	-	Time.
t_1	-	Duration of heat input.
p	-	Spark (pulse) duration.
κ	-	Thermal diffusivity.
R_o	-	Radius vector of a point in the heated body.
α	-	Azimuth angle in the polar co-ordinates system of the heated body.
q	-	Heat input intensity per unit area per second.
T	-	Temperature of a point in the heated body.
ω	-	Angular frequency of the spark, rads./sec.
$\mathcal{L} = 2\,l$	-	Length of the ligament strips in the reduction unit.
R	-	Ballast resistance.
R_m or R_{min}	-	Minimum permissible ballast resistance.
C	-	Capacity.
L	-	Inductance.
U	-	Breakdown voltage.
CLA	-	Centre line average surface finish index.
ψ	-	Non-linear resistance of the spark.
ρ	-	Resistance of the discharge circuit (includ. ψ).
γ	-	Charge in the condenser.

$\mathcal{E}$	-	Potential difference of the charging source.
Θ	-	Charging time for one spark.
n	-	Spark repetition rate.
N	-	Average power transmitted to the condenser.
e	-	The base of natural logarithms.
k	-	Charging-time to time-constant ratio.
U_v	-	Average voltage, voltmeter reading.
N_{inp}	-	Power requirement of the relaxation circuit.
g	-	Earth acceleration.
I'	-	Charging current.
I, I_s	-	Spark current.
δ	-	Damping coefficient
U_s	-	Spark voltage.
U_1	-	Spark voltage at the beginning of the discharge.
U_2	-	Spark voltage at the end of the first half-wave.
U_3	-	Spark voltage at the beginning of the second half-wave.
U_4	-	Spark voltage at the end of the second half-wave.
I_m, I_{1m},	-	Amplitude of spark current in the first half-wave.
I_{2m}	-	Amplitude of the spark current in the second half-wave.
h_c	-	Crater depth.
k' K n' m' β , λ	-	Different constants (factors of proportionality).

R', R'',	-	Radii of curvature.
d	-	Thickness of the stressed layer.
a	-	Thickness of the strip.
b	-	Width of the strip.
E	-	Young's Modulus.
f	-	Average residual stress.
m	-	Reciprocal of Poisson's ratio.
S	-	Chord length.
h	-	Bow of arc.
d_c	-	Crater diameter.
v	-	Crater volume.

The notation used in the Appendices is not included.

LIST OF FIGURES

FOREWORD

The present thesis describes investigations into some aspects of spark erosion. The work was started towards the end of 1955 and carried out in the Royce Laboratory of the Department of Mechanical Engineering in The Manchester College of Science and Technology.

At the time the investigations were started, the method of spark machining was still largely a novelty, although the equipment for this purpose had been manufactured by then for about three years. The available literature was scarce, and was mostly a repetition of the same few original sources. The information pertaining to the fundamentals was even more scarce and confined to description rather than to analysis.

In view of this situation it was decided to pursue the research in several fields simultaneously, namely in electrical as well as mechanical ones. It was felt that a deep breach in a narrow section would lead to amassing facts which could not be properly appreciated because of the lack of general knowledge on the subject.

Since then, many new investigations by other workers in different countries have become known, some of them on similar lines to the present one. Some of the findings presented here have been confirmed by other work, some are still awaiting such confirmation.

It is hoped that the questions left open will eventually find their solution; there is still more to be learnt about the subject than is already known.

CHAPTER I

INTRODUCTION

1. HISTORICAL NOTES

Electric spark machining is one of the several methods in which electric energy is directly applied to the working of metals. The erosion produced by the electric spark was observed and mentioned already by Priestley in 1762 (1)*. It has been considered an adverse phenomenon by electrical engineers since the first days of electric contacts. Early useful application of the electric spark discharged in a liquid dielectric is mentioned by Rudorff (2) who quotes Svedberg - 1906 , and Kohlschütter - 1919 . They produced colloidal metal by eroding electrodes submerged in a liquid, and they used a condenser for the production of the sparks.

The spark had been, of course, applied even earlier for the ignition in petrol engines, but the erosion in this case was always detrimental and the discharge took place in a gas.

Other forms of electric energy were applied to metal cutting, with varying success. Arc cutting is relatively common, friction-disc cutting is sometimes assisted by electric arc, and disintegrators have been used for some time for the removal of broken drills and taps, but are being replaced by spark disintegrators. Still other forms are the electrolytic etching with or without mechanical assistance and other similar methods.

---

* Numbers in parenthesis refer to the Bibliography listed at the end.

All these cannot, however, be termed "machining" in the sense of producing accurate geometrical forms in a controllable manner. The first practical application of spark erosion for the controlled and accurate reproduction of geometrical forms is generally attributed to B. R. Lazarenko and his wife N. I. Lazarenko who in 1943 designed a spark eroder operating on a simple relaxation circuit, i.e. a condenser charged through a resistance and periodically discharged through the spark gap. This development was a result of a prolonged study (since 1935) of the behaviour of electric contacts under various conditions, including operation in a liquid dielectric. The phenomena associated with erosion in liquids were described by the Lazarenkos in 1944 in a treatise on electric contacts, while the application to machining was described in a book published in 1946. These and other early references are quoted in a recent work by the same authors (3). The method thus became more widely known and many developments have taken place since. In 1950 spark erosion machines were already manufactured in several countries and it is estimated that the number of models produced now in the world is about 100. The relaxation circuit and its modifications prevail in the majority of the presently produced equipment, but other means of producing electric pulses have been attempted as well, some with success.

2. PRESENT APPLICATIONS OF THE METHOD

The application of the method is derived from its basic characteristics. The spark will erode any material irrespective of its properties, provided it conducts electricity. (Some non-conductors,

notably diamonds can be machined by special procedures, but these are rare exceptions). The tool may be softer than the workpiece but has also to be a conductor. No mechanical contact is required for the machining operation and the mechanical forces are therefore almost nil. The erosion occurs on both the workpiece and the tool, though not to the same extent. Spark machining has therefore been employed for producing parts from hard metals, e.g. various tools made from hardened steel or cemented carbides, or for "drilling" fine holes and non-circular openings in various metals. It would by far exceed the scope of the present work to describe all the known applications of spark machining, but a short list will indicate the versatility of this method. The main applications are:-

Manufacture of press and forging tools.

Manufacture of form cutting tools.

Manufacture of drawing and extrusion dies.

Manufacture of metallic casting moulds.

Drilling holes with a curved axis.

Drilling holes of small diameter (down to 0.0004 in.).

Machining of awkward metals such as Nimonic or manganese steels.

Tapping hardened steel and cemented carbides.

Metal sawing.

Circular and surface grinding.

Sharpening of tools.

Removal of broken taps, drills, studs, etc.

Toughening. (This is a reversed application of the erosion, namely depositing a hard layer on the workpiece by operating in air instead of

in a liquid dielectric).

An extensive, though by no means complete description of the technology and applications is given in the book by Nosov and Bykov (4).

3. FUNDAMENTAL CONDITIONS, SPARK AND ARC

There are two fundamental conditions for maintaining the erosion process used in spark machining:

I. The spark gap which separates the two electrodes must be filled with liquid dielectric, at least during the occurrence of the breakdown and the discharge.

II. The discharge must be of a true transient nature and must not degenerate into an arc, i.e. it must be a spark.

It has been found by various investigators - Lazarenko (3), Mironoff and Pfau (5), Koncz (6), Zolotikh (7), Bruma (8) that a single spark discharged in liquid dielectric will always produce a well-defined circular crater and remove the same volume if repeated under identical conditions. It was also found that if the sparks are produced at a constant frequency, the amount removed is proportional to time, i.e. to the released energy, provided the gap does not become too congested with the swarf.

This is a phenomenon which cannot be observed with a gaseous dielectric, in which case the crater is of a very irregular form and the amount removed varies considerably from spark to spark. The presence of a liquid dielectric brings about a qualitative and a quantitative change in the nature of the erosion. The amount eroded

in a liquid dielectric may be ten times greater than in air, according to Nosov and Bykov (4). Different dielectric liquids produce different rates of erosion, but the variation is not wide, i.e. in the order of ± 30% at the most. Only water has a much smaller rate of erosion, approximately a half of that of paraffin, but this can be attributed to the electric conductivity which develops even in initially distilled water. The reasons for this increased erosion, as well as for breakdown in liquid dielectrics in general are not yet fully understood. Lazarenko (3) suggests that the spark in a liquid is more concentrated because of the pressure caused by the inertia of the liquid on the walls of the expanding conducting channel in the gap. This suggestion is supported by the fact that a shock wave inevitably develops in the liquid with the passage of a spark.

Another important property of the liquid dielectric is the prevention of adhesion between the eroded particles and the cathode. When a spark is discharged in a short gap (in the order of one thousandth of an inch) in air, particles eroded from the anode strongly adhere to the cathode. This phenomenon has been observed a long time ago and is being utilized for depositing processes since 1941 - Lazarenko (3), Nosov and Bykov (4).

Such adhesion can occasionally also be observed with liquid dielectrics if the gap space becomes too congested with the products of erosion.

4. THE MECHANISM OF DIELECTRIC BREAKDOWN

In the course of the last 50 years the mechanism of the electrical breakdown of dielectrics has been the subject of very extensive studies by many investigators. Most of the work was done in the field of gaseous dielectrics, some in solid and relatively little in liquids. Until recently the breakdown of a gas was explained by the Townsend electron avalanche, but this was insufficient in some cases and the theory of a "streamer" was proposed. Very recent investigations indicate that the actual mechanism is rather close to the original electron avalanche theory. The literature on this subject is very large and is quoted in Llewellyn Jones' book (9), and the works by Loeb (10) and by Meek and Craggs (11). The breakdown of a liquid dielectric is thought to be established by a similar mechanism, namely of initial electron emission caused by the electrostatic field and subsequent ionization of the gap by collision processes.

There is a very great difference between the dielectric strength of a pure and a contaminated dielectric. This was shown by Goodwin and MacFadyen (12), Higham and Meek (13) and Lewis (14). Even a small contamination may reduce the strength to a fraction of that observed in a purified liquid. Stekolnikov (15) found that if fine metal powder is dispersed in purified transformer oil, the conductivity rose and a voltage of 250 volts was sufficient to produce a breakdown in gaps of the length of 1 mm. Zolotikh (7) doubts that erosion products have any influence on the conductivity of the dielectric, because the eroded particles were found to be coated with an insulating layer of

hydrocarbon resin (in the case of paraffin dielectric). The conductivity of the fluid did not change even when the erosion products constituted 50% of the weight. On the other hand, Zolotikh thinks that the effective gap is diminished by the presence of the swarf and the irregularity in the electrostatic field may enhance cold emission. In the present work the importance of the swarf for the breakdown was demonstrated by a simple experiment: The two electrodes were separated by a distance of 0.004 cm. in clear (not purified, only settled) paraffin and a voltage of 130 volts DC applied. No break-down occurred. When a small amount of contaminated paraffin was injected into the gap space, breakdown occurred and continuous sparking developed. This experiment was repeated several times with identical results. Zolotikh (7) found that contamination with swarf increases the distance between the electrodes which can be broken down by a given voltage. He found that while the first breakdown at 300 volts occurred at the distance of 26 μ in a purified paraffin, the second breakdown occurred at 34 μ and the third and all following breakdowns occurred at the distance of 64 μ. The gap conditions are thus most important for the breakdown. The amount of swarf also controls the surface finish; Opitz (16) found that flushing the gap will greatly improve it.

It can thus be seen that the mechanism of the breakdown is not yet completely known, but it has been established that the breakdown occurs within a fraction of one microsecond (Zolotikh, 7, Crowe, 17). During that time a conducting channel is established and the subsequent history of the discharge depends upon the external electric circuit.

In the case of a circuit with relatively small inductivity, and sufficient energy storage, the current will grow at a very fast rate, up to 10^8 amp./sec. It has been found that this is about the limit of rate of growth, and if exceeded, the spark channel splits into several channels (Sommerville and Grainger 18). The rates of growth in sparks produced by relaxation circuits seldom reach this value; from the photographs of currents in the present work it can be seen that the average value is approximately 2×10^7 amp./sec. The current density in sparks has been investigated by Froome (19), Cobine and Gallagher (20), Craig and Craggs (21) who found that it varied from 10^4 to 10^6 amp./cm.^{2}, but was seldom below 10^5 amp./cm.^{2}. Williams (22) has produced very intensive sparks by special pulse circuits and found current density approaching 10^7 amp./cm.^{2}. The current density in the present work judged by dividing the current amplitude by the crater area, appears to be in the order of 10^5 amp./cm.^{2}.

Current densities of such magnitude cannot be maintained for long, certainly not for more than 10^{-3} sec. Within this time the metallic vapours will fill the gap and the conducting channel will diffuse sufficiently to provide a low-resistance path with ensuing arc. If the source continues to provide energy, a stable arc will develop. The current density in an arc is smaller by several orders of magnitude than in a spark and can be 10^2 amp./cm.^{2} and less. There is also a great difference in temperatures; while an electric arc has a temperature of not more than 4,000° C., the values given for sparks vary from 10,000 to 50,000° C., according to Obrig (26). With the

development of an arc the highly localized action as well as the accuracy are lost. The surface sustains a deep damage not observed with a spark. The difference in accuracy is best illustrated by Figure 1, which is reproduced from Lazarenko (3). Both holes were produced by an octagonal electrode and in both cases the average power was the same. The only difference was that one hole was produced by arcs and the other by sparks.

The surface damage can be seen in Figures 2 and 3 which were prepared in the course of the present work. It is notable that the surface produced by arcs with a capacity of 1.5 μF is much rougher than the surface produced by sparks with 100 μF in the charging circuit. The reason for the different action is the very different length of duration. A spark does not exist for longer than 10^{-3} sec., while an arc, once it starts, will maintain itself from the source and exist continuously. The thermal effect will be prolonged and will penetrate deeply with adverse consequences.

5. THE MECHANISM OF EROSION

The passage of an electric spark is accompanied by erosion of both electrodes. Under usual conditions, i.e. in a circuit of the type used in the present investigation, the erosion of the anode is greater than that of the cathode, if both are of the same metal. If hardened steel is eroded with a copper tool electrode as the cathode, the ratio of tool/workpiece erosion is of the order of $\frac{1}{4}$. However, if the workpiece is a cemented carbide, the copper tool will erode faster.

The rate of erosion and the tool/workpiece erosion ratio are most important technological parameters, the control of which clearly requires a complete understanding of the mechanism of erosion. Such understanding does not appear to have been achieved as yet. Several different explanations are given for the erosion. According to Mandelshtam and Raiski (23), Haynes (24) and Finkelnburg (25), fine vapour jets or "flares" stream from one electrode to the other, causing erosion. Such streams were observed in high tension discharges in gases, but it is doubtful whether they can exist in liquids. Nevertheless, this hypothesis is brought forward by these workers to explain spark erosion in general.

An entirely different explanation is given by Williams (22), who discards the thermal effect altogether. According to Williams the erosion is caused by the electrostatic field produced by the electrons coming from the cathode and hitting the anode. The sudden influx of electrons is said to upset the electrostatic equilibrium with ensuing tearing out of metal particles. The erosion of the cathode is explained by the impact of the particles torn from the anode. This hypothesis cannot explain why hardened steel, despite its great tensile strength, is eroded more quickly than mild steel, nor can it explain other phenomena such as residual stresses or structural changes. Mironoff and Pfau (5) who have coined a new term, the "hyperthermal" shock, consider that the erosion and other phenomena of spark cannot be explained by referring to phenomena occurring at lower temperatures and longer times. They do not offer, however, any real proof to substantiate their assertion.

A thermal basis of the erosion mechanism is suggested by Llewellyn Jones (27), and in a somewhat different manner by Zolotikh (7). Llewellyn Jones analysed the data on spark erosion, mainly of sparking plugs (from the extensive work by Debenham and Haydon, 28) and found that the heat generated by the spark should suffice to melt the electrodes. He assumed a point source and did not try to compare the shape of the crater with the theoretical isothermal surface. Zolotikh went further and calculated the isothermal surface corresponding to the melting point of the electrode material. He did not show the way in which the calculation was carried out and it appears that there are no tabulated functions which could be referred to in such a calculation. Assuming that the heat quantity q is fed into the electrode in one second per unit area, and that the spark duration is p, the temperature T at any point (r, z) at the time p is given by Carslaw - Jaeger (29) as:

$$T = \int_0^{r_0} \int_0^{2\pi} \int_0^{p} \frac{q}{[4\pi\kappa(p-t_1)]^{3/2}} e^{-\frac{R_0^2 + R^2}{4\kappa(p-t_1)}} r_1 \, dr_1 \, d\alpha \, dt_1$$

Figure 4 shows the relevant geometry of this calculation. As seen from the above formula, the integrand is the heat conduction equation for a continuous point source in an infinite body. The function q, however, is not known either in time or in radius. The time distribution can be found from the power curve of the spark, calculated from the voltage and current values, and its general shape is shown in Figure 5.

The space (radial) distribution of q is not yet known, but it can be assumed that it would be similar to a Gaussian distribution, Figure 6. Another difficulty is the variation of the thermal constants (diffusivity) with the temperature. Assuming average values for q and for the thermal diffusivity, Zolotikh (7) obtained isothermal surfaces of the melting point closely congruent with the observed craters. Despite the great interest in this calculation, it was decided not to pursue it as this would require extensive numerical, point for point calculations. It is considered, however, that it would be of considerable value if the calculation of temperature distribution in the case of continuous disc sources is attacked as a separate problem and the special functions required (integrals of error function) computed with the aid of an electronic computer. The results would benefit not only spark erosion but also investigations of spot welding, flame hardening, etc.

Both Llewellyn-Jones and Zolotikh showed that the amount of heat liberated in a spark is sufficient to melt a volume of metal equal to the observed crater. The question as to the nature of the forces which lift this molten metal and throw it into the gap space has not been yet answered. The electromagnetic forces caused by the spark current could be sufficient at the moment the current is at its peak, but a very recent paper by Zolotikh (30) shows high speed cinematographic pictures, taken at over 60,000 frames/sec., according to which the crater is only $\frac{1}{4}$ of its final size when the current is at the maximum. Moreover, most surprisingly, the crater is not more than

half of its final size when the spark is over, and continues to grow after the spark had ended. The sparks investigated were rather long, over 100 μ sec., but there is every reason to assume that at least to some extent, this phenomenon is common to all sparks. No fully satisfactory explanation has yet been offered for the last phenomenon, though it may hold the key to the mechanism of the spark erosion process.

6. THE RESEARCH PROGRAMME

The research work was divided into two parts:-

1. Investigation of the electrical properties of the circuit.

   This covered:-

   I. The relationship between the minimum ballast resistance R_m which still prevents arcing and the capacity C of the condenser.

   II. The voltage and current forms of the spark discharge.

2. Investigation of the mechanical properties of the workpiece.

   This covered:-

   I. Surface finish.

   II. Residual stresses in spark eroded metal strips.

   III. Fatigue of spark eroded mild steel components.

C H A P T E R I I

THE EQUIPMENT

1. THE ELECTRIC AND ELECTRONIC EQUIPMENT

I. The Spark Erosion Machine

The spark erosion machine used was the Mark I Sparcatron machine, the first spark eroder produced in the United Kingdom. The machine has a nominal power of ½ kW net and operates on the normal 400 V. 3 phase supply. The direct current is obtained by metallic rectifiers and the voltage of the D.C. source is 130 volts. A bank of condensers enables combinations of capacity from 0.5 to 610 μF. Alternatively, a D.C. voltage of 28 V. can also be obtained. The power supply unit and the condensers are located in a cabinet which is connected by cables with the proper eroder, or drilling unit. The latter consists of a head with a vertical spindle to which the tool electrodes are fastened and a table with a basin for the dielectric fluid. A pump system with filters enables circulation of the fluid if necessary. The tool electrode is always the cathode, and the earthed table which holds the workpiece, is the anode. The cabinet and the drilling unit are shown in Figure 7. A special servo-mechanism automatically controls the gap length, keeping it within the required length. The operation of the servo mechanism, which is shown diagramatically in Figure 8 is as follows:-

The electric motor has a split field and is at rest when each field receives the same current. When the current in one field drops, the motor rotates clockwise, and when the current in this field rises,

it rotates anti-clockwise. Rotation of the motor brings about lowering or raising of the spindle by means of a pinion and rack. The field is connected by means of an amplifier across a bridge, composed of two arms. One arm is the ballast resistance R and the upper portion of the potential divider P, while the other arm consists of the lower portion of P and of the equivalent resistance of the discharge side. When the gap is too long, there is no spark and the one arm of the bridge being open unbalances it with subsequent downward movement of the spindle. On the other hand, in the case of a contact between the two electrodes, the resistance of this arm of the bridge is too low, because the resistance of the spark is missing. This causes an upward movement of the spindle. Balance is obtained at a certain gap length, which is thus automatically maintained.

This bridge method of gap control is universally used in all relaxation-circuit operated modern machines. The electronic amplifier, however, is not used anymore, and the field of the motor is directly connected to the bridge. The new Sparcatron machine uses for example a permanent magnet rotor for the motor. Older methods, as well as variants of the bridge method are described by Gutkin (31).

The machine used performed satisfactorily for research purposes, but it was rather unstable when operating at low capacities at 130 volts. Automatic gap control at 28 V. was almost impossible.

The inductance of the discharge branch of the circuit was measured with the Wayne-Kerr B.221 Universal Bridge and was found to be 3.22 μH. The resistance at ω = 10,000 was 0.011 Ohm, and this

value can be taken as the approximate ohmic resistance. At high frequencies the resistance was higher because of the skin effect.

The machine was provided with both voltmeter and amperemeter (for the average current), but for experimental measurements an Avometer was used because of the better accuracy obtainable.

II. The Oscilloscope

The oscilloscope used for measuring and recording spark voltages and currents was a Solartron make, type Solarscope CD.711. A Cossor oscilloscope was tried, but was found too slow for the purpose. The oscilloscope was fitted with a 35 mm. camera capable of taking single pictures or continuous picture a film speeds up to 80 in./sec. The response of this oscilloscope is up to 5 mc./sec. It was possible to measure voltage and current simultaneously, with one beam, by switching it from one input to the other 150,000 times per second. This method has advantages over the two-beam method in that the two beams may interfere with each other. The disadvantage is the difficulty of simultaneous measurements of very short time phenomena. It was also possible to measure each input separately. The 300 V DC range was used for the voltage and 10 V or 3 V ranges were used to measure the current, with the use of a shunt. The shunt had a DC resistance of 0.0012 Ohm. It was made of a thin strip (0.003 in.), and its resistance would, therefore, be practically unchanged for all measured cases. The inductance of the shunt was negligible - 0.02 μ H.

The shunt remained cold in all cases, except in some short circuit experiments. Thus there was no need for a material with low temperature-resistance coefficient and copper was sufficient. Tests were made with the shunt submerged in the dielectric liquid, which acted as coolant, but this was found unnecessary. The oscilloscope is ~~shown in Figure 7, the~~ shunt in Figure 9.

III. The Sparking Lathe

The lathe on which the fatigue specimens were "sparked" was a small bench type machine adapted for this purpose by attaching a brass disc on the spindle to which current was fed by means of a carbon brush. The brush was connected to the anode and was earthed. The tool electrode was mounted on a block of insulating material clamped in the tool post. The leads were connected to the cathode and the anode respectively of the drilling unit, so that the total inductance of the discharge branch thus formed was 6.5 μH (as compared with 3.22 μH of the drilling unit alone) and the total DC resistance was 0.049 Ohm. The specimens were held between centres and driven by a turn-about. The contact between the driving pin and the turn-about was sufficient for the fine sparking required.

The lathe was capable of speeds up to 1,000 r.p.m., but above 200 r.p.m. considerable vibrations developed and speeds in excess of 200 r.p.m. were, therefore, avoided.

The dielectric was provided by the pumping system of the drilling unit, plastic tubes being used to convey it to and from the lathe. The use of paraffin limited the maximum capacity permissible

to prevent fire risk. It may be mentioned that for heavy spark turning transformer oil is generally used. The lathe and the set-up are shown in Figure 10a and b.

2. MECHANICAL EQUIPMENT

I. Surface Finish Measuring Equipment

The surface finish measurements were carried out on the Talysurf Mark I. This instrument produces a pen record of the surface by moving a fine diamond stylus across it. The radius of the stylus is 0.0001 in., the range of magnifications is from 400 to 40,000 times in the vertical direction and 50 or 200 times in the horizontal direction. The magnification in the vertical direction is achieved by electronic amplification of electric pulses obtained by the movements of a coil connected to the stylus lever.

The instrument is also provided with a meter which gives the average height of the surface roughness (Centre Line Average), by integrating the electric impulses. The CLA shown by the meter is obtained as an average of five values from five lengths of 0.04 in. each. In this way undulations of the surface of 0.04 in. wave length or more are largely eliminated and only the fine texture is accounted for. The pickup carrying the stylus assembly is moving on a straight line generated by the instrument itself; it is of the so-called skid-less type. (The magnification of 400 x was obtained by means of a special electronic unit ordered for this purpose, the lowest magnification of the instrument as normally supplied is 2,000 x and the maximum CLA value indicated 150 μin.). The horizontal magnification is obtained by

a suitable ratio of the velocity of the paper to the velocity of the pickup movement. The instrument, a product of Taylor-Hobson, performed extremely well, despite its delicate elements and age (15 years). The Talysurf set-up is shown in Figure 11.

For the measurement of surfaces with a CLA value over 300-400 μin. a special reduction unit was built, because of the danger to the diamond stylus when it has to traverse a very rough surface, and in particular at the speed of meter measurement. The reduction unit is composed of a separate stylus holder, connected by two parallel ligament springs to a base which can be clamped to the Talysurf pickup. The stylus of the Talysurf rests on the upper spring and the movement of the special stylus thus produces a smaller movement of the original Talysurf stylus. As shown in Figure 13, the ratio between the two displacements is constant and is higher than the ratio of the two relative distances from the basis. This forms a kind of a "shortened leverage". In addition, the design ensures freedom from friction and backlash. The ratio was found to be constant over a vertical displacement of 0.1 in., which is much more than required. A thumb-screw enables the adjustment of the relative position between the Talysurf stylus and the upper spring. A gramophone needle ground to a cone of 90° with a radius of approximately 0.0002 in. was used as the special stylus. The "unit" is shown in Figures 11 and 12. Only pen records were produced with this unit, because when it was traversed at the higher speed of meter measurement, vibrations developed. Damping was tried with some success, but the very rough surface required

planimetration of the pen records in any case, and the experiments with damping were not continued. The steel strips used for ligaments are 0.005 in. thick and 0.5 in. wide. The distance between the strips is 5/16 in. and the length of the deflecting part 2ℓ is $2\frac{7}{8}$ in.

II. The Fixture for Measuring the Curvature of Metal Strips (Investigation of Residual Stresses)

The fixture devised for the measurement of the curvature of the eroded strips consisted basically of a surface plate, a three point support for the strip, a micrometer head and a microscope. The three point support was achieved by three gramophone needles mounted in a block which could slide on the surface plate. The plane represented by the three points was parallel to the surface plate. A micrometer head of $2\frac{1}{2}$ in. diameter, reading directly 0.0001 in. with the possibility of estimating 0.00001 in. was mounted on a magnetic base which was clamped to the surface plate. (In order to prevent lifting of the strips by the magnetic force, the holder of the head was made of brass). The spindle of the micrometer head was adjusted so that it was perpendicular to the surface plate. The measuring end of the spindle carried a $\frac{1}{8}$ in. diameter steel bearing ball which was mounted in a suitable socket and was concentric with the spindle axis. The ball could be viewed through a microscope of a (variable) magnification of approximately 30 x and which was mounted on the same magnetic base and adjusted parallel to the surface plate. The method of measuring is described in Chapter III, Page 25. The fixture is shown in Figure 14.

CHAPTER III.

THE EXPERIMENTAL WORK

1. INVESTIGATION OF THE CIRCUIT

I. The R_m-C Relationship

The experiments were carried out by using a $\frac{3}{4}$ in. diameter brass electrode on a mild steel workpiece, in paraffin, with automatic gap control and approximately 50 volts average breakdown voltage.

An oscilloscope was connected to the voltage across the gap and adjusted in a way which gave a picture of many charging traces simultaneously. When the ballast resistance R was reduced, at a certain point bright specks appeared on the lower portion of the oscillograms, and with further slight reduction of the resistance these specks formed a line, as shown in Figure 15a. The traces were not quite stationary and therefore difficult to photograph because the picture became rather blurred. The bright specks indicate incidence of arcing, and this was checked by observing the surface produced in such a case. Figures 2b and 3b show that in the case of incidence of arcing pitting starts on the surface, and a molten layer becomes visible in the cross-section. When the resistance was reduced further, arcing became more frequent, until, at a much lower resistance a visible continuous arc developed. The oscillogram changed its form suddenly, the trace did not reach the value of the breakdown voltage any more but remained low, as shown in Figure 15b. The gap was lit by the arc and the surface produced completely ruined, as shown in Figures 2c and 3c. The hardness of the

white layer shown in Figure 3c was nearly 900 kg./mm.^{2}, Vickers Hardness Number, while the unaffected metal (mild steel) had a hardness of 240 VHN only.

For plotting the R_m-C relationship, the value of R_m used corresponded to the first incidence of the bright specks, i.e. just before the bright line shown in Figure 15a appeared.

The R_m-C plot is shown in Figure 16, the relationship being approximately $R_m = 60\ C^{-\frac{1}{2}}$.

The duration of the spark, p, was found to be $p \approx 2\pi(LC)^{\frac{1}{2}}$, from the plot in Figure 35.

II. Measurement of Spark Voltage and Current

The spark voltage was measured directly by connecting the gap to a suitable range of an oscilloscope. For current measurements a low-inductance shunt made of thin copper strip was used and the oscilloscope was triggered from the voltage, the shunt being on the earthed (positive) side of the circuit. The oscilloscope had to be disconnected from earth because of disturbances. Both the shunt and the voltage measuring points were as near as possible to the gap itself, to prevent phase displacement between the voltage and the current readings. It was found that the shunt had to be made of thin strip because of the skin effect. The shunt is shown in Figure 9. All leads to the oscilloscope were screened.

Measurements were made for both continuous sparking and for single sparks. In the latter case the source was disconnected before the spark was produced, in order to avoid the influence of the source

voltage. All values used in the calculations were averages obtained from numerous visual observations. Photographs were taken too, for better illustration, but in most cases it was impossible to obtain a photograph showing the average value.

A special technique was used in measuring single sparks. Three types of single sparks were produced. The first one was produced by charging the condenser, disconnecting the source and then lowering the cathode until a breakdown occurred. By suitably adjusting the spindle holding the cathode it was possible to stop the electrode at the distance at which the spark occurred. In the second method the cathode was released from a very small height, approximately 1 mm., and allowed to drop down until it touched the anode. The spark occurred before the contact was effected. In the third case the cathode was released from a distance of 100 mm. and dropped freely onto the anode. The spark occurred again before the contact was effected but in the case of sparks above a certain duration the contact prevented continuation of the spark. The various oscillograms are shown and explained in Figure 17.

2. INVESTIGATION OF THE MECHANICAL PROPERTIES OF THE WORKPIECE

I. The Investigation of Surface Finish

Mild steel and hardened tool steel surfaces were spark eroded with different capacities and at different discharge voltages. Mild steel was eroded with round brass electrodes $\frac{3}{4}$ in. diameter at 85 and 130 volts and $\frac{3}{8}$ in. diameter electrodes at 27 volts. Hardened tool specimens, blocks $\frac{3}{4}$ x $\frac{1}{2}$ in. were eroded with brass electrodes, at 70 - 85 volts. (All voltages are breakdown values U).

Care was taken to use a high ballast resistance to prevent any incidence of arcing. Surface finish was measured by Talysurf, for finishes up to approximately 300 μin. by the average meter, above this value by planimetration of records. Records of the surface were also made on the Talysurf, and for finishes above approximately 300 μin. the special reduction unit was used.

Single craters were also investigated, the diameter being measured with a microscope and the depth by means of the Talysurf record. The specimens are shown in Figure 18, the various records in Figure 19.

Experiments were made on the effect of slight hand polishing on the eroded surface, and the results are shown in Figure 20. All results of surface finish measurements are given in Tables I and II. The values quoted are averages of approximately 20 measurements each. The results are plotted in Figure 21 and Figure 22.

II. The Measuring of Residual Stresses

Strips of annealed mild steel, hard rolled brass, tempered spring steel and hardened high speed steel were spark eroded on one side, the ensuing curvature measured and then the eroded layer removed, until the strip nearly straightened out again. The strips were $\frac{1}{2}$ in. wide and approximately 0.02 in. thick, and an H.S.S. strip 0.04 in. thick was also used.

The spark eroded portion of the strips was $2\frac{1}{2}$ in. long. The capacity used was 1.5 μF., the breakdown voltage approximately 85 v., the gap was automatically controlled. To ensure uniform removal, a

narrow brass electrode was used, $\frac{1}{8}$ in. wide and $2\frac{1}{2}$ in. long. The eroded strips were clamped by means of springs to a plane surface and that surface was adjusted to be parallel to the electrode. During erosion the strip was traversed in such a way that the electrode moved across the width of it. This ensured uniform thickness of the strip after erosion and produced better results than a flat electrode covering the entire eroded surface at a time, a procedure which was tried previously. The flat surface to which the strips were fastened was actually the bottom of a small tank, so that different dielectric fluids could be used. Most experiments were carried out in paraffin, some in distilled water. The 0.04 in. thick H.S.S. strip was eroded at 300 μF, in paraffin.

The curvature was measured by the chord-bow method. Three circles, $\frac{1}{8}$ in. diameter were marked on the uneroded surface of the strip, at the distance of 1 in. from each other and opposite the eroded face. They constituted the base and the peak of the measured arc. The strips were then placed on three point supports parallel to a surface plate and a vertical micrometer was used to measure the heights of the three points (i.e. the centres of the marked circles). Since measurement had to be effected without contact, as otherwise the strip might deflect, a special method was employed. The micrometer spindle was provided with a spherical end and as it approached the surface of the strip, the sphere was reflected from the surface of the strip. The sphere and its reflection were observed with a microscope and it was found possible to bring the two images almost together without actual contact. With

care the achieved accuracy of repetition was 1/100 000 in. which was much better than required. The sphere and its reflection are shown in Figure 14.

After the curvature had been measured, the eroded and stressed layer was removed. A 25% solution of nitric acid was used, which according to Richards (32) does not introduce new residual stresses. Strips of annealed mild steel, brass and spring steel identical to those spark eroded were etched in order to find if the material was stress free, which was actually the case.

The thickness of the strips before and after etching was measured with a micrometer having a 1/10000 in. vernier. Care was taken to leave a small curvature after removing the stressed layer in order to ensure that not more than this layer was removed. The high speed steel strips could not be etched by nitric acid, and the layer was therefore ground off instead. Grinding was also used in order to check whether the strips were stress-free prior to spark eroding.

In connection with grinding, a series of experiments were carried out both on mild steel and H.S.S. to find the influence of grinding on residual stresses. Details of the results of residual stress measurements and the grinding experiments are given in the Analysis and Discussion.

III. Fatigue Investigation

The fatigue specimens were of mild steel with 0.15% C. content. The material was specially ordered to be from one cast and was normalized. The shape of the specimen is shown in Figure 23.

Tests were carried out in Wöhler type cantilever machines which were capable of 100 lb. max. load, obtained by dead-weights. The speed was 2,800 r.p.m. Rubber sheets were interposed between the shackle and the weights to minimize the effect of minor eccentricity of the rotating specimen. An automatic cut-out stopped the machine in case the specimens broke. Counters showed the number of stress reversals sustained by the specimens.

Three series of specimens were tested:

(a) Turned,

(b) Spark eroded,

(c) Spark eroded and stress relieved.

The turned specimens were carefully machined with a sharp tool and small depths of cut (not over 0.010 in.); the finishing cuts were taken at a feed of 0.003 in./rev. and depths of 0.005 in., 0.003 in. and 0.002 in. with a slightly rounded diamond-lapped tool. The surface finish of these specimens was 60 - 100 μin. CLA.

The spark eroded specimens were first machined as the turned ones and subsequently "sparked" on a small lathe which was converted for this purpose. A capacity of $3\frac{1}{2}$ μF was used, and in order to ensure roundness the average voltage was approximately 80 volts instead of 50 - 60 v. for maximum efficiency. The tool was a block of brass which was trued by rotating a cutter mounted on a mandrel between the centres of the lathe. After truing the mandrel was removed and the fatigue specimen inserted instead.

The sparking was done at approximately 200 r.p.m. and at a feed of 0.05 in. per revolution. The leads were connected to the anode and the cathode of the drilling unit, so that the total discharge circuit was of a rather large resistance, which resulted in a relatively better surface finish that would have been obtained by the same voltage and capacity in the drilling unit itself. The sparking was continued until the surface was completely covered. The dielectric was paraffin.

The stress-relieved specimens were prepared in the same way, namely turned and subsequently sparked, and were eventually heated to a temperature of approximately 700° C. for half an hour in an argon atmosphere, and then cooled slowly in the furnace for another half hour. This procedure aimed at relieving the residual stresses induced by spark machining.

The results of the endurance tests are shown in Figure 24. The turned mild steel specimens fractured still at 33,750 lbs./in.^{2}, and the endurance limit was found to be between this value and 32,600 lb./in.^{2}, say approximately 33,000 lb./in.^{2}. The curve shows a bend at 6-9 x 10^6 cycles.

The endurance limit of the spark eroded specimens was found to be 27,250 lb./in.^{2} and that of the spark eroded and stress relieved specimens was at 30,750 lb./in.^{2}. The two latter curves show a bend at 3-4 x 10^6 cycles.

CHAPTER IV

ANALYSIS AND DISCUSSION

1. ANALYSIS OF THE RELAXATION CIRCUIT

I. Maximum Power Transmission

The complete relaxation circuit (Figure 25) consists of a charging branch and a discharge branch. In the charging branch is a source of direct current, a ballast resistance R and a condenser C. The condenser is connected in series with the ballast resistance. The inductance of the charging circuit is assumed to be negligibly small. The condensers used are of the non-inductive type and with a very small leakage.

The discharge branch consists of the spark gap with a non-linear resistance ψ, inductance L (which however small, plays an important part in the performance), and the ohmic resistance ρ' of the leads etc., which is usually kept as small as possible.

The spark gap is automatically adjusted to such magnitude that a voltage U is required to break down the dielectric. The potential difference impressed by the D.C. source is $\mathcal{E}$.

If the charge in the condenser is γ, we have:

$\frac{d\gamma}{dt}R + \frac{\gamma}{C} = \mathcal{E}$, where the current $I' = \frac{d\gamma}{dt}$ and $U = \frac{\gamma}{C}$

The solution is: $\gamma = \mathcal{E}C(1 - e^{-t/RC})$ or

$$U = \mathcal{E}(1 - e^{-t/RC}) \qquad \text{Equation (1)}$$

When the voltage across the condenser, i.e. across the gap reaches the breakdown value U, a spark occurs, the energy stored in the condenser is released and the condenser starts recharging. Under normal operating conditions the gap will become deionized and the discharge branch will thus be open. This requires a sufficiently high value of the ballast resistance R. If the resistance R is below this value, an arc develops and the process is disturbed. The duration of the spark is between a few to several hundred microseconds, while the charging time is very much longer. For given values of R and C the charging time Θ depends on the required value of $U/\mathcal{E}$, i.e. on the length of the gap.

From Equation (1) the charging time Θ is given by

$\Theta = -RC \log_e (1-U/\mathcal{E})$ and the spark repetition rate $n = \frac{1}{\Theta}$ is

$$n = -\left[RC \log_e (1-U/\mathcal{E})\right]^{-1} \qquad \text{Equation (2)}$$

The voltage-time curve is shown in Figure 26.

The duration of the spark p is very short compared to Θ, so that for the practical purpose of evaluating the optimum ratio $U/\mathcal{E}$ it has been assumed that $\Theta + p \approx \Theta$.

It has been established by Lazarenko (3), Zolotikh (7) and others that the amount of the metal eroded is closely proportional to the energy spent, hence the rate of removal is proportional to the transmitted power. (This proportionality holds for operation within certain limits; if the capacity C is increased beyond about 500 microfarads, there is no substantial gain in removal; therefore equipment having more than this is rarely used).

The power transmitted to the condenser at any instant is equal to UI, I being the instantaneous charging current, where

$$I = \frac{\mathcal{E}-U}{R} = \frac{1}{R}\left[\mathcal{E}-\mathcal{E}(1-e^{-t/RC})\right] = \frac{\mathcal{E}}{R}e^{-t/RC}$$

The power is thus equal (using Equation (1)) to:

$$\frac{\mathcal{E}^2}{R}(1-e^{-t/RC})e^{-t/RC}$$

and the average power transmitted during one cycle is

$$N = \frac{1}{\Theta}\int_0^{\Theta}\frac{\mathcal{E}^2}{R}(1-e^{-t/RC})e^{-t/RC}\,dt$$

$$= \frac{\mathcal{E}^2}{R}\frac{RC}{\Theta}\left(\tfrac{1}{2}e^{-2\Theta/RC} - e^{-t/RC} + \tfrac{1}{2}\right) \qquad \text{Equation (3)}$$

or $$N = \frac{\mathcal{E}^2}{R}k\left(\tfrac{1}{2}e^{-2k} - e^{-k} + \tfrac{1}{2}\right) \quad , \text{ where } \frac{\Theta}{RC} = k$$

The function N(k) is shown in Figure 27.

From Equation (1) we have $U/\mathcal{E} = 1-e^{-k}$ or $k = -\log_e(1-U/\mathcal{E})$, so that N is a function of $U/\mathcal{E}$. The function $N(U/\mathcal{E})$ is shown in Figure 28. Since the length of the gap is proportional to the voltage U, the function N=f(gap length) is of the same shape as $N(U/\mathcal{E})$.

The value of k which corresponds to the maximum power transmission can be found by differentiating Equation (3) in respect to k and equating to zero.

$$\frac{dN}{dk} = \mathcal{E}^2C\left[(-e^{-2k} + e^{-k})k - \left(\tfrac{1}{2}e^{-2k} - e^{-k} + \tfrac{1}{2}\right)\right]k^{-2} = 0$$

or

$$k = \frac{\frac{1}{2}e^{-2k} - e^{-k} + \frac{1}{2}}{e^{-k} - e^{-2k}}$$

The numerical solution of this transcendetal equation renders k = 1.26 or U = 0.72

A voltmeter indicating average voltage (as it is normally used) will read U_v which is found by integrating the area under the U(t) curve for one charging cycle.

$$U_v = \frac{1}{\theta}\int_0^{\theta} U\,dt = \frac{1}{\theta}\mathcal{E}\int_0^{\theta}(1-e^{-t/RC})\,dt = \mathcal{E} - \mathcal{E}\frac{RC}{\theta} + \mathcal{E}\frac{RC}{\theta}e^{-\theta/RC}$$

and by putting $\theta/RC = k = 1.26$ we obtain $\underline{U_v = 0.434\,\mathcal{E}}$ for the maximum power transmission.

It has been assumed that the duration of the spark p can be neglected; that assumption can now be checked. As shown on Page 22 the minimum value of the ballast resistance which still prevents arcing was found to be approximately $R_{min} = 60\,C^{-\frac{1}{2}}$. On the other hand, the duration of the spark was found (Page 22) to closely equal $p = 2\pi(LC)^{\frac{1}{2}}$. Since L equals approximately 3 microhenry, the duration of the spark $p \approx 10\,C^{\frac{1}{2}}$. Hence the ratio p/θ

$$p/\theta = p/RC\log_e(1-U/\mathcal{E}) = 10C^{\frac{1}{2}}/60C^{-\frac{1}{2}}C\log_e(1-U/\mathcal{E}) =$$

$$1/6\log_e(1-U/\mathcal{E}) \approx 0.13 \quad (\text{taking } U/\mathcal{E} = 0.72).$$

This means that the energy accumulated during the time θ has to be divided by 1.13 θ in order to obtain the true average power. Since, however, the ratio p/θ is constant for the case of most intensive erosion, the optimum value of $U/\mathcal{E}$ will not be affected and remains 0.72. Moreover, since it can be assumed that the minimum value of the ballast resistance is a characteristics of the spark phenomenon, the ratio p/θ will be a constant for a relaxation circuit with a different inductance

L, so that the ratio $U/\mathcal{E} = 0.72$ for the highest power transmission should hold for all cases.

By substituting the value $k = 1.26$ in Equation (3) the maximum theoretical power is found to be

$$N_{max} = 0.21\ \mathcal{E}^2/R_{min} \qquad \text{Equation (4)}$$

(R_{min} or R_m is the minimum ballast resistance which may be used).

II. The Efficiency of the Relaxation Circuit

The efficiency η of the relaxation circuit is the ratio of the transmitted power to the sum of the transmitted power and the power lost in the resistance.*)

Hence:

$$\eta = \frac{\int_0^{\Theta} I\,U\,dt}{\int_0^{\Theta} I\,U\,dt + \int_0^{\Theta} I^2 R\,dt} = \frac{\frac{1}{2}e^{-2\Theta/RC} - e^{-\Theta/RC} + \frac{1}{2}}{} =$$

$$= \frac{\frac{1}{2}e^{-2k} - e^{-k} + \frac{1}{2}}{1 - e^{-k}}$$

The maximum possible efficiency is 0.5 which corresponds to an infinitely long charging cycle. For the case of $k = 1.26$ the efficiency is 36.5%. Taking into account that owing to fluctuation in gap length the charging voltage cannot be maintained constant (Figure 29), the actual efficiency cannot be assumed to be much over 25%. By substituting in Equation (4) the value $R_m = 60\ C^{-\frac{1}{2}}$ and dividing by the actual efficiency, an expression is obtained for the maximum power requirement N_{inp} of a circuit which has to operate at the highest possible rate of erosion:

*) Assuming that the condensers cause no losses.

$$N_{inp} = 0.015\,\mathcal{E}^2\,C^{\frac{1}{2}} \qquad \text{Equation (5)}$$

(N_{inp} - Watts; $\mathcal{E}$ - Volts; C - microfarads).

Vasiliev (39) measured the craters produced by various breakdown voltages and came to the conclusion that the highest rate of removal is obtained when $U/\mathcal{E} = 0.85$. This is somewhat higher than the theoretical ratio of 0.72, and the power transmitted at $U/\mathcal{E} = 0.85$ is only 0.93 of the maximum. No other information on actual experimental results appears to have been published.

III. Spark Turning

Departure from the optimum ratio $U/\mathcal{E}$ will result in reduced rate of removal. In the case of "drilling", i.e. in the normal application of the common spark machining equipment the departure to higher values of $U/\mathcal{E}$ than the optimum or to the lower ones will only affect the surface finish; it will improve as the ratio $U/\mathcal{E}$ becomes smaller. The rate of removal will decrease in both cases, so that operation in the lower region may sometimes be of advantage. The position is different in spark turning. In the course of preparation of fatigue specimens for the present investigation it was found that perfectly round parts often lost their circular shape and acquired errors of one and more thousands of an inch. Eventually it was found that for the production of a truly circular shape it is essential to operate in the region where $U/\mathcal{E}$ is well above the optimum value. The ensuing loss of productivity has to be accepted, as it is theoretically impossible to operate the relaxation circuit in the optimum $U/\mathcal{E}$ range without producing errors in the round workpiece. The explanation is as

follows: It can be seen from Figure 28 that if the ratio $U/\mathcal{E}$ is less than optimum, the rate of removal decreases with the decrease in $U/\mathcal{E}$, i.e. with the decrease in the gap length. The opposite occurs when $U/\mathcal{E}$ is more than the optimum. Owing to the fluctuation in the gap conditions, setting for any value of $U/\mathcal{E}$ will result in operation within a certain range of values for $U/\mathcal{E}$, the chosen one being the average. Thus, if the operation is to be performed at the optimum ratio of $U/\mathcal{E}$ and the gap is adjusted accordingly, some sparks will occur when the gap is larger than the optimum and some when it is smaller. Consider the case when the gap is below the optimum - a decrease in gap size reduces the rate of removal, which means that points on the workpiece more distant from the axis are removed more slowly than those somewhat nearer to it. This will cause eccentricity of a magnitude equal to the variation in gap length. Brought to the extreme - when the tool electrode touches the workpiece there is no removal at all. The mechanism is reversed for operations entirely above the optimum value of $U/\mathcal{E}$. Here the rate of removal decreases with increase in gap length and the operation is self-correcting. A similar phenomenon is observed when spark turning is employed for producing round components from non-circular material. The form of the material is "copied" in a way not dissimilar to the "copying" encountered in the use of not very rigid metal cutting lathes. It is therefore essential to operate entirely above the optimum gap length of circular components are to be produced.

IV. Arcing

The fundamental requirement of spark machining is that no current should pass in the gap between sparks. After the completion of a spark the gap must become non-conducting, the breakdown occurring only when sufficient energy has again accumulated in the condenser. Since the D.C. source is connected all the time to the gap, there is a danger that once the dielectric breaks down, current will flow continuously through the conducting path and short-circuit the source and the condenser. This will prevent the build-up of energy in the condenser, required for the pulse, and will also result in an arc, detrimental to the surface finish and structure of the machined metal. The characteristics (voltage-current curves) of spark and arc are entirely different, but they can have a common point - Figures 30 and 31. If the conditions are conducive to the development of a stable arc, it will indeed occur. The conditions for a stable arc are different for circuits with different ratios of L/C, but in any case a stable arc will develop if the charging resistance is less than $(L/C)^{\frac{1}{2}}$. (Andronov and Haikin (42)).

It was found in the present investigation that a continuous arc developed when the capacity was 1.5 microfarad and the resistance approximately 2 - 3 ohms. As the inductance of the circuit was approximately 3 microhenries, the condition for a stable arc was about the same as predicted. It was not possible to maintain continuous arcs with higher capacities because of the ~~limitation of the~~

limitation of the permissible current in the equipment. On the other hand, it was found that if the resistance R was reduced below the value $60\ C^{-\frac{1}{2}}$, occasional arcing would start (Chapter III-1-I). This relationship was found to hold for a capacity range of $\frac{1}{2}$ to 100 microfarads. Thus, while the theoretical relationship for continuous arc $R = L^{\frac{1}{2}}C^{-\frac{1}{2}} = 1.8\ C^{-\frac{1}{2}}$ was found to be nearly true (at least for small capacities), the larger constant (60 instead of 1.8) for first incidence of arcs would indicate that arcing is also possible at a different condition of equilibrium, possibly because of occasional short circuits. Since even the occasional arcing may be detrimental to the surface, for reasons given in Chapter III-1-I, some means should be incorporated in the machine to indicate arcing. A number of commercial machines provide it by either an oscilloscope or a neon tube.

V. Analysis of the Spark Discharges

The shapes of current and voltage curves of spark discharges were observed with the aid of an oscilloscope. Measurements were made for a range of capacities from $\frac{1}{2}$ to 500 microfarads, mostly for those voltages which could be maintained automatically by the servomechanism, but also for some higher voltages approaching the potential difference of the D.C. source. The current and voltage forms were also observed for discharges produced after the source had been disconnected; owing to the leakage of the condensers the lower limit of capacity in this case was 10 microfarads. In the latter case the breakdown was initiated in three different ways:-

(a) By bringing the two electrodes closely together without making contact;

(b) As in (a), but with subsequent contact;

(c) By making the electrodes approach each other with considerable velocity until contact was established.

Photographs of some of the current and voltage forms are shown in Figure 17. Observations of these figures show that both the voltage and the current shapes have a characteristic common for all the ways of producing the discharge. (It will be seen that the only exception is for the case in which the electrodes hit each other with a velocity above a certain limit). The voltage curve starts at a value between 35 to 45 volts and drops to 10 - 12 volts with a nearly constant slope, then it suddenly drops to zero and in most cases goes over the zero line to a negative value. These values are independent of the capacity. A single spark with the source disconnected and the electrodes not in contact will show either a second discharge, this time of the reversed shape, or a constant voltage of negative sign. When the sparks are produced continuously (i.e. in succession), in which case the source is connected, the two forms occur, but it can be noticed that the complete reversed discharge is relatively rare here. Moreover, the source voltage frequently suppresses the reversed voltage, as can be seen in Figure 17.

The typical forms are shown in Figure 32 with the reversed half-wave both present and absent.

The current forms possess a similar duality; while the first half-cycle is nearly a sine wave of an amplitude increasing with the capacity, the second half of the cycle is either a smaller sinusoidal or zero current.

The current is lagging behind the voltage by an angle φ which diminishes with increased capacity. The current form is shown in Figure 33.

Both the current and the voltage forms are somewhat distorted by superimposed high frequency oscillations, especially at low capacities. The forms shown in Figures 32 and 33 have been "cleaned" of the parasitic high frequency.

The erosive action of the spark discharge begins from the moment the current starts to flow. The breakdown of the dielectric occurs in an extremely short time, a fraction of one microsecond (Crowe, 17 ; Zolotikh, 7) and its mechanism is not directly affecting the erosion. For the investigation of the spark itself it is sufficient to assume that the conducting channel is established practically instantly. The equipment used was not capable of measuring the time of the breakdown.

The discharge circuit possessed both capacity and inductance, therefore it would exhibit oscillation if the energy stored in the condenser would be released by suddenly short-circuiting the gap. Sine waveforms for both voltage and current were actually observed when a large capacity (50 microfarads or more) was used and the gap was suddenly closed by letting the spindle with the cathode fall freely

from a height of approximately 4 inches onto the anode surface. Taking the height as 10 cm. and the gap length as 0.0025 cm., the time in which the gap will be closed is $0.0025/(2g \times 10)^{\frac{1}{2}} = 0.0025/(19700)^{\frac{1}{2}} = 18$ microseconds. If the pulse is several times longer, it will be of a nearly-sine waveform., Figure 17 . Therefore, these forms of current and voltage cannot be regarded as representative for a spark.

When the breakdown had taken place and the conducting channel begins to form, and at the same time the gap is maintained, the discharge is of an oscillatory nature and of nearly the same frequency as before but of a different character. The charge in the condenser is discharged through the growing channel, the resistance of which decreases rapidly because of its expansion. The inductance of the circuit causes the current to "overshoot", so that after reaching a maximum it decreases. If the energy stored in the condenser, $U^2C/2$ is completely spent by losses in the gap, the leads and by radiation, the spark is over when the current and the voltage reached zero. The current reaches zero gradually, while the voltage drops suddenly. If, however, some energy is still left over, the condenser will be recharged, but with reversed polarity. The gap deionizes apparently very quickly, because it has been observed that the reverse charge will quite often remain in the condenser; this observation was made by both oscilloscope and voltmeter. The latter swung over to below zero and returned to zero only when the gap was short-circuited. With larger capacities a visible second spark could be observed. In some cases, however, the reverse charge was discharged through the gap, either by probably

producing another breakdown or by conduction of the accumulated swarf, or possibly by a combination of both, i.e. breakdown of a minute effective gap left as the swarf nearly filled the space. Therefore, the shape of the second half-wave of the voltage depends on the gap condition in this particular instant.

The current wave is of a corresponding form - if the reverse charge is discharged, a current will flow, and it exhibits a sine form. It has been observed that while the first current amplitude increases with the capacity (for a constant charging voltage), the reversed amplitude is nearly constant (Table III). A similar result was obtained by Zolotich (7).

VI. The Oscillatory Behaviour

A simple ρLC circuit, with the three elements in series is defined by the equation

$$L\frac{d^2I}{dt^2} + \rho\frac{dI}{dt} + \frac{I}{C} = 0$$ I being the current.

This Equation has a simple solution if ρ, L and C are constants. In the case of a spark the resistance is not constant, but nevertheless if the simple solution is applied, the experimental results agree quite well with the calculations. If $\rho^2 < 4L/C$, the solution is an under-damped oscillation given by $I = I_m e^{-\delta t} \sin(\omega t)$, $\delta = \rho/2L$ and $\omega = (1/LC - \rho^2/4L^2)^{\frac{1}{2}}$.

It can be seen from the voltage and current forms that the resistance of the spark is very small during almost the entire period, and therefore the frequency can be taken as $1/2\pi(LC)^{\frac{1}{2}}$. The duration of one half of one period is then $\frac{p}{2} = \pi(LC)^{\frac{1}{2}}$.

The measured times p were plotted against the capacities C in Figure 35. The graph confirmed the assumption and the induction was found to be 3.1 microhenries, as compared to 3.22 μH measured.

The lagging of current behind the voltage must be attributed to the measuring technique, since there can be no inductance of the corresponding magnitude in a spark gap. The resistance of the spark is ohmic, though non-linear, and the inductance of the channel as a conductor is extremely small because of its small length. Screened earthed leads were used to connect the oscilloscope, but a short length of each was unscreened. Moreover, the shunt which was used to measure the current was some distance from the spark gap and this could add some more inductance in the measuring circuit. A plot of the tangent of the phase displacement against pulse length p gave a straight line (Figure 34), which means that the ratio resistance/inductance of the disturbing element was constant, an indication of a metallic conductor. The shunt itself had such a small inductance (0.02 μH) that it could not cause the lag.

The reverse "overshooting" of the current, shown especially with the smaller capacities, was probably due to a reflected wave caused by mismatching of the impedance of the shunt circuit with the oscilloscope. At any rate, moving the leads up and down had some effect on this phenomenon. The overshooting was observed in cases in which the condenser remained reversely charged and no current could possibly flow through the gap in the reverse direction. The phenomenon was less disturbing with capacities above 50 microfarads, i.e. with pulses above a certain duration (approximately 75 microseconds).

No detailed study was made of the high frequency oscillations seen in some photographs. It was found that their frequency was nearly constant, actually increasing slightly with increased capacity. A change in the inductance of the discharge circuit, obtained by connecting pieces of thick wire, only affected the amplitude of the h.f. wave-forms. It was assumed, therefore, that the h.f. oscillations were imposed on the discharge circuit, and were created probably by the condensers themselves. The condensers, nominally non-inductive, possessed a very small inductance each, which together with the capacity constituted an oscillatory circuit. Assuming the inductance of the condensers proportional to their size, i.e. to their capacity, a constant frequency would be expected by connecting the condensers in parallel, since the total inductance would be inversely proportional to the sum of the capacities and their product would be constant. The slight increase in frequency occurring with the connection in parallel of more condensers would indicate that the larger condensers have a relatively higher inductance than the smaller ones. This is quite possible, and the difference in frequencies was small anyway, (approximately 0.2 with 5 fold increase of capacity). Owing to the relative proximity of the frequency of the h.f. parasitic oscillations to the natural frequency of the discharge circuit when using small capacities (up to 5 microfarads), the distortion of the current amplitude of the latter were very large and measurement was difficult.

It is assumed that accurate investigation of discharges produced by small capacities would require very carefully designed circuits with condensers of extremely small inductance.

A system like the discharge circuit, having a distributed inductance would have theoretically a large (actually infinite) number of natural frequencies; a close observation indeed disclosed a few more oscillations of much higher frequencies, but their amplitudes were vanishingly small, except in the case of the pulse produced by the 0.5 microfarad condenser. (The oscilloscope used was said to have a response up to 5 megacycles per second).

VII. Calculation of the Current

An attempt was made to calculate the amplitude of the first current half-wave. It was observed that the voltage in the condenser which happened to charge reversely without losing the charge by a reversed half-wave, was never more than $\frac{1}{3}$ of the original breakdown voltage. It was assumed, therefore, that approximately 8/9 of the energy originally stored in the condenser must have been spent during the first half of the pulse, i.e. during the first half-wave. For the purpose of the calculation it was assumed that the voltage form of the spark follows a straight line, although actually it was some kind of an exponential curve. Had the resistance of the spark been constant, ψ = const., the curve would be $U_s = U_1 e^{-t/\psi C}$, U_1 being the voltage at the beginning of the breakdown (35 - 45 v). The resistance of the spark could then be calculated from the knowledge of the voltage

U_2 (10 - 12v) when the time t = p/2. The resistance of the spark, however, is far from constant, and in the first half of the first half-wave it drops from infinity to a few hundredths of one ohm, and then goes up again. The idea of "effective resistance", calculated sometimes (Zolotikh, 7) from the damping of the first current amplitude to the amplitude of the reversed half-wave has little meaning either. It was therefore thought that assuming the voltage curve to be a straight line would introduce an insignificant error. The current was assumed to be of a sine form, and for the purpose of calculation the sine was expanded in series. The first four terms of the sine series were found to be sufficient for the practically required convergence.

It would be, of course, quite possible to follow a different procedure, e.g. by assuming that the resistance of the spark ψ is inversely proportional to time during the first half of the first half-cycle and directly proportional in the second half, the exponential function could then be expanded in series as well and the energy obtained by integration. It was believed, however, that the elaborate calculation would not justify itself, since the departure of the observed voltage curve from a straight line appeared to be very small.

According to calorimetric measurements carried out by Zolotikh (7), the energy dissipated in the spark gap amounts to 0.4 - 0.6 of the energy stored in the condenser. By taking an average value of 0.5, the current amplitude of the first half-wave is given by:-

$$I_m = 26\ C^{\frac{1}{2}}$$

The complete calculation is shown in Appendix III.

The log-log plot of the measured I_m against C (Figure 36) shows reasonable agreement with the calculated relationship.

The losses in the leads calculated on the basis of the measured resistance (0.011 ohm) and the current I_m amount to approximately $\frac{1}{8}$ of the energy stored in the condenser. It can, therefore, be assumed that other losses, such as in the condensers and the electromagnetic radiation amount to $\frac{1}{4}$ - $\frac{1}{3}$ of the total energy. At very short sparks, however, the losses in the leads may be considerably higher because of the skin effect.

The results obtained in our case show somewhat higher values for the current amplitude I_m than those obtained by Zolotikh (7). The value given by Zolotikh for current amplitude in the case of approximately 90 volts and 200 microfarads is approximately 220 amps as compared with approximately 390 amps from our measurements or 370 from the formula $I_m = 26C^{\frac{1}{2}}$.

Taking into account that Zolotikh quotes approximately 2.2 μH for the inductance of his circuit, as compared to 3.1 in our case, the formula, if corrected for that inductance renders:
$I_m = (2.2/3.1)^{\frac{1}{2}} \times 370 = 310$ amps, which is still nearly 50% higher than 220. It is, however, possible that the different dielectric fluids are responsible for the discrepancy. While Zolotikh used a double-purified paraffin, which was replaced after each discharge, ordinary contaminated paraffin was used in the present investigation and was not renewed.

The presence of a considerable amount of swarf was not objectionable, because only a dielectric fluid so contaminated is representative of normal operating conditions of spark machining. Therefore, the initial voltage after the breakdown U_1 was mostly 35 volts and sometimes less, rarely 45 volts, and was never observed to reach the value of 60 V. quoted by Zolotikh. It appears not improbable that the presence of swarf enables faster growth of the conducting channel. If the formula for I_m is modified for U_1 = 45 instead of 35 volts, the current in question would be 220 amps. only. However, both the current measurements and the most common voltage curves observed disagree with such a low value. The difference of the dielectrics may therefore probably be the main cause of the discrepancy. There is certainly scope for investigation of the effect of the dielectric and the degree of its contamination on the parameters of spark erosion.

VIII. Productivity of the R-C Circuit

A striking feature of the relaxation circuit is its low efficiency and small productivity. The efficiency of the circuit is at the most 25%, as was shown already in Paragraph II of this Chapter. Some improvement of the efficiency can be obtained by including an inductance in the charging circuit, which results in an "overshoot" of the voltage across the condenser for the same source voltage. Such circuits are sometimes used and are described by Blake (38), Livshits (33), and Opitz (16). The main disadvantage of these circuits is the need for a vibratory movement of the tool electrode in order to obtain

synchronization between the instant of the discharge and the state of maximum voltage. This imposes a limit on the spark repetition frequency which can be reasonably high only when the tool electrode and its assembly are very light. Such machines are used for the drilling of small holes.

A far more serious limitation is the low productivity. It can be easily shown that if the minimum permissible resistance is used, the ratio of charging time to spark duration is 10 to 1 or more. This means that only 10% of the total time is utilised for actual machining and the remaining 90% for charging. When roughing with a relaxation circuit, the maximum possible rate of removal is 1 cm.^{3} per minute (for hardened tool steel). This corresponds to a rate of removal of 10 cm.^{3} per minute during spark duration. Such a rate of removal is already very high, especially for a tough material. It can thus be seen that the spark is an excellent machining medium, but the method of its generation is inefficient. It would be theoretically possible to vary the ballast resistance during the charging cycle so as to shorten its duration; this would require vacuum tubes capable of carrying currents of dozens of amps., but such valves are not manufactured.

IX. Other Pulse Generators

It is understandable that other circuits have been developed in recent years, which can produce sparks of a certain energy much faster than the relaxation circuit. The development was in two directions:

mechanical pulse generators, using specially wound AC generators or DC commutator machines on one hand, and electronic pulse generators, basically similar to those used in radar techniques, on the other hand. The mechanical generators achieve rates of removal of 5 times or more than obtained with relaxation circuits, but only for roughing, while the electronic generators show a good rate of removal in finishing. The latter, however, are rather complicated and prone to break-downs. The relaxation circuit has the great virtue of cheapness and simplicity and will undoubtedly hold its place for a long time. The majority of the equipment as present manufactured operates on a relaxation circuit. Some have a repetition rate of up to 100,000 sparks per second, but though the machines can be acquired commercially, the makers refuse to disclose the circuits employed. The mechanical generators are described in detail by Livshits (33) and Zolotikh et al (34), while electronic and similar (rotating gap and pulse transformers with electronic elements) are described by Williams (35), Martin (36), Lazarenko (37) and others (with less detail). No known generator appears to work at a frequency higher than 100,000 c/s. It is doubtful if it would be worthwhile to exceed this because of the losses due to the skin effect. The high repetition rate of some relaxation circuit machines, if true, is most probably obtained by very small capacities and inductances. The figures quoted for the rate of erosion are about the same as those obtainable with circuits of normal design, but the surface finish quoted is better. Another important point is the stability of the servo-mechanism which maintains the gap length. A hunting servo can reduce the productivity to a fraction of the possible maximum.

X. Polarity of Erosion

The mechanical pulse generators are characterized by relatively long pulses of several hundred microseconds. An interesting phenomenon occurs with the use of these long-pulse machines, in that the polarity has to be reversed in order to reduce the tool erosion to a few per cent. According to a very recent source (Livshits et al. 40), the erosion of tools made of a copper-graphite composition is only 0.1% of the erosion of the workpiece, i.e. the tool wear is already in the order of wear of ordinary cutting tools. This phenomenon has been called "polarity of erosion"; it was observed by Lazarenko (3) in his original work and later confirmed by others. Zolotikh (7) quotes ratios of cathode/anode erosion of 10% for pulses 1 μsecond long, 25% for 10 μsecond and 58% for 140 μsecond long pulses. With much longer pulses the ratio becomes much more than unity. In such cases the polarity has to be reversed, i.e. the tool made the anode and the workpiece the cathode. This indicates that the governing factor in the erosion is the time, i.e. the rate of heat input. (All comparisons are made for pulses of the same energy). It was observed in the present work that sparks without the reverse half-wave produced erosion on the tool electrode which was practically identical with the erosion produced by sparks with the reverse half-wave. Thus the reverse flow of electrons cannot be blamed for the major part of the tool erosion. The "polarity of erosion" confirms this. The difference between an intensive and a slow spark is the rate of heat input which is reflected in the temperature gradient in the electrodes. An intensive spark produces a

steep gradient and a considerable part of the crater is boiled and vapourized. Zolotikh assumes (7) that an average (150 μF) spark causes boiling and vapourizing of 25% of the crater volume. The same energy discharged in a much longer time will thus cause smaller relative vapourization, and in a much shorter time the reverse will be the case. Very short sparks completely vapourize the eroded volume. It can be shown that the anode ions can reach the cathode in a time of the order of 10^{-9} second, i.e. practically instantaneously. If this is correct, the question arises - why is the relative cathode erosion low when the anode produces relatively much vapour - as in the case of the short spark - while in a long "soft" spark with relatively little vapour the cathode erosion is much greater. This appears to be the fundamental problem of the spark erosion process from the technological point of view, because tool wear is the most important aspect of the method. It appears that as far as tool wear is concerned, the type of circuit used in the present investigation is almost the worst possible one, because the sparks are of a duration which produces a nearly equal erosion of both electrodes.

The mechanism of erosion and its ramifications should be the subject of an extensive study, since the knowledge available at present is far from sufficient for a scientific approach to electro-spark technology. It would appear, however, that the situation is more satisfactory as far as roughing is concerned than it is in the case of finishing. Roughing can now be carried out at great speed and with low tool wear by using the long-pulse generators, but there is as yet no

method capable of producing finished surfaces both quickly and with low tool wear.

2. PROPERTIES OF THE SPARK ERODED SURFACE

I. The Surface Finish

If one assumes that the amount of eroded metal is proportional to the amount of energy spent, and that the shape of the crater is similar for small and large craters, a relationship between the expected surface finish, the capacity and the voltage can be worked out.

Thus, for a crater of the depth h_c - Figure 37a, the volume will be proportional to h_c^3 on the one hand, and to the energy of a single spark $CU^2/2$ on the other. The craters are not, however, arranged in a straight line as shown in (a) but rather in a random way as shown in (b). It is, moreover, assumed that if the length upon which the surface finish is measured is many times longer than the diameter of a single crater, the average depth obtained would be proportional to h_c.

The instrument employed - Talysurf - indicates the centre line average CLA which is proportional to h_c. Thus:

$$(CLA)^3 \propto CU^2 \quad \text{or} \quad CLA = K\, C^{\frac{1}{3}}\, U^{\frac{2}{3}}$$

Measurements were carried out on specimens of mild steel for three different voltages and for capacities from $\frac{1}{2}$ to 200 microfarads, as shown in Table I. The results were plotted in Figure 21. It can be seen that the relationship for a constant voltage is near to CLA proportional to $C^{\frac{1}{3}}$, but on the basis of these results it is difficult to reach a conclusion concerning the effect of the voltage. Three

different voltages were apparently not enough, but it was not possible to operate the equipment on other voltages because of the available setting of the servo-mechanism. In any case, the nearest approximation would be that the CLA is proportional to $U^{0.4}$, which means that with increased voltage the crater grows more slowly than the energy of the spark. This is quite understandable, since with a higher voltage the gap is longer and the proportion of the energy losses in the gap is higher than in the case of a lower voltage and shorter gap. The only available reference on similar measurements is by Dumpe (41) who gives the relationship as Root Mean Square = constant x $C^{0.25}$ $U_v^{0.45}$. This is not very different from results obtained in our case.

Since in most cases industrial equipment is designed for one voltage only, the effect of the voltage on the surface finish is of much less importance than that of the capacity. The predicted relationship can be thus used for practically any voltage, i.e.

*) $$\underline{\text{CLA} = \text{constant} \times C^{\frac{1}{3}}}$$ Equation (6)

Measurements carried out on surfaces of specimens of hardened tool steel showed the same relationship between surface finish and capacity; it is of interest to point out that the surface finish produced on tool steel was slightly worse (higher CLA) than that for corresponding erosion conditions on mild steel specimens, (Figure 22). This would mean that craters on hardened tool steel are slightly greater than for the same

*) This is true for constant breakdown voltage; if that is changed, e.g. by changing the gap length (servo adjustment), the constant in the Equation (6) will change too. However, the change will be very small because of the low exponent (0.4) of the voltage. Details of calculation of voltage are shown in Appendix I.

conditions on mild steel. This ties up quite well with data for relative rates of erosion, which are given (e.g. Wickman Publication No. W165, 1957) as 1.2 to 1 for hardened tool steel to mild steel. Thus, measurement of the surface finish produced on a certain material could serve as a first, rough guide to the expected rate of erosion.

The range of finishes investigated was well beyond the usual needs, it exceeded that of the standard capacity of the measuring equipment. The Talysurf I which was used could normally measure only up to 150 microinches CLA at the lowest magnification of 2,000. A special electronic unit was ordered to reduce the lowest magnification to 400, but the average readings were not taken above 400 microinches at the most, in order to prevent damage of the stylus.

For rougher surfaces the mechanical reduction unit was employed. It can be concluded that stylus measurement of sparked surfaces is quite possible, representative and reproducable (plus or minus 20% of the average), provided it is carried out in the range in which surface finish is normally measured. If that range is exceeded, the stylus may sustain damage, but this applies equally well to surfaces produced by other methods.

It must be pointed out, however, that the possibility of measuring the surface finish does not necessarily mean that the properties of the surface are thus asserted. The spark eroded surface has a peculiar geometry which is quite different from the geometry of surfaces produced by conventional machining. Its oil retaining and wearing properties cannot be deduced from the CLA value alone; this

value can only be employed for the comparison of various spark eroded surfaces, but not for comparing such surfaces with ground, milled or turned ones.

The performance of spark eroded surfaces and the importance of the quality of surface finish are not sufficiently known and should be investigated in great detail.

II. Residual Stresses

The measurement of residual stresses was based on the deflection method. When narrow strips of metal were eroded on one side the residual stresses thus created caused bending. After the curvature had been measured a layer of metal was removed from the eroded side. The change in curvature was then measured and the residual stresses in the removal layer calculated.

(a) The calculation of the stresses

Assume that a flat strip of metal, free from residual stresses has been bent to a curvature of the radius R' after being spark eroded on one side. It was observed that the eroded side was always concave, which indicated that the affected layer must be in tension. The tension in the layer exercised a bending moment and as a result of it the strip was bent to the radius R'. After a layer of the thickness d was removed from the eroded surface the strip straightened out and its curvature was then of the radius R". The bending moment caused by the residual stresses which were contained in the removed layer changed the curvature, therefore, from $1/R'$ to $1/R"$. If the Young's Modulus of the strip is E, the thickness of the strip a and the width b, we obtain

$1/R' - 1/R'' = M/EI$ where $M = fbda/2$, f being the average residual stress, and I the second moment of the area of the cross-section of the strip. $I = ba^3/12$. This procedure can be repeated, but account has to be taken for the effect of the straightening on the stresses in the subsequent layers and the calculations are rather lengthy. The procedure of such a case is fully described in the literature (32).

In the present investigation the affected layers were found to be so thin that it was extremely difficult to subdivide them with the necessary accuracy and therefore only one layer was removed. This was of such thickness as to bring the strip to nearly the original flatness (as mentioned earlier).

A correction has to be made for the reason that the stresses in spark erosion are in all directions in the plane, and since the radius of curvature is a measure of strains, the lateral strain has to be taken into account as well. Thus, if m is the reciprocate value of Poisson's ratio, the correct formula is

$1/R' - 1/R'' = M(1-1/m)/EI$

The curvature was determined by measuring the length of the chord S and the bow h (Figure 14). For large radii and small bows, as in our case, the radius of curvature is $S^2/8h$. If the initial curvature $1/R'$ corresponds to a bow h' and the final curvature $1/R''$ corresponds to a bow h", the value $h = h'-h''$ enables the calculation of the change in curvature.

The value h was obtained by measuring the bows before and after removing the stressed layer and the average residual stress f was calculated.

Taking m = 10/3 and using h in the previous formula, the residual stress f is given by:

$$f = 1.9Ea^2h/dS^2 \qquad \text{Equation (7)}$$

Measurements were carried out on strips of annealed mild steel 0.024 in. thick, on hard rolled brass 0.024 in. thick, on hardened and tempered spring steel 0.020 in. thick and on hardened high speed steel strips of 0.020 and 0.040 in. thickness. The width of the strips was 0.5 in.

The mild steel strips were annealed by heating to over 700° C. for approximately four hours in an argon atmosphere. They were spark eroded with 1.5 μF and approximately 80 V breakdown voltage in paraffin which resulted in a surface finish of approximately 120 μ in. CLA.

As mentioned before, the eroded surface was etched with 25% solution of nitric acid. It was found that the stresses were confined to a layer 0.0008 - 0.001 in. thick and the average value was 30 tons/in.^{2}. For comparison, a similar strip was eroded in distilled water, which resulted in 80 microin. CLA surface finish. The residual stresses in this case were found to be much lower, approximately 17 tons/in.^{2} and the stressed layer approximately 0.0005 in. thick.

Hard rolled brass strips were spark eroded at 1.5 microfarads and the residual stresses were measured by similar procedure. The same solution of nitric acid was used. The affected layer was found to be approximately 0.0015 in. thick and the residual stress 26 T/in.^{2}.

The residual stress in spring steel was found to be approximately 33 tons/in.^{2} in a layer of 0.001 in., eroded in paraffin at 1.5 microfarad. Under similar eroding conditions the stresses in high speed steel were found to be confined to a layer approximately 0.0007 in. thick and were approximately 65 tons/in.^{2}.

In order to find the growth of the affected layer with increased capacity, i.e. in the case of roughing, the 0.04 in. thick high speed steel strip was eroded at 300 microfarads. The very rough surface made measurements very difficult, but it was found that after removing 2 to 4 x 10^{-3} in., the strip straightened out again. The stressed layer could thus be assumed to be within these limits. The high speed steel was not etched, since nitric acid hardly attacks it, but ground away on a surface grinder, using manual feed with great care. Prior to this, experiments were carried out to establish the conditions for grinding which would not introduce appreciable stresses. It was found that if the depth of cut is 0.0005 in. or less, the traversing speed very low (manually done, approximately 1in./sec.) and the wheel sharp, the so induced tensile stress in H.S. Steel in the longitudinal direction is very small and can be neutralized by slightly polishing manually with polishing paper. In this context measurements were also made of stresses produced by surface grinding and by polishing with fine emery. It was found that if annealed mild steel was lapped by fine emery paper (No. 2/0) with a pressure of 2 - 3 lb./in.^{2}, a compressive residual stress equal to the yield point developed in a layer 2/10,000 in. thick. In grinding annealed mild steel with a sharp

wheel, 0.0005 in. deep cuts and travers speed of 3 in./sec. tensile residual stresses were set up in the longitudinal direction (i.e. in the direction of the grinding) and compressive stresses in the direction perpendicular to it. In both cases the stresses were over the yield point and confined to approximately 0.0005 in. This shows that even in a quickly strain-hardening material such as mild steel, careful grinding produces only thin affected layers.

The values obtained for the magnitude of the residual stresses and for the depth of the affected layers are approximate only, since the relatively coarse finish and the non-uniformity of etching did not enable more accurate measurements.

No attempt was therefore made to find stress gradients, but even the values obtained indicate that the residual stresses are above the initial yield point of mild steel and are of considerable magnitude in all the investigated cases.

(b) The causes of the residual stresses

It is assumed that the residual stresses induced by spark erosion are caused by the thermal effect of the spark. The localized heating of a small volume of the metal causes its thermal expansion which cannot be taken up by elastic deformation. Thus plastic deformation occurs while the metal is still hot, and on cooling the thermal contraction causes residual tension. The occurrence of plastic deformation of metal crystals after erosion by sparks has been observed by electron microscopy and by X-ray diffraction (Zolotikh, 7 ; Wilms and Wade, 44). The plastic deformation will occur wherever the

temperature gradient causes shearing strains above the elastic limit, but if the metal is heated above a certain temperature, it becomes incapable of any elastic strain and the thermal expansion changes entirely into plastic deformation. It is assumed, therefore, that the most affected layer will be in the neighbourhood of the isothermal line representing this temperature. (The temperature in question is 600° C. approximately for mild steel and 300 - 350° C. for brass).

Although the isothermal lines have not been accurately plotted (as explained in Chapter I-5) an attempt was made to evaluate the relative displacement of the isothermal lines for different spark energies.

The shallow shape of the craters indicates that the hot spot is not a point but a disc approaching the crater in size. For the purpose of the calculation it was assumed that the energy is delivered to the workpiece over the entire crater area and at the rate of q calories per cm.^{2} per second.

The volume of the crater is proportional to the energy of the spark, and the form of the crater, i.e. the ratio of the diameter to the depth is the same for different craters. Thus the volume of a crater is proportional to the cube of its diameter:

$$v = k' d_c^3$$

On the other hand, the volume is proportional to the energy of the spark which is $CU^2/2$ where C is the capacity and U the breakdown voltage. The energy is also proportional (without losses it would be equal) to the heat flow x duration of the spark. We can thus write:

$$v = k'd_c^3 = mCU^2 = n'qd_c^2p, \quad p \text{ being the duration of the spark.}$$

Since $p = 2\pi(LC)^{\frac{1}{2}}$ (see Chapter IV-1-VI) and L - the inductivity of the circuit is constant, we can write $p = \beta C^{\frac{1}{2}}$. If from the given Equations q is expressed in terms of C we obtain $q = q_o C^{-\frac{1}{3}}$ where q_o is the appropriate constant.

The reduction in the heat flow intensity with the increase in capacity is not improbable as it is quite possible that with longer pulses the conducting channel spreads by ionization and the current density decreases. The values given by the various sources for current density are varying within very wide limits indeed (see Chapter I - 4)

Since the diameter of the crater is at least ten times greater than the thickness of the affected layer, the Equation of the heat conduction in a semi-infinite body with a continuous plane source can be applied for approximate calculation. The temperature in a semi-infinite body with a plane source of the intensity q which acts for the time p is given by Carslaw-Jaeger (29)

$$Temp. = \frac{q}{2}\left(\frac{p}{\pi K}\right)^{1/2} e^{-z^2/4Kp} - \frac{qz}{4K}\, erfc\left(\frac{z}{2\sqrt{Kp}}\right)$$

K being the thermal diffusivity and z the distance from the heated plane.

Using this Equation and substituting actual values for K , p and z as well as taking into account the change of q with the capacity C it was found that the temperature which occurred at the depth of 10^{-3} in. when the spark was produced by 0.5 microfarad would be expected at approximately 10^{-2} in. when the spark would be produced by 500 microfarads.

Thus increasing the capacity by 10^3 times would increase the thickness of the layer contained between the bottom of the crater and the given temperature line by approximately 10 times. This compares well with the actual measurement of the thickness of the stressed layer produced by 300 microfarad spark on the 0.04 in. high speed steel strip:

From a thickness of 0.0007 in. at 1.5 microfarad the layer increased to 0.002 - 0.004 in. at 300 microfarads. Taking the theoretical relationship as a straight line on log-log basis, meaning that thickness increases with the cubic root of the capacity, we obtain theoretically a thickness of 1.9×10^{-3} for 300 microfarads. The actual result is quite near to this value, especially when it is taken into account that the thickness was measured from the top of the craters and not from the bottom.

A similar relationship was obtained between the surface finish (CLA value) and the capacity (see Chapter IV-2-I); it can be concluded that the "subsurface" grows at the same rate as the geometrical shape. From the actual values it could be concluded that the stressed layer is several - up to ten - times greater than the CLA value.

(c) Carburization of the eroded surface

The difference between the residual stresses in mild steel sparked in water and the same sparked in paraffin is quite interesting. It has been observed that mild steel sparked in paraffin acquires a hard layer which resists filing. This layer, however, is very thin and its hardness could not be measured by microhardness methods;

neither could it be easily distinguished in metallographic investigation.

It was assumed that this layer was formed by carburization of the steel in the cracked paraffin and thus constituted a high carbon steel capable of very high residual stresses. On the other hand, carburization and hardening would increase the volume which would tend to reduce the tensile stress. This is an interesting question worthy of future investigation, perhaps in context with research into the resistance to abrasion of spark eroded steels, which is sometimes claimed to be very high (Nosov and Bykov 4).

(d) The effect of the residual stresses

The implications of the residual stresses in spark eroded metals are not clear. Their detrimental influence on fatigue was suspected and investigated in the case of mild steel (Chapter IV-3-I). The majority of the present applications, however, is for production of workpieces not subjected to fatigue. Dies are subject to impacts, perhaps quickly repeated impacts, pressure, abrasion; so are cutting tools. It is not at all clear where the residual stresses enter here; their effect could even be beneficial, e.g. by pre-stressing in the case of compressive loads. Until extensive research is carried out into the effects of these residual stresses, it will not be possible to decide, except in very few cases such as fatigue, whether they should be avoided or intentionally produced. The answer to this question may be of importance when a certain type of equipment has to be selected for a particular purpose. The various methods of spark

generation vary mainly in the intensity of the energy flow, i.e. in the gradient of the temperature, which means the depth of the stressed layer. This can be proved easily by changing the time p in the Equation of heat conduction, while leaving other variables constant and maintaining a constant qp. A short but intensive spark will produce a thinner stressed layer for the same crater size, but whether this is really desirable can only be decided in the future.

III. Fatigue Investigations

(a) Detailed results

The creation of residual tensile stresses as a result of spark erosion brought about not unnaturally the question as to what effect spark erosion has on the endurance of the workpiece. In view of the prevailing use of spark erosion the question was rather academic; the only material which could possibly be machined by this method and later subjected to fatigue loading in usage in the true sense was Nimonic, the material of gas turbine blades. In view of the great difficulties in obtaining sufficient quantities and machining of this type of metals, it was decided to carry out a series of tests in mild steel only. It was assumed that if a significant effect would be discovered in testing mild steel, which is rather insensitive to the influence of residual tensile stresses on fatigue (e.g. Roŝ and Eichinger, 45), this would be sufficient to point out the importance of these residual stresses for cases in which fatigue is really critical.

The material chosen was mild steel with 0.15% carbon content, normalized. All specimens were of one cast which was specially ordered for this purpose. Tests were carried out in Wöhler type cantilever machines which were capable of carrying a load of up to 100 lb. The specimen is shown in Figure 23.

Simple cantilever loading was decided upon, as it was calculated that the shearing stresses would be only 2½% of the maximum bending stress. The principal stress was thus practically identical with the bending stress. The tapered shape of the cantilever facilitates the localization of the fracture in the central portion of the length, and the bending stress varies only slightly in the neighbourhood of the critical section, as shown in Appendix III and in Figure 38.

The specimens were machined as accurately as was possible, the variations in the smallest diameter were ± 0.001 in. and were mainly due to the difficulty of measuring it with a micrometer. As shown in Appendix III, the ensuing error in calculating the stresses in unbroken specimens was approximately 2%. The stresses in the broken specimens were calculated from actual dimensions of the broken section and its distance from the point of load application. In view of the difficulty of measuring these, e.g. when the specimen showed several initiations of fatigue fracture which were not in the same plane, the accuracy of these measurements could not be considered better than 2% either.

Three series of specimens were tested: One series of turned, one series of spark eroded and one series of spark eroded and stress relieved specimens.

As mentioned before, (Chapter III-2-III) the turned specimens fractured still at 33,750 lb./in.^{2}, and the endurance limit was found to be between this value and 32,600 lb./in.^{2}, say approximately 33,000 lb./in.^{2}. The curve shows a bend at 6-9 x 10^6 cycles.

The endurance of the spark eroded specimens was found to be 27,250 lb./in.^{2} and that of the spark eroded and stress relieved specimens was at 30,750 lb./in.^{2}. The two latter curves show a bend at 3-4 x 10^6 cycles.

Observation of the fracture of the sparked specimens, both heat treated and untreated revealed that at higher loads the fatigue fracture started at several points simultaneously, all located around the periphery of the cross-section, while at the loads still causing fracture, the fatigue failure originated in one point only.

(b) Probable causes of the lowered endurance limit

The results of the fatigue tests show beyond doubt that spark erosion lowers the endurance limit of soft mild steel by at least 15%. If the unsparked specimens were polished, their endurance limit would undoubtedly be higher than 33,000 lb./in.^{2}. It was, however, thought that a better picture would be obtained if the surface finish of both groups would be comparable. A range from 75 microin. CLA to 180 microin. CLA is negligible as far as its effect on fatigue of mild steel is concerned. Both values are almost belonging to one surface finish class, and both can be termed "medium turning". From the sparse data available in the literature (Moore and Kommers 46, Matalin 47) it is evident that the difference between the two finishes

is much less than between "rough turning and finish turning" and even in the latter case the difference in fatigue is only 3%, according to Moore and Kommers (46).

Since it was not possible to reproduce the pattern left by spark erosion by any mechanical method, the finishes were assumed as comparable in their effect on the endurance limit. At any rate, a possible difference would be within the order of the accuracy of evaluating the results.*)

It can thus be said that the effect of spark erosion on the endurance of mild steel is as detrimental as that of artificially induced tensile stresses quoted by Rôs and Eichinger (45).

This occurs despite the fact that eroding in paraffin causes some carburization in the surface which should improve the endurance limit. Apparently the thickness of the carburized layer is far too small to outweigh the detrimental effect of the tensile stress locked up in the surface.

Two recent sources (which became available after the present work had been concluded) mention the effect of spark erosion on fatigue. According to Matalin (47) spark erosion will reduce the endurance of heat treated alloy steels to less than half of the normal value. A catastrophic effect of spark erosion on fatigue - down to 5% of the original value, was very recently reported by Lines (43). Few details were given as to the material, but apparently it was a gas

*) Slight polishing would reduce the CLA value of the sparked specimens to less than half the original value; since only peaks would be removed, the effect of craters as stress raisers would be unchanged.

turbine blade steel. Lines attributes the detrimental effect to the presence of nitrogen in the paraffin used and to the formation of nitrides. Change over to distilled water was said to have improved the fatigue properties, but vapour blasting was subsequently applied to restore the values to a satisfactory level. Lines did not give any further details, in particular on the lowering of the endurance after eroding in water but before vapour blasting. Also the electrical conditions were very vaguely stated and from the photographs shown it would appear that there was considerable arcing in the condemned case.

From the present work it appears that the beneficial influence of water could be also attributed to the gentler action, caused by partial conduction which diminished the spark energy, and not only to the absence of nitrides. It was found in the present investigation that under identical electric conditions the surface finish was better and residual stresses lower when water was used instead of paraffin. There appears to be little doubt that the tensile residual stress produced by spark erosion contributes to lowering the endurance limit.

This assumption is at least partly supported by the improvement shown by the series of specimens heat treated after spark erosion. Whatever the metallurgical changes produced by heat treatment, there is no doubt that stresses were relieved. On the other hand, the recovery was not complete, which indicated some permanent damage. However, rather than to attribute this to the formation of some special phases such as nitrides, it would appear simpler to assume that the severe

tensile stresses, exceeding in all cases the initial yield point, caused some microcracks which could not close again and thus facilitated the fatigue failure. It is agreed, however, that nitrides may be detrimental especially in highly alloyed steels, although a continuous nitrided layer is, similarly to a carburized layer, one of the means of improving fatigue properties. The detrimental effect could be attributed to the interruptions in the layer and the nitride inclusions causing stress concentrations.

It can be therefore concluded that spark erosion in its usual form brings about a reduction of the endurance limit of mild steel of the order of 15%. In view of the relative insensitivity of annealed mild steel to the effect of residual tensile stresses on fatigue, this reduction should be considered as serious and in all cases in which spark machined components are to be subjected to cyclic loading, great care has to be exercised and suitable investigations carried out, in order to gain information on the degree of deterioration of the fatigue properties for various materials. The lowering of the endurance limit can be attributed mainly to the residual tensile stresses which, according to the latest view on the fatigue phenomena, help to open microcracks. It is also conceivable that deeper cracks exist, which will not close even after stress relief. This appears to be indicated in the present work, and it is suggested that an investigation into the problem of permanent damage would be most valuable.

IV. Other Mechanical Properties

Many workers claim that tools sharpened or produced by spark erosion show high wear resistance and longer life. There is, as yet, no explanation for this. It was found that spark eroded high carbon steels possess a very hard surface layer (e.g. Rudorff, 2) which could improve the wear properties. Improved life is, however, also claimed for press tools (Nosov and Bykov, 4) which are subjected to impact and impact-fatigue loads. If the hardened layer is beneficial, it might appear worthwhile to operate under slight arcing conditions, in which case such a layer is easily formed. The question of the best spark type would also have to be considered, i.e. whether a long or a short spark is preferable, in view of the different temperature effects of each. A long spark may appear more suitable, though it will produce a thicker stressed layer.

It is thus shown that the few phenomena observed in the present investigation call for a very detailed continuation of research in order to obtain a better knowledge and eventually a mastery of the new and most promising branch of engineering called electro-spark technology.

C O N C L U S I O N S

The results of the present work can be summed up as follows:-

1. In cases when the erosion has to be caused by sparks only and the formation of arcs has to be prevented, the minimum permissible ballast resistance in a relaxation circuit is a definite function of the capacity used. The knowledge of the relationship between these two parameters makes it possible to calculate and to design a relaxation circuit and to estimate the power requirements, once the voltage and the maximum capacity are chosen. The cathode ray oscilloscope is a convenient means for indicating the limit of non-arcing operation.

2. Conditions were established for the successful application of a relaxation circuit for spark turning and the reasons for unsuitable voltage causing out-of-roundness of the workpiece were found.

3. The typical forms of spark voltage and currents were found. Both in the case of single sparks and in the case of continuous sparking the reverse half-wave may be either present or absent. Its presence must be due to the swarf in the process, because the dielectric used (paraffin) was shown to be capable of very fast deionization. Values of inductance and current amplitudes were both calculated and measured, and the results were found to be in reasonable agreement. Skin effect, parasitic oscillations and other secondary phenomena were noted.

4. The theoretically predictable relationship between the centre line average value of a spark eroded surface and the energy of a single spark is very close to the actual one if the voltage is kept constant. When different voltages are applied the surface finish relationship indicates that the energy losses are growing with increasing gap length. The surface finish can be measured by means of the usual methods and with existing equipment, and the consistency of the results is comparable to that obtained on surfaces produced by machining.

5. Residual stresses arise as a result of spark erosion. They are tensile and of a high magnitude. The depth of the affected layer is small and is approximately proportional to the surface finish value. There are good reasons to attribute the creation of the residual stresses to the thermal effect of the spark.

6. Spark erosion reduces the endurance limit of mild steel. The effect of the residual stresses on this phenomenon could be demonstrated by considerable improvement in the endurance limit of specimens which were stress relieved after being spark eroded. There was, however, also indication of some permanent damage attributable to microcracks.

TABLE I

SURFACE FINISH MEASUREMENTS (MILD STEEL)

SURFACE FINISH MEASUREMENTS (MILD STEEL)

I. Average voltage 18 volts; E = 28 V.
(U = 27 V. appr.)

Capacity Microfarads	CLA Microinches (Average)	CLA Variation
5.5	130	120 - 140
10.5	155	135 - 175
20.5	178	160 - 190
50.5	210	180 - 220
100.5	320	290 - 360
200.5	348	310 - 420

II. Average voltage 45 volts; E = 130 V.
(U = 85 V. appr.)

Capacity Microfarads	CLA Microinches (Average)	CLA Variation
0.5	66	62 - 70
1.5	92	82 - 102
2.5	124	110 - 140
5.5	155	150 - 170
12.5	220	180 - 260
30.5	277	235 - 320
40.5	340	280 - 400

III. Average Voltage 125 V (E = 130 V)
(U = 130 V appr.)

Capacity Microfarads	CLA Microinches (Average)	CLA Variation
0.5	90	85 - 100
2.5	180	150 - 200
10.5	260	210 - 310
30.5	360	280 - 410

All measurements carried out on the Talysurf, from meter readings.

Values of CLA for surfaces too rough to be measured directly by the meter, which were obtained by planimetration of pen records produced with the help of the specially built "reduction unit":

U = 80 V. C = 120 F CLA = 460 microinches.

C = 250 F CLA = 600 microinches.

TABLE II

SURFACE FINISH MEASUREMENTS OF HARDENED TOOL STEEL

Capacity Microfarads	CLA value Microinches
0.5	85
2.5	130
5.5	200
12.5	240
30	320
100	470

Breakdown voltage U = 85 volts appr.

All values are averages. Fluctuations up to 20%.

TABLE III

SPARK CURRENT AMPLITUDES

U = 90 V appr.

Capacity Microfarads	First Half-Wave Amperes	Second Half-Wave Amperes
10.5	125	65
20.5	150	70
50	208	70
100	293	75
200	390	75
500	680	80

APPENDIX I

CALCULATING THE BREAKDOWN VOLTAGE FROM VOLTMETER READING

Evaluation of the surface finish required the knowledge of the breakdown voltage U; the only available value, however, was the average voltage U_v given by the voltmeter. As shown on page 29, the breakdown voltage U at the time θ is given by

$U = \mathcal{E}(1 - e^{-\theta/RC})$, $\mathcal{E}$ being the voltage of the source.

The average voltage is given, from page 32, by

$$U_v = \mathcal{E}(1 - RC/\theta + \frac{RC}{\theta}e^{-\theta/RC})$$

The curves $U/\mathcal{E}$ and $\mathcal{E}/U_v$ were drawn as functions of θ/RC and then a curve of U/U_v was derived from them. Thus, by measuring the average voltage U_v and knowing the voltage of the source $\mathcal{E}$, the corresponding value of θ/RC could be found, which in turn made it possible to find (from the curves) the required breakdown voltage U. All three curves are drawn in Figure 39.

APPENDIX II

CALCULATION OF THE MAXIMUM CURRENT I_m OF THE SPARK

This calculation is based on the following assumptions:

(a) Nearly all the energy (at least 8/9) stored in the condenser is dissipated during the first half of the spark discharge.

(b) The current form of the first half-wave is sinusoidal.

(c) The voltage form during the first half of the spark is a straight line beginning with the voltage U_1 and ending with U_2.

If the voltage of the spark at time t is U_s and the duration of the spark is p, we have

$$U_s = U_2 + \frac{U_1 - U_2}{p/2} t \qquad \text{and if } p/2 = s$$

$$U_s = U_2 + \frac{U_1 - U_2}{s} t$$

The current I_s is a sine wave given by

$$I_s = I_m \sin \frac{t}{s} \pi$$

Expanding in series, we have

$$\sin \frac{t}{s}\pi = t\frac{\pi}{s} - \frac{t^3}{3!}\left(\frac{\pi}{s}\right)^3 + \frac{t^5}{5!}\left(\frac{\pi}{s}\right)^5 - \frac{t^7}{7!}\left(\frac{\pi}{s}\right)^7 + \cdots$$

Now, the power of the spark N_s is given by $N_s = U_s I_s$, so

$$N_s = \left(U_2 + \frac{U_1 - U_2}{s} t\right) I_m \left[t\frac{\pi}{s} - \frac{t^3}{3!}\left(\frac{\pi}{s}\right)^3 + \frac{t^5}{5!}\left(\frac{\pi}{s}\right)^5 - \frac{t^7}{7!}\left(\frac{\pi}{s}\right)^7 + \cdots\right]$$

Putting $\pi/s = a$ $\qquad \frac{U_1 - U_2}{s} = b$ we obtain

$$N_s = I_m U_2 \left(ta - \frac{t^3 a^3}{3!} + \frac{t^5 a^5}{5!} - \frac{t^7 a^7}{7!} + \cdots\right) +$$

$$+ I_m b \left(t^2 a - \frac{t^4 a^3}{3!} + \frac{t^6 a^5}{5!} - \frac{t^8 a^7}{7!} + \cdots\right)$$

The energy is given by $A = \int_0^s N_s \, dt$

$$A = I_m \int_0^s \left[U_2 \left(ta - \frac{t^3 a^3}{3!} + \frac{t^5 a^5}{5!} - \frac{t^7 a^7}{7!} + \cdots\right) + \right.$$

$$\left. + b\left(t^2 a - \frac{t^4 a^3}{3!} + \frac{t^6 a^5}{5!} - \frac{t^8 a^7}{7!} + \cdots\right)\right] dt =$$

$$= I_m \left[U_2 \left(\frac{s^2 a}{2} - \frac{s^4 a^3}{3!} + \frac{s^6 a^5}{6 \times 5!} - \frac{s^8 a^7}{8 \times 7!}\right) + \right.$$

$$\left. + b\left(\frac{s^3 a}{3!} - \frac{s^5 a^3}{5 \times 3!} + \frac{s^7 a^5}{7 \times 5!} - \frac{s^9 a^7}{9 \times 7!} + \cdots\right)\right] =$$

$$= I_m s \left[U_2 \left(\frac{\pi}{2} - \frac{\pi^3}{4 \times 3!} + \frac{\pi^5}{6 \times 5!} - \frac{\pi^7}{8 \times 7!} + \cdots \right) + \right.$$

$$\left. + (U_1 - U_2) \left(\frac{\pi}{3} - \frac{\pi^3}{5 \times 3!} + \frac{\pi^5}{7 \times 5!} - \frac{\pi^7}{9 \times 7!} + \cdots \right) \right] =$$

$$= I_m s \left[U_2 \left(1.57 - 1.29 + 0.424 - 0.074 + \cdots \right) + \right.$$

$$\left. + (U_1 - U_2) \left(1.05 - 1.03 + 0.363 - 0.066 + \cdots \right) \right] =$$

$$= I_m s \left[0.63\, U_2 + 0.317 (U_1 - U_2) \right]$$

Since $s = p/2 = \pi \sqrt{LC} = \pi \sqrt{L}\sqrt{C}$

we obtain

$$A = I_m \pi \sqrt{L}\sqrt{C} \left[0.63\, U_2 + 0.317 (U_1 - U_2) \right]$$

Assuming that $A = \lambda \frac{C U^2}{2}$, where $\frac{C U^2}{2}$ is the energy stored in the condenser, the maximum current is given by

$$I_m = \frac{\lambda C U^2}{2\pi\sqrt{L}\sqrt{C}\,[0.63\,U_2 + 0.317(U_1 - U_2)]} \quad \text{or}$$

$$I_m = \frac{\lambda U^2}{2\pi\sqrt{L}\,[0.63\,U_2 + 0.317(U_1 - U_2)]}\sqrt{C}$$

λ = ratio of the energy spent in the gap to the energy stored in the condenser.

Taking $\lambda = 0.5$ (Zolotikh, 7), and substituting

$U_1 = 35$ V $\quad U_2 = 10$ V

$U = 90$ V $\quad L = 3.1\ \mu H$

we obtain

$$I_m = 26\sqrt{C}$$

APPENDIX III

STRESSES IN THE FATIGUE SPECIMEN

The fatigue specimen, shown in Figure 23 is a tapered cantilever of diameter d_2 at the large end. The load P is applied at the small end. The diameter of the taper, if continued to the point of load application, is d_1. The length of the taper (i.e. the cantilever) from the diameter d_1 to the large end (diameter d_2) is L.

The bending stress at any point is

$$\sigma = \frac{P x}{\pi d^3/64}$$

d being the diameter at the distance x from the point of load application. The diameter d is a function of x, namely

$$d = d_1 + \frac{d_2 - d_1}{L} x$$

The bending stress is thus

$$\sigma = 64 P \frac{x}{\pi \left(d_1 + \frac{d_2 - d_1}{L} x\right)^3}$$

The dimensions of the specimen are $d_1 = 0.224$ in. and $(d_2 - d_1)/L = 0.06$.

Substituting these values, the function $\sigma(x)$ was calculated and plotted in Figure 38. It can be seen that the stress varies slowly in the vicinity of its maximum.

The maximum stress occurs at the point in which $\frac{d\sigma}{dx} = 0$

By differentiating the expression for stress and equating to zero, the distance of the point with the maximum stress, X_m is:

$$X_m = \frac{L d_1}{2(d_2 - d_1)}$$

In the specimen used in the present case this distance is 1.866 in. The magnitude of the maximum stress is thus given by:

$$\sigma_m = \frac{256}{27} \frac{PL}{\pi d_1^2 (d_2 - d_1)}$$

Substituting the values of d_1 and $(d_2 - d_1)/L$, we obtain

$$\sigma_m = 1002\, P \approx 1000\, P$$

The accuracy of this calculation as function of the diameter d_1 is given by:

$$\left| \frac{\Delta \sigma}{\sigma} \right| = \frac{2 \Delta d_1}{d_1}$$

Assuming an error of measurement of up to 0.002 in. on the diameter d_1 (actually on a diameter at the neck of the specimen, which is proportional to d_1), the accuracy of stress calculation in an unbroken specimen is 2×2/224 or approximately 2%.

BIBLIOGRAPHY

1. J. Priestley: History and Present State of Electricity. 2nd Edit. London, 1769, p. 623.

2. D. W. Rudorff: Principles and Applications of Spark Machining Proc.I.Mech.E., 1957, vol. 171, No.14.

3. B. R. Lazarenko & N. I. Lazarenko: Electrospark Machining of Conductive Materials, Acad.Sc.USSR, 1958.

4. A. V. Nosov & D. V. Bykov: Working Metals by Electrosparking, H.M.Stat. Office, London, 1956.

5. N. Mironoff & J. Pfau: Machine Moderne, Jan. 1955, p. 33 - 37.

6. J. Koncz: Engin. Digest, vol. 11, 1950, p. 108 - 111; 165 - 168.

7. B. N. Zolotikh: The Physical Principles of Electrospark Machining of Metals, Verlag Technik, Berlin, 1955.

8. M. Bruma: Revue Universelle des Minues, 1955, 9 Serie, vol. 11, No.11.

9. F. Llewellyn-Jones: Ionization and Breakdown in Gases, Methuen, London, 1957.

10. L. B. Loeb: Fundamental Processes of Electrical Discharges in Gases, Wiley, New York, 1939.

11. J. M. Meek & J. D. Craggs: Electrical Breakdown of Gases, Clarendon Press, Oxford, 1953.

12. D. W. Goodwin & K. A. MacFadyen: Proc.Phys.Soc., vol. B66, 1953, p. 85.

13. J. B. Higham & J. M. Meek: Proc.Phys.Soc., vol. B63, 1950, p. 633 & 649.

14. T. J. Lewis: Proc.Phys.Soc., vol. B66, 1953, p. 425.

15. I. S. Stekolnikov: Acad.Sc.USSR, Tech. Bull. 7, 1950, p. 985.

16. H. Opitz: Revue Universelle des Mines, 1955, 9 Serie, vol. 11, No. 11.

17. R. W. Crowe: Journ.Appl.Phys., 1956, vol. 27, No. 2, pp. 156 - 160.

18. J. M. Sommerville & C. T. Grainger: Brit. Journ.Appl.Phys., vol. 7, Nov. 1956, pp. 400 - 405.

19. K. D. Froome: Proc.Phys.Soc., vol. 60, 1948, p. 424.

20. J. D. Cobine & C. J. Gallagher: Phys.Rev., 1948, vol. 74, p. 1,524.

21. R. D. Craig & J. D. Craggs: Proc.Phys.Soc., 1953, vol. B66, p. 500.

22. E. M. Williams: Electr. Engin., March, 1952, vol. 71, No. 3, pp. 252 - 260.

23. S. L. Mandelshtam & S. M. Raiski: Acad.Sc.USSR, Phys.Bull., 1949, vol. 13, No. 5, p. 549.

24. J. R. Haynes: Phys.Rev., 1948, vol. 73, p. 891.

25. W. Finkelnburg: Phys.Rev., 1948, vol. 74, p. 1,475.

26. H. Obrig: Industrie-Anzeiger, 13, June, 1958, vol. 80, No. 47, p. 685.

27. F. Llewellyn-Jones: Brit.Journ.Appl.Phys., 1950, vol. 1, p. 60.

28. Debenham & Haydon: Aero.Res.Com.R and M., No. 1,744, 1936.

29. H. S. Carslaw & J. C. Jaeger: Conduction of Heat in Solids, Clarendon Press, Oxford, 1947.

30. B. N. Zolotikh: Electrospark Machining of Metals, Issue 1, Acad.Sc.USSR, 1957, p. 55.

31. B. G. Gutkin & A. L. Vishnitski: Control Gear for Electrosparking and Anodic Machine Tools, Verlag Technik, Berlin, 1954.

32. D. G. Richards: Residual Stress Measurement, Am.Soc.Metals, Cleveland, 1952, p. 194.

33. A. L. Livshits: Electro-erosive Machining of Metals, Mashgiz, Moscow, 1957.

34. B. N. Zolotikh et al: Electrospark Machining of Metals, Issue 1, Acad.Sc.USSR, 1957, pp. 133 - 158.

35. E. M. Williams & J. A. Woodford: Trans.I.R.E., Industr. Electron., March, 1955, p. 78.

36. A. Martin: Electronique Industrielle, Nov. - Dec., 1955, pp. 171 - 176.

37. B. R. Lazarenko: Elektrichestvo, No. 8, 1955, pp. 63 - 68.

38. L. R. Blake: The Engineer, 18 Feb. 1955, p. 222.

39. D. T. Vasiliev: Stanki i instrument, vol. 18, No. 5, 1947, pp. 1 - 8, (Henry Brutcher Translation No. 2490).

40. A. L. Livshits et al: Stanki i instrument, No. 5, 1958, p. 24.

41. V. E. Dumpe: Symposium on Electric Machining, Mashgiz, Moscow, 1955.

42. A. A. Andronov & C. E. Chaikin: Theory of Oscillations, Princeton University Press, 1949, Ch. V, Par. 5.

43. A. H. Lines: Discussion on the Paper by Rudorff (2).

44. G. R. Wilms & J. F. Wade: Metallurgia, Vol. 54, No. 326, Dec. 1956, pp. 263 - 268.

45. M. Roš & A. Eichinger: Eidgenossische Materialprüfungs und Versuchsanstalt, Report no. 173, Zurich, Sept. 1950.

46. H. F. Moore & J. B. Kommers: The Fatigue of Metals, McGraw-Hill, 1927.

47. A. A. Matalin: Surface Finish and Performance of Machine Parts, Mashgiz, Moscow, 1956.

OPENING PRODUCED BY :

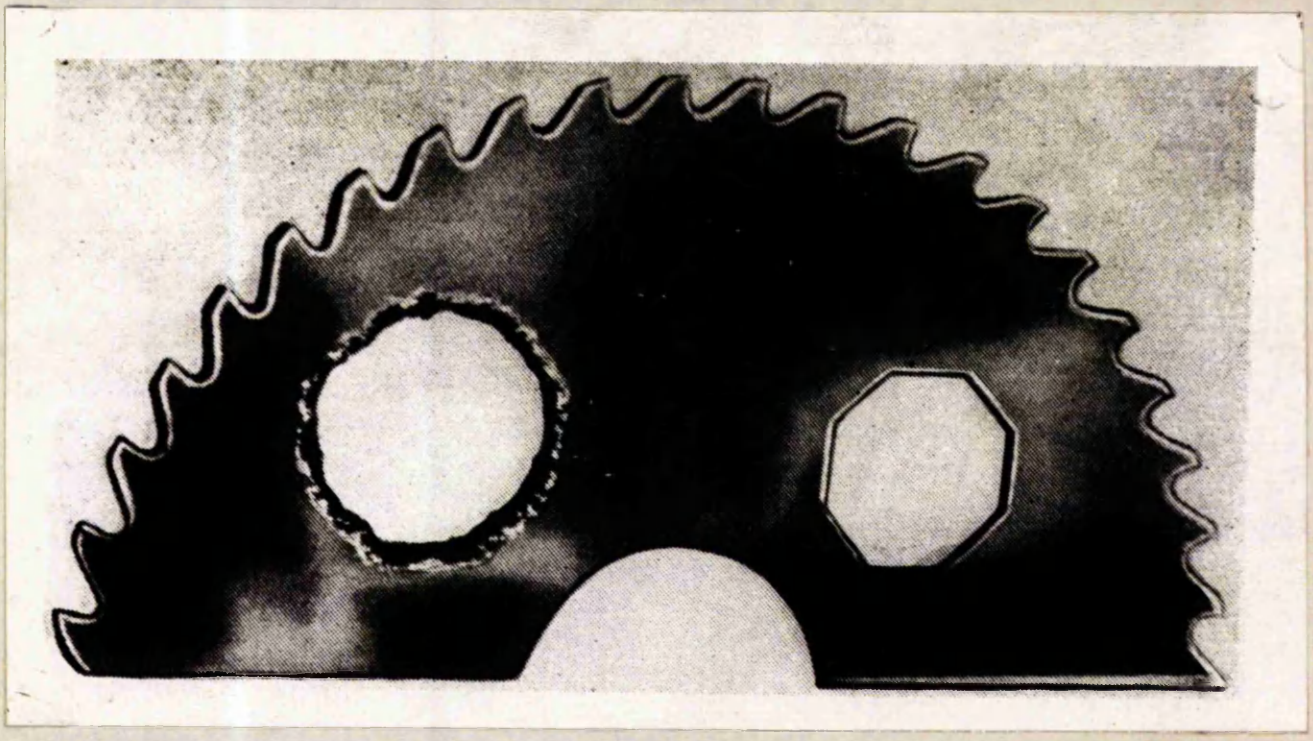

ARCING SPARKING

THE DIFFERENCE IN PERFORMANCE BETWEEN ARCS AND SPARKS

Fig. 1

1.5 μF

a

SPARKING

1.5 μF

b

SPARKING AND
SLIGHT ARCING

100 μF

d

SPARKING

1.5 μF

c

ARCING

SURFACES PRODUCED BY SPARKS AND ARCS (Magnif. 4 x)

Fig. 2

a

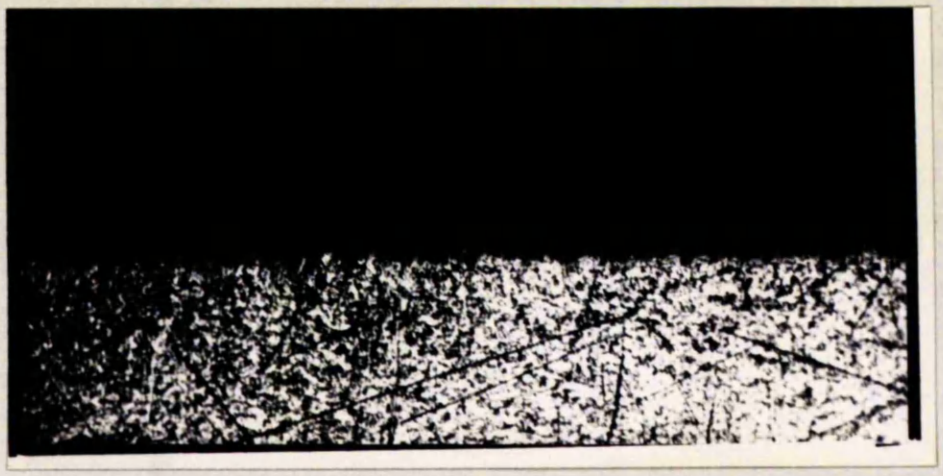

SPARKED 1.5 μF

b

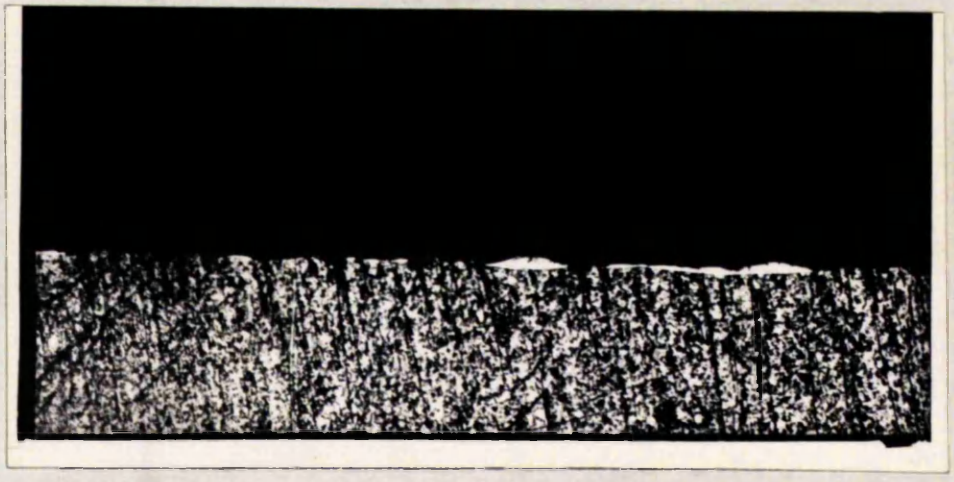

SPARKING AND SLIGHT ARCING 1.5μF

MICROSECTIONS OF SURFACES PRODUCED BY SPARKS AND ARCS

(Magnif. 50 x)

Fig. 3 a&b

c

ARCING 1.5 μF

d

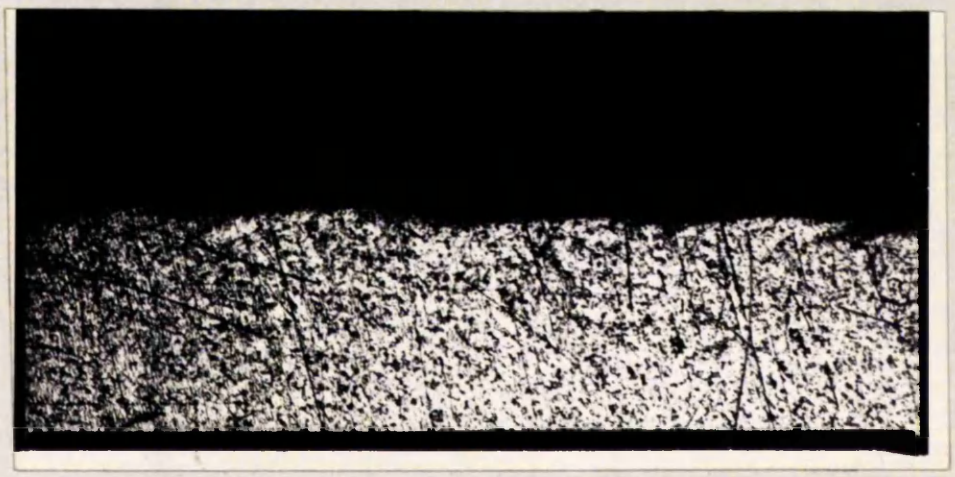

SPARKING 100 μF

Fig. 3 c & d

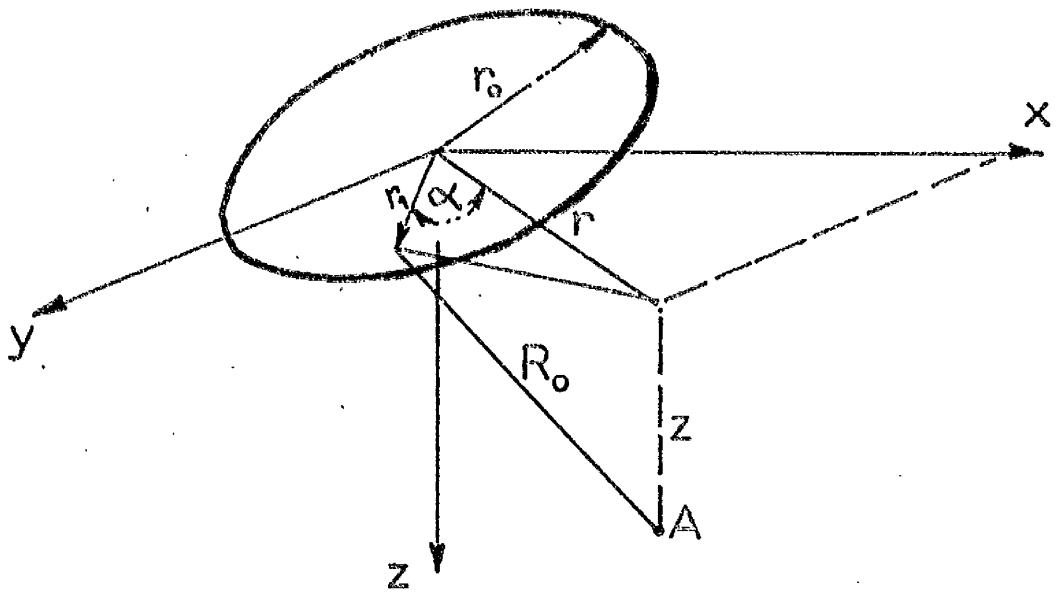

r_o = radius of heat source

$R_o^2 = r^2 + r_1^2 + z^2 - 2 r r_1 \cos\alpha$

A = point with temperature T

TO THE CALCULATION OF THE TEMPERATURE.

Fig. 4

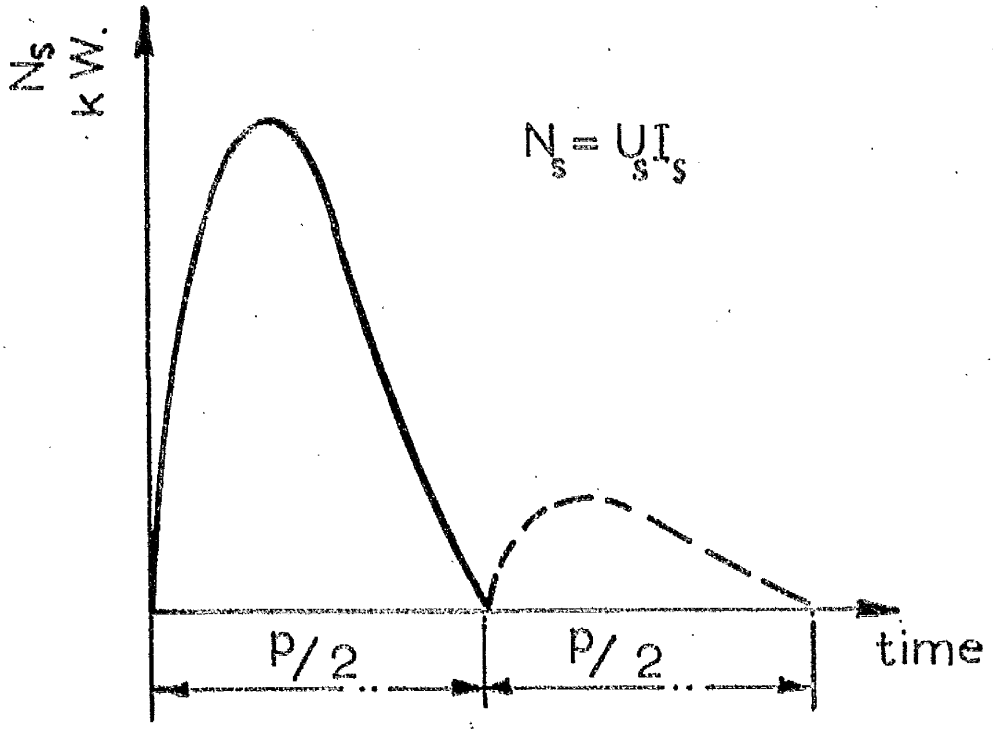

TYPICAL POWER (N_s) CURVE OF A SPARK

Fig. 5

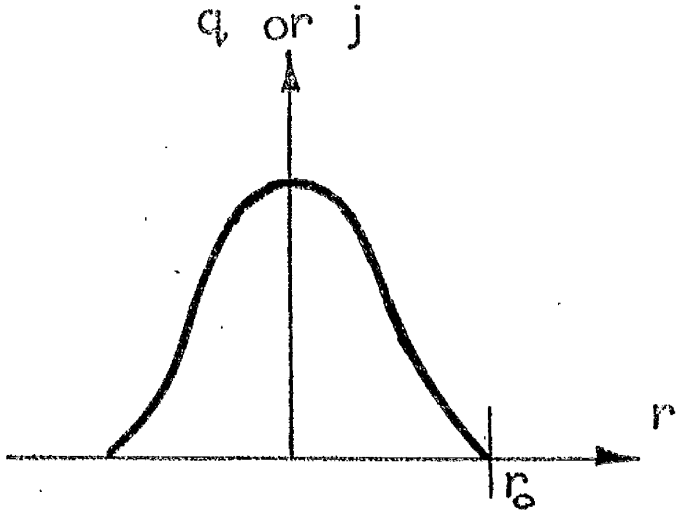

PROBABLE DISTRIBUTION OF HEAT INPUT q OR CURRENT DENSITY j IN THE SPARK.

Fig. 6

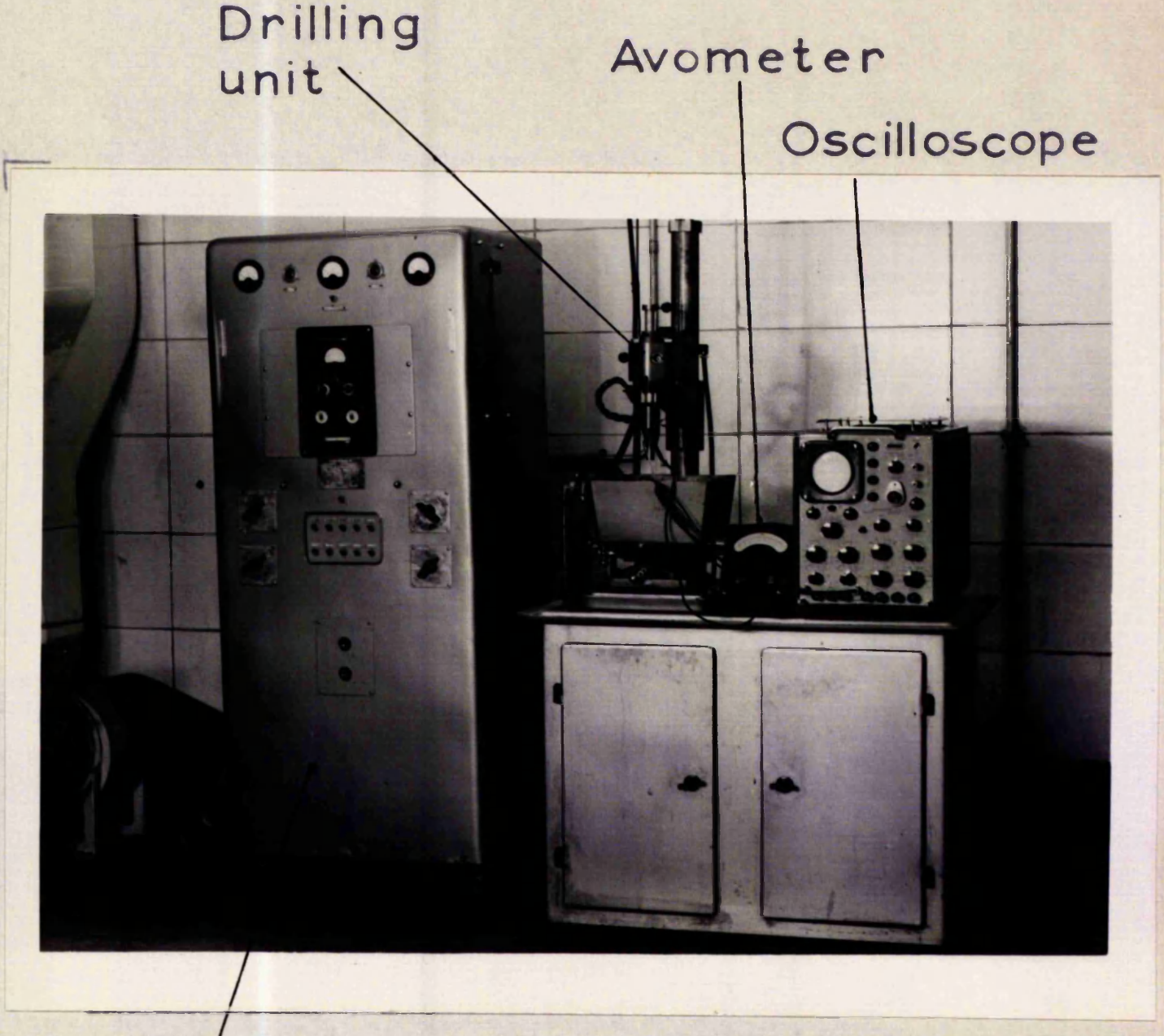

THE EXPERIMENTAL SET-UP ON THE „SPARCATRON-I" MACHINE

Fig. 7a

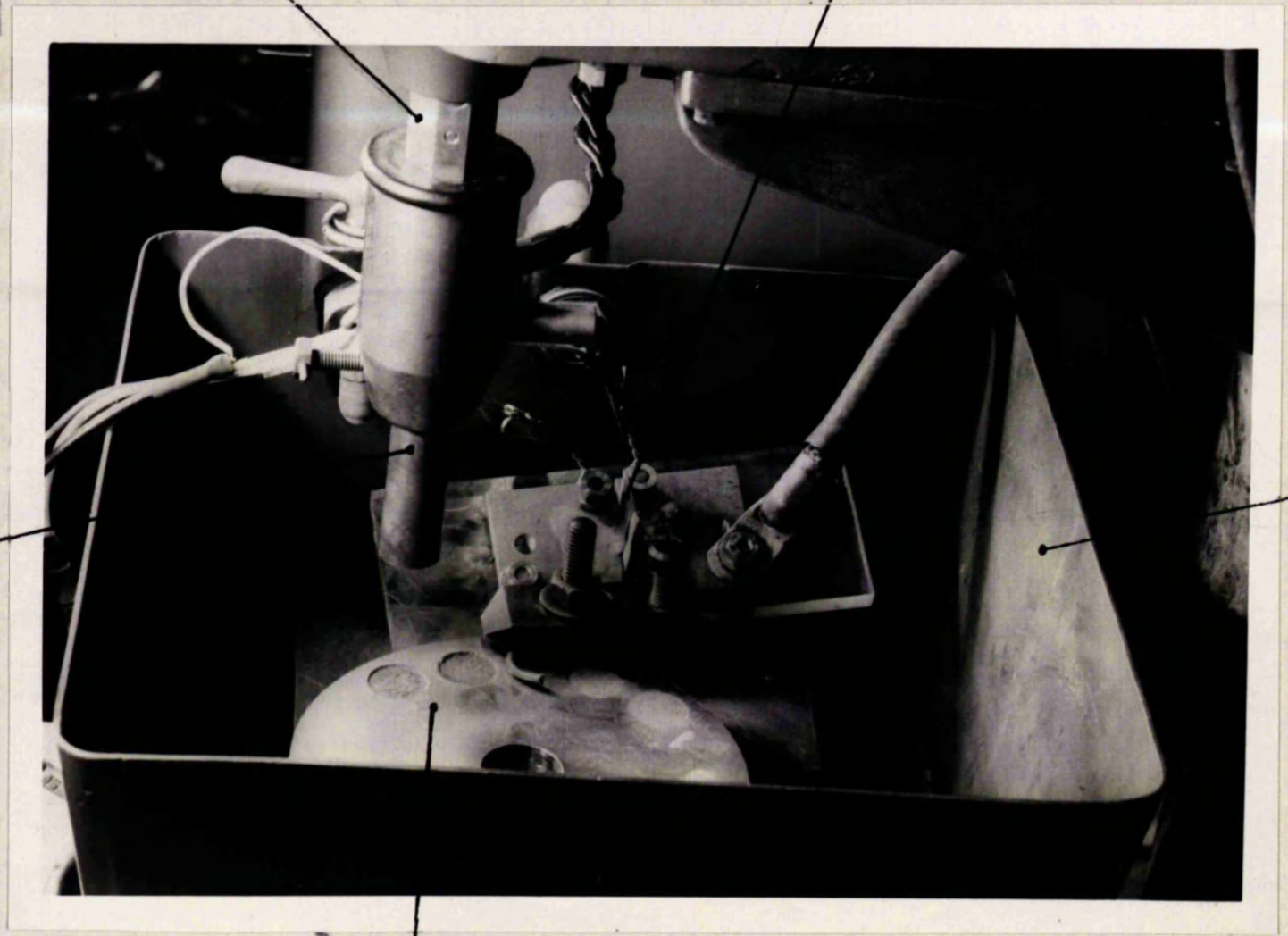

"SPARCATRON" DRILLING UNIT CLOSE-UP

Fig. 7 b

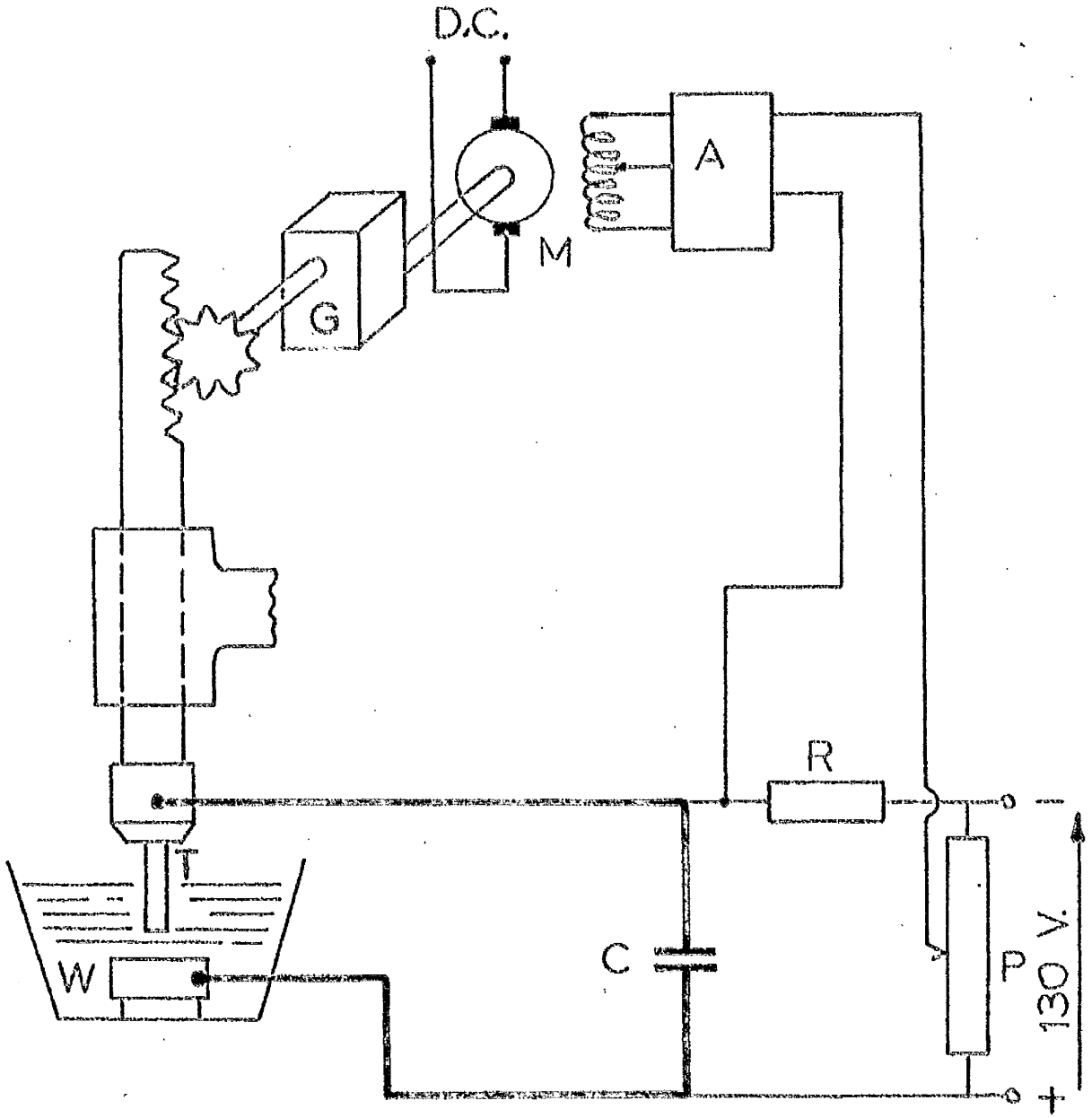

G – Reduction gearbox.
M – Reversible motor.
A – Electronic amplifier.
C – Capacity.
R – Ballast resistance.
P – Potential divider.
T – Tool.
W – Workpiece.

DIAGRAM OF THE SPARCATRON I MACHINE

Fig. 8

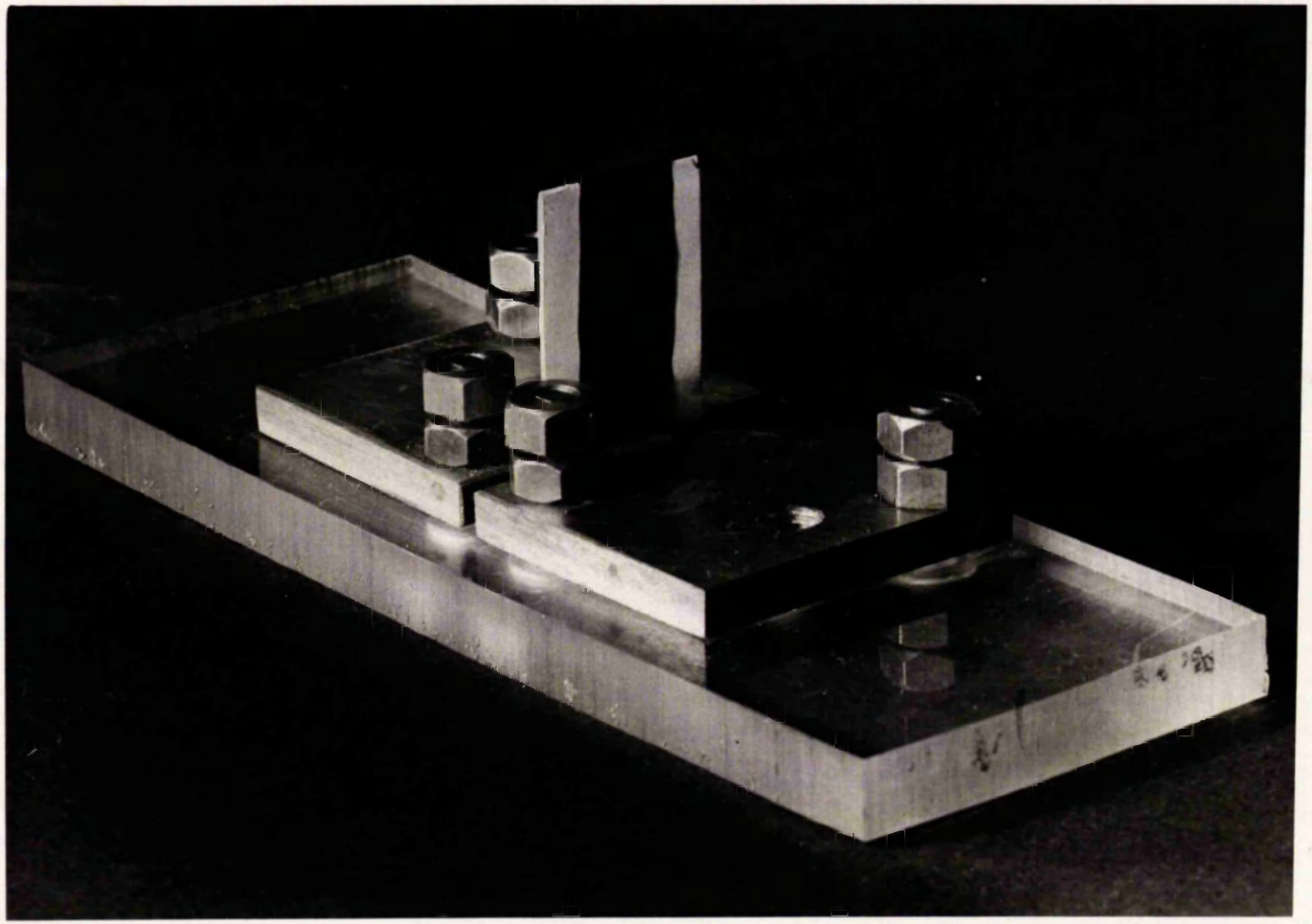

THE SHUNT FOR SPARK CURRENT MEASUREMENTS

(Appr. actual size)

Fig. 9

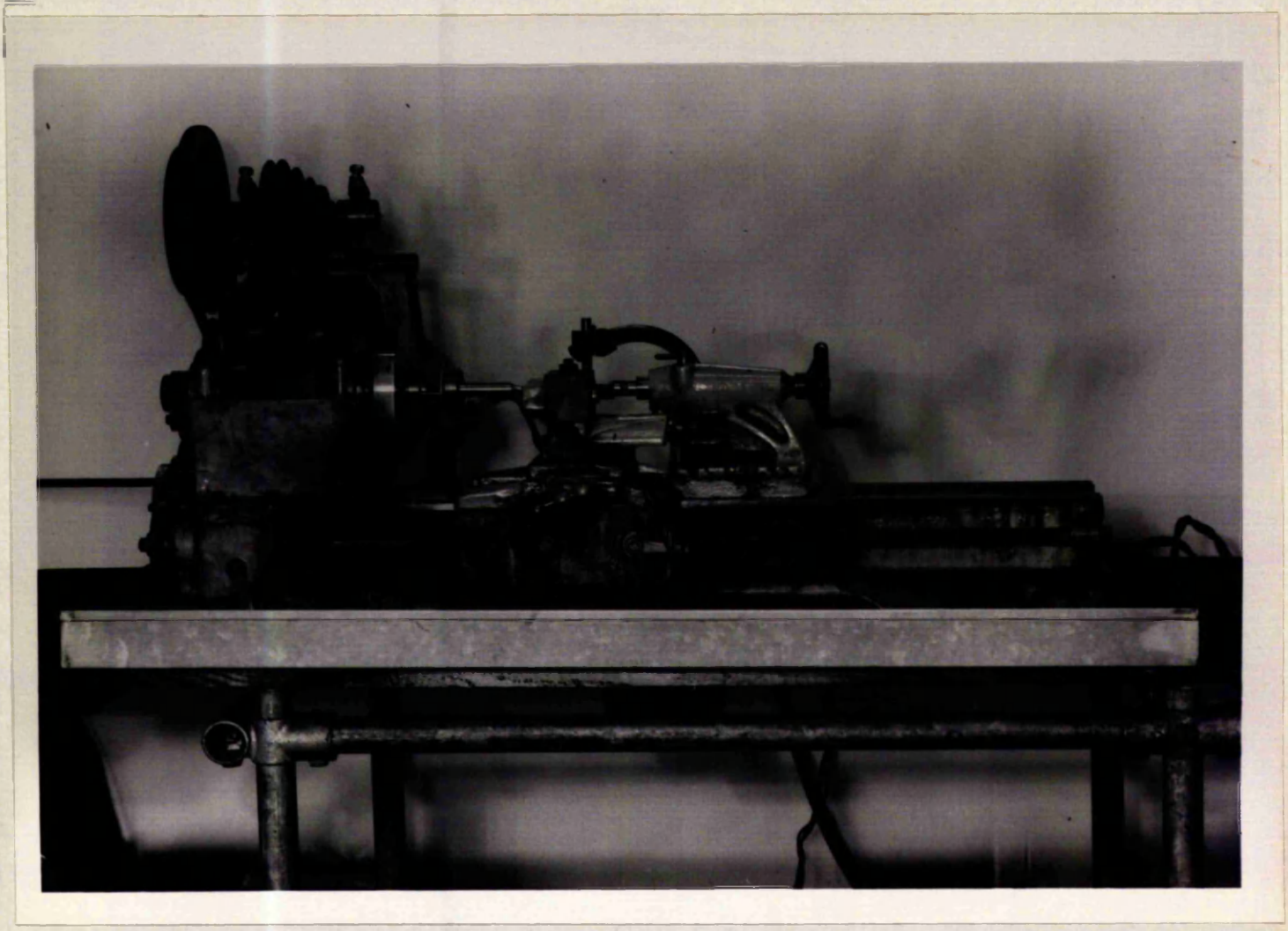

THE „SPARKING" LATHE

Fig. 10 a

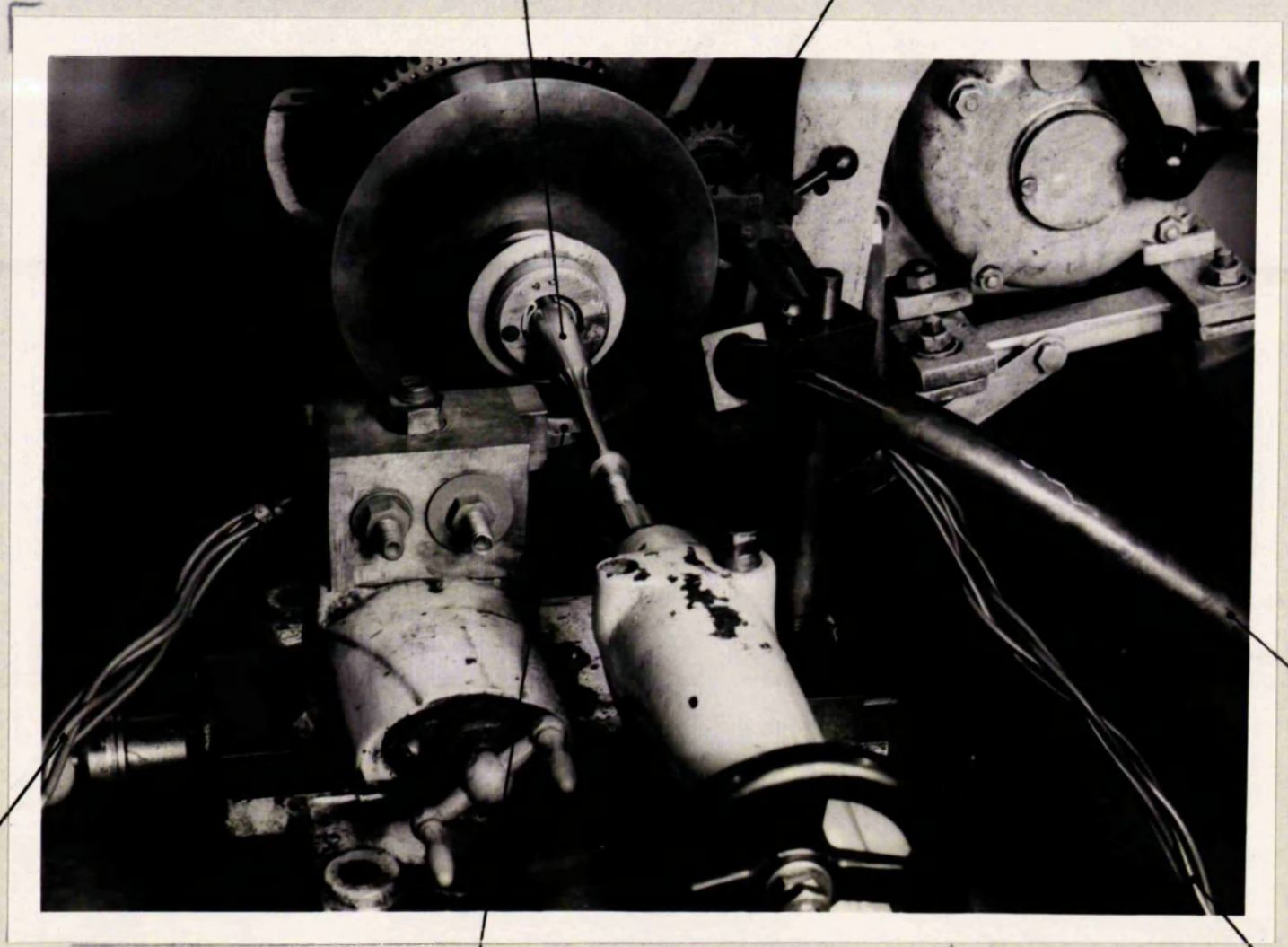

"SPARKING" LATHE CLOSE-UP

Fig. 10 b

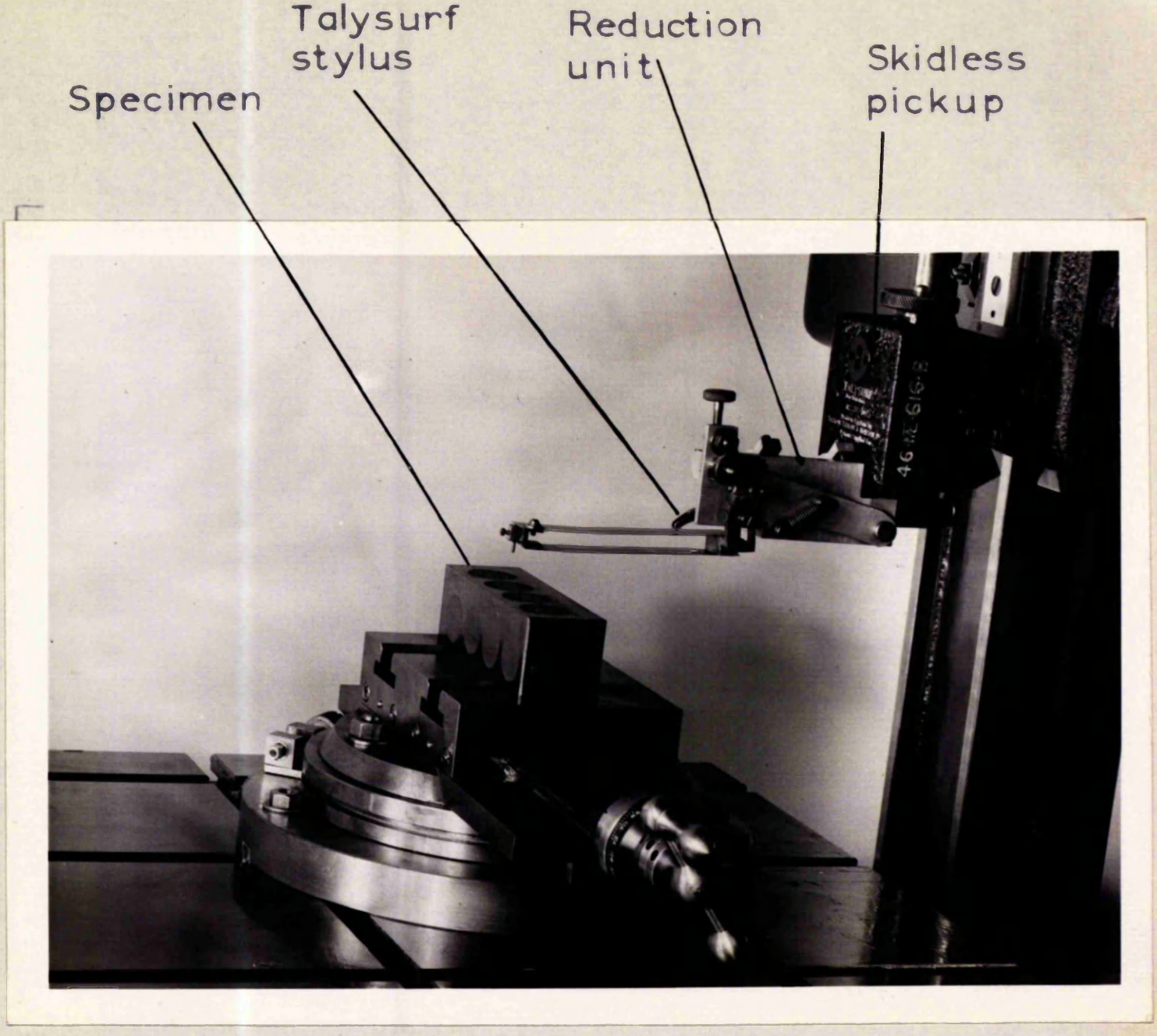

TALYSURF SET-UP WITH
THE REDUCTION UNIT

Fig. 11

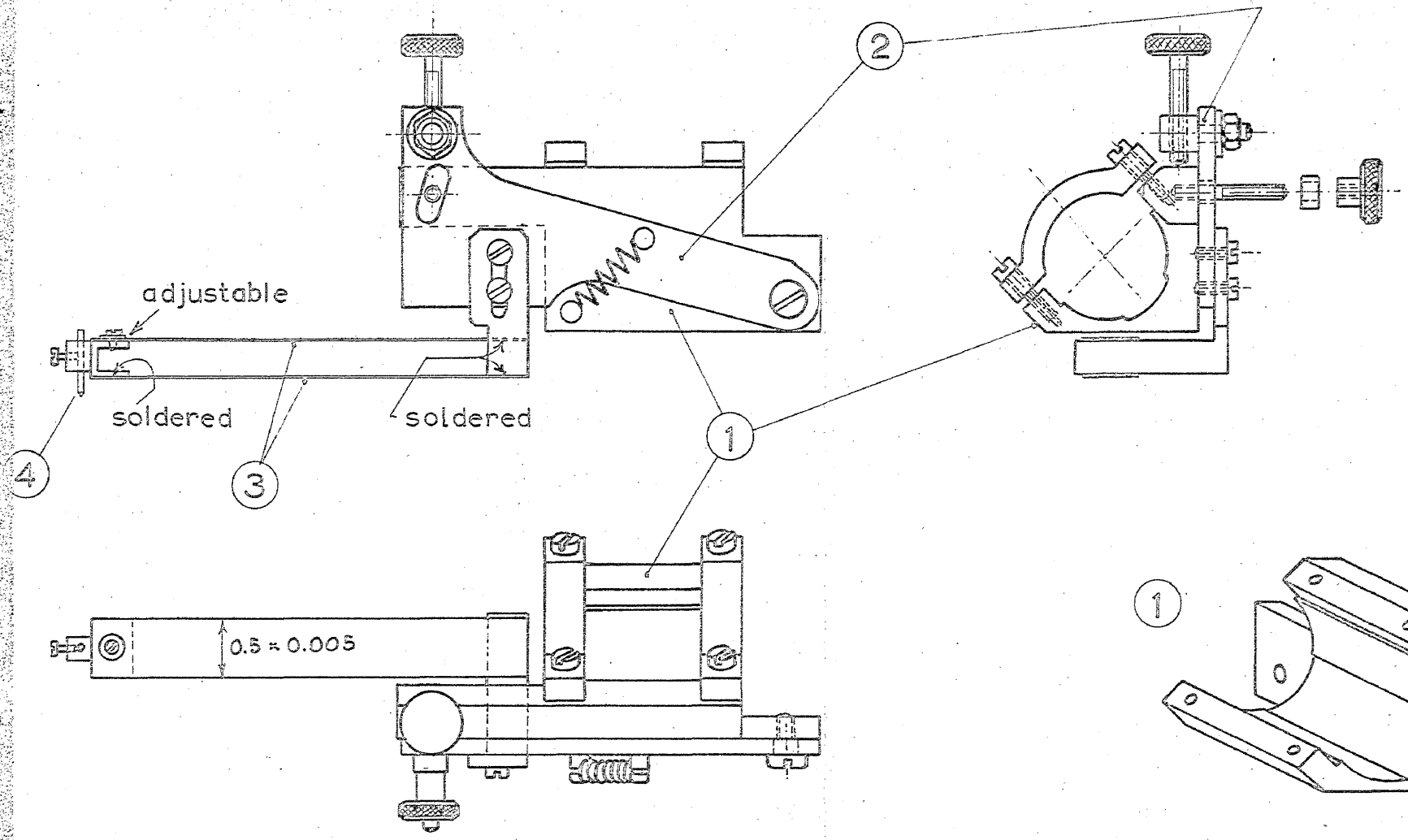

"REDUCTION UNIT" FOR SURFACE FINISH MEASUREMENTS

TO SCALE 1 : 1

Fig. 12

No.	MAIN PARTS, NAME	MATERIAL
4	STYLUS	HARD. STEEL
3	LIGAMENT SPRINGS	SPRING STEEL
2	MOVING PLATE	ALUM. ALLOY
1	BASE	ALUM. ALLOY

Fig. 12

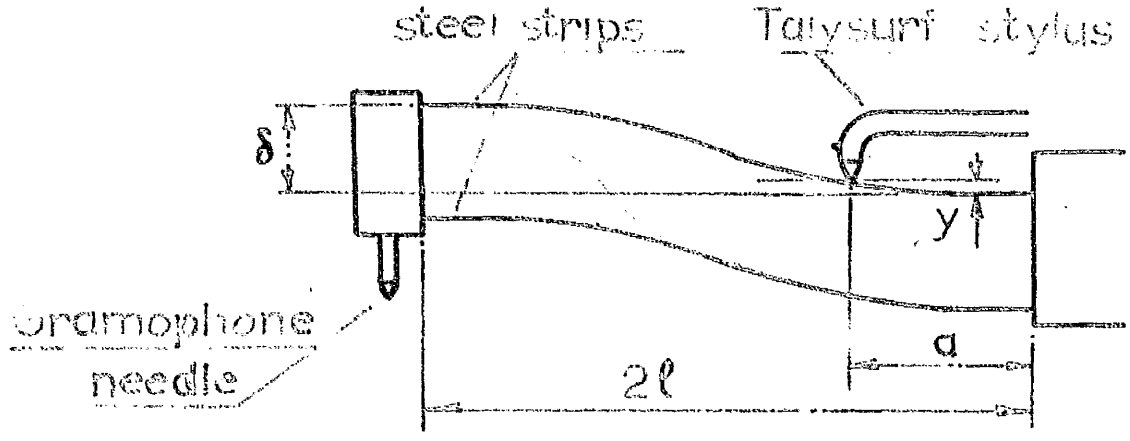

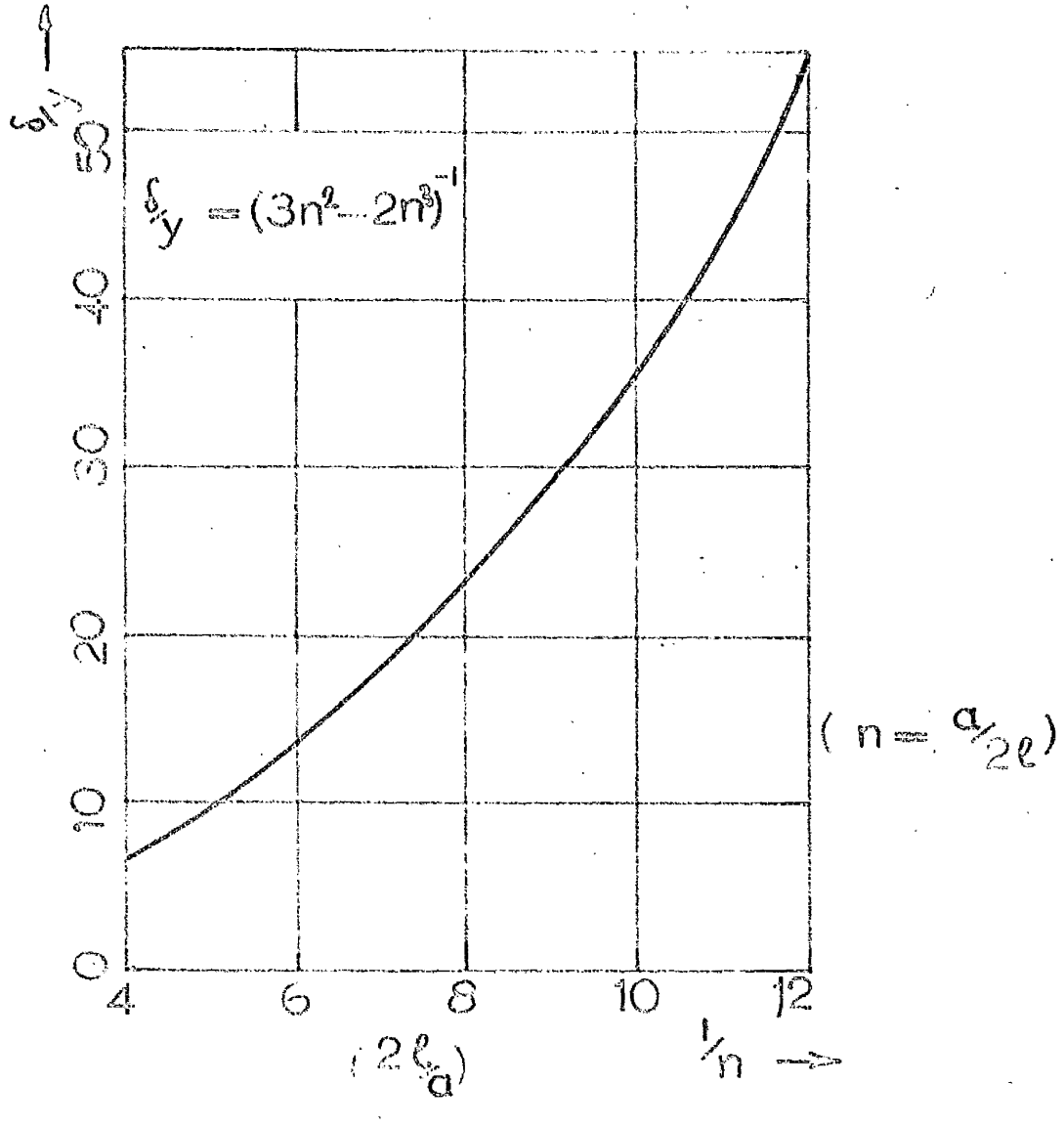

REDUCTION RATIO δ/y OF THE "REDUCTION UNIT" FOR SURFACE FINISH MEASUREMENTS

Fig. 13

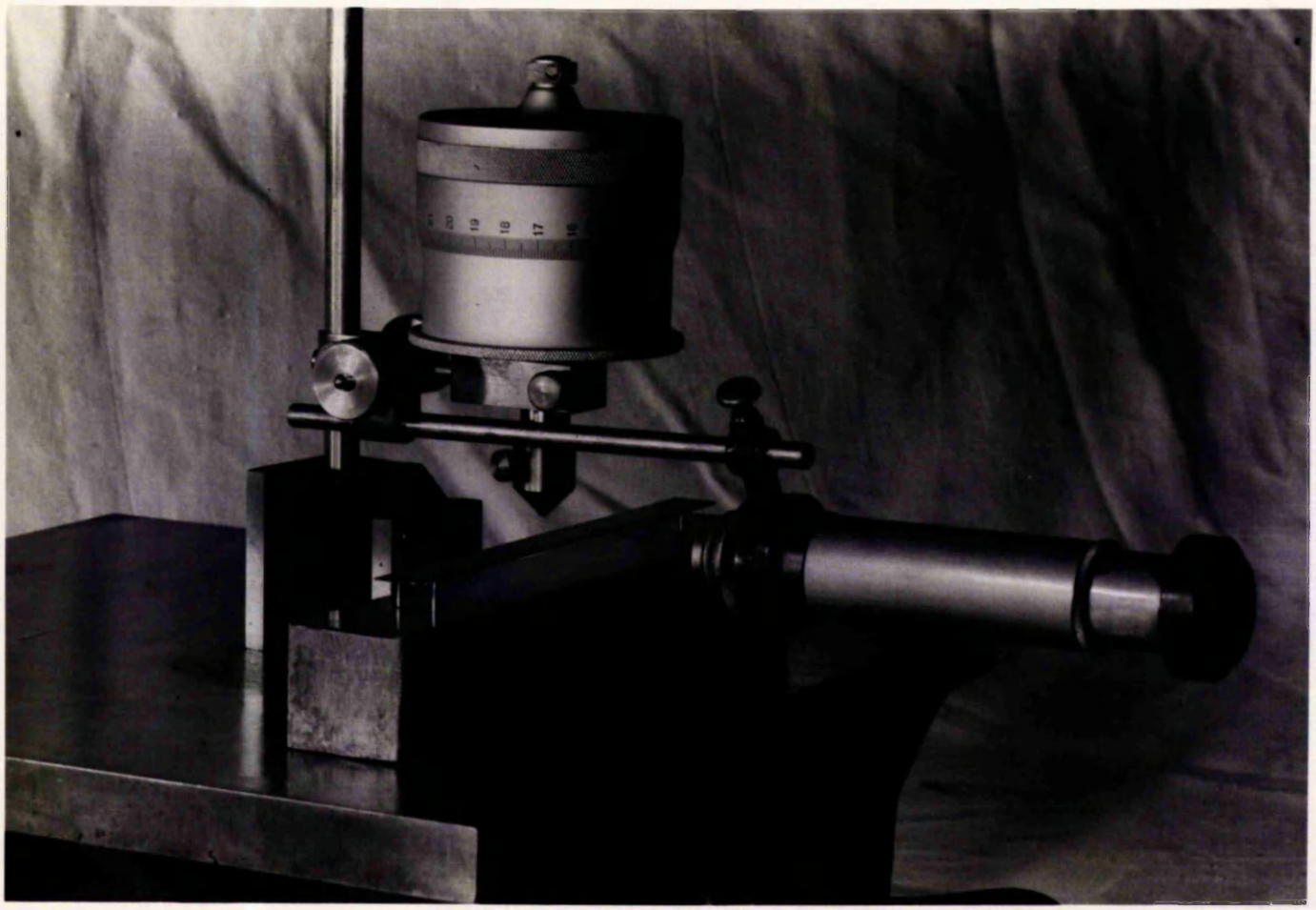

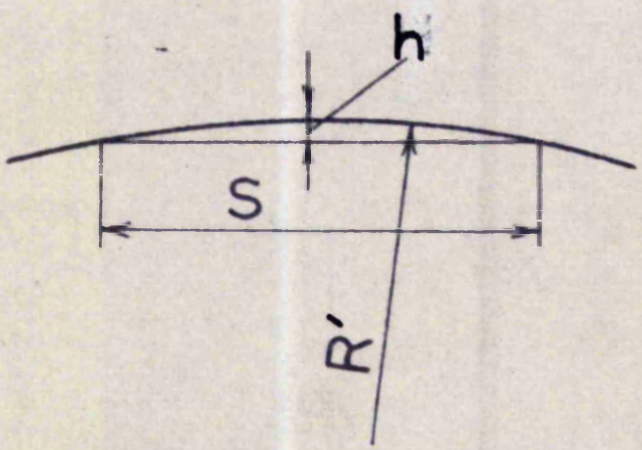

FIXTURE FOR MEASURING CURVATURE OF STRIPS

Fig. 14

a

2.5μF (E=130V)

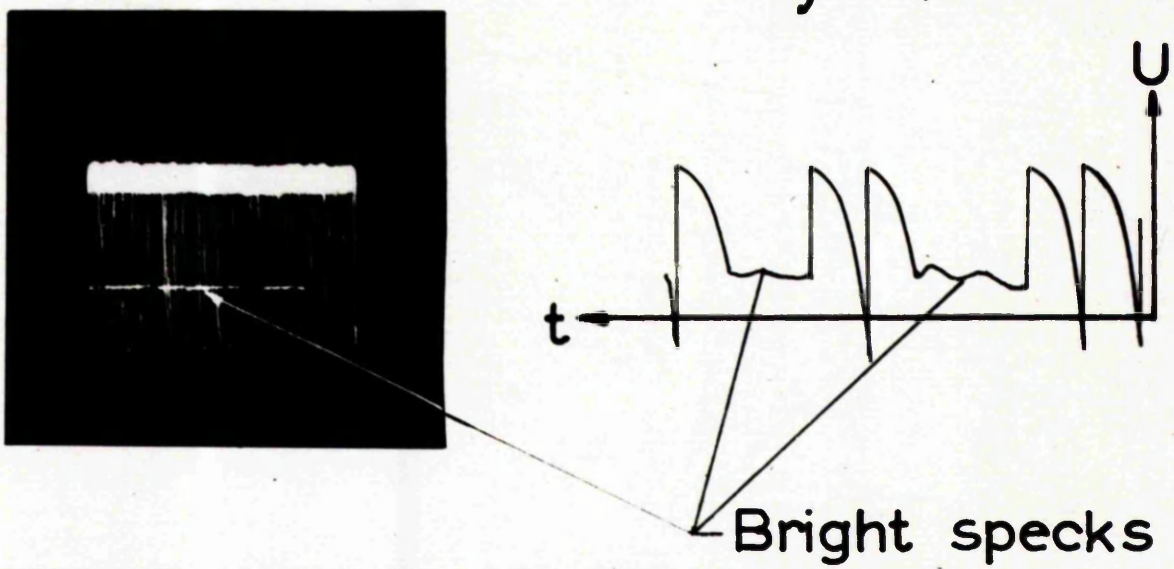

FIRST INCIDENCE OF ARCING

b

(retraced)

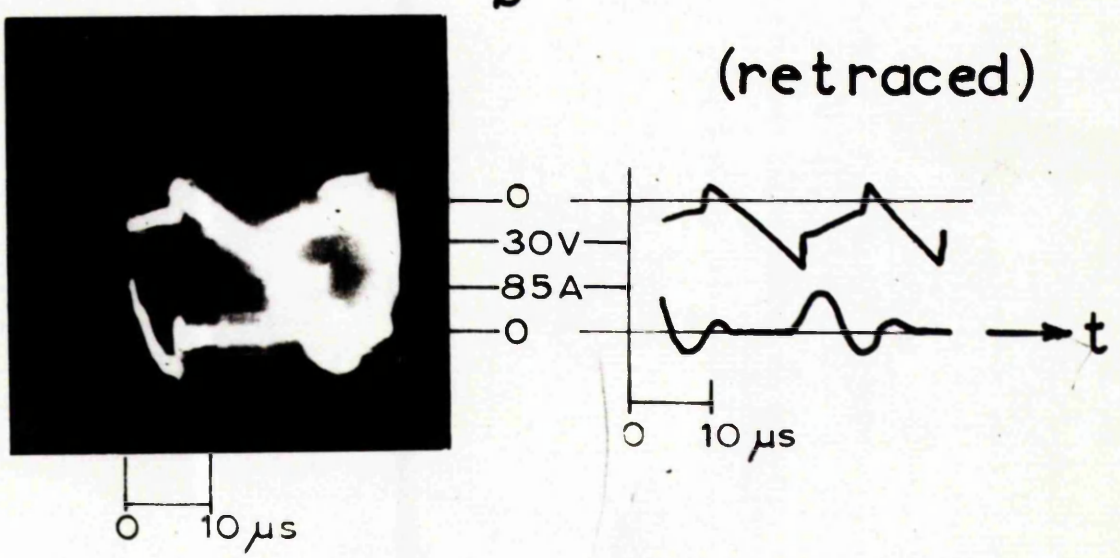

1.5μF (E=130V)

CONTINUOUS ARC

Fig. 15 a & b

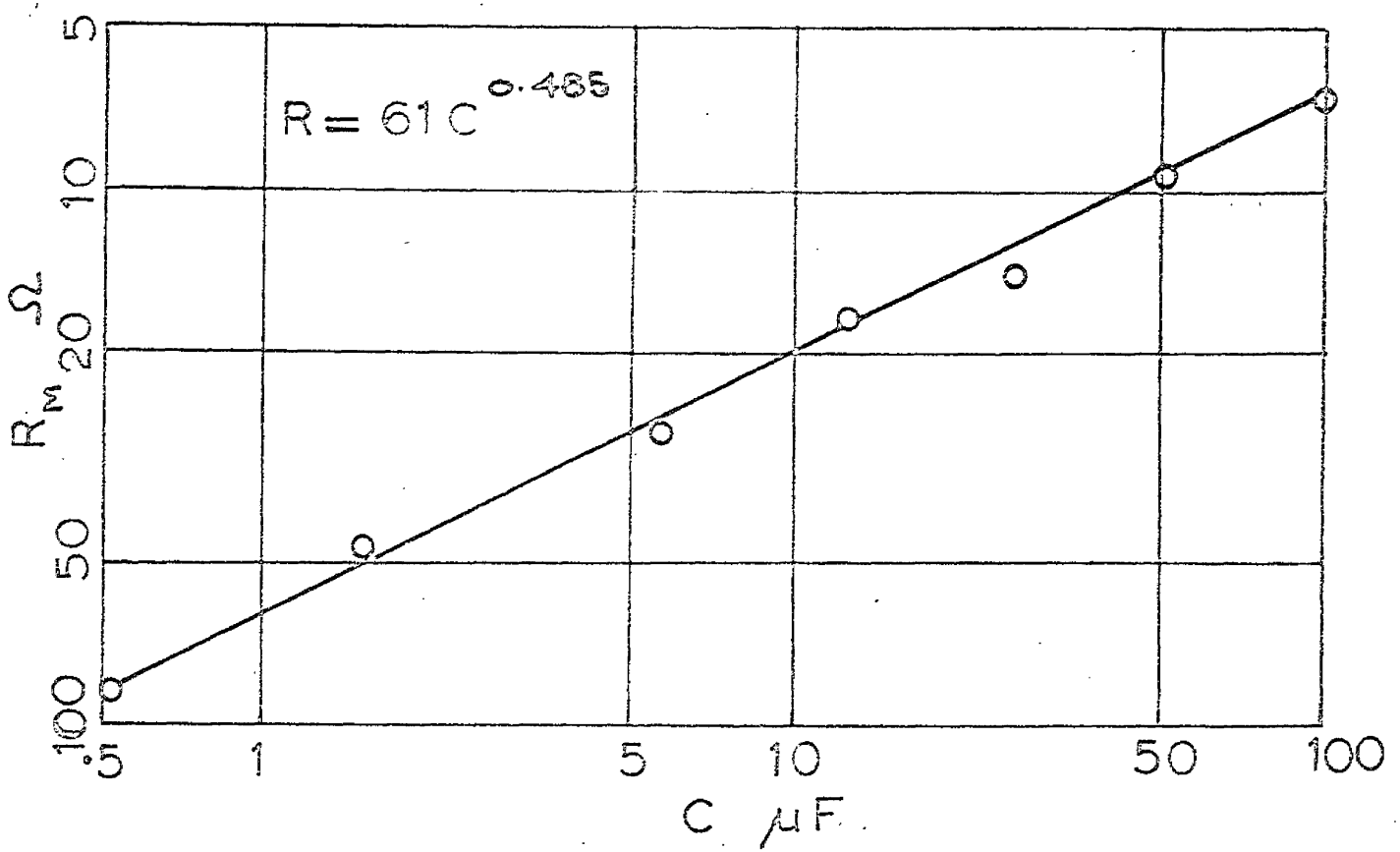

MINIMUM PERMISSIBLE CHARGING RESISTANCE R_M – FUNCTION OF CAPACITY C

Fig. 16

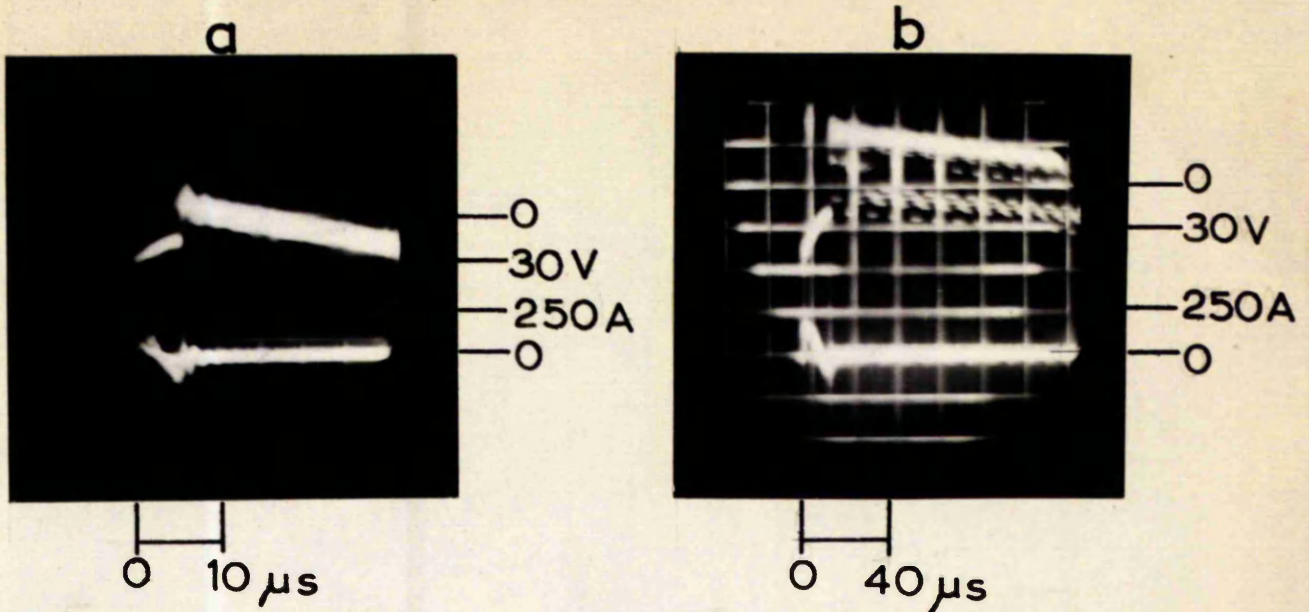

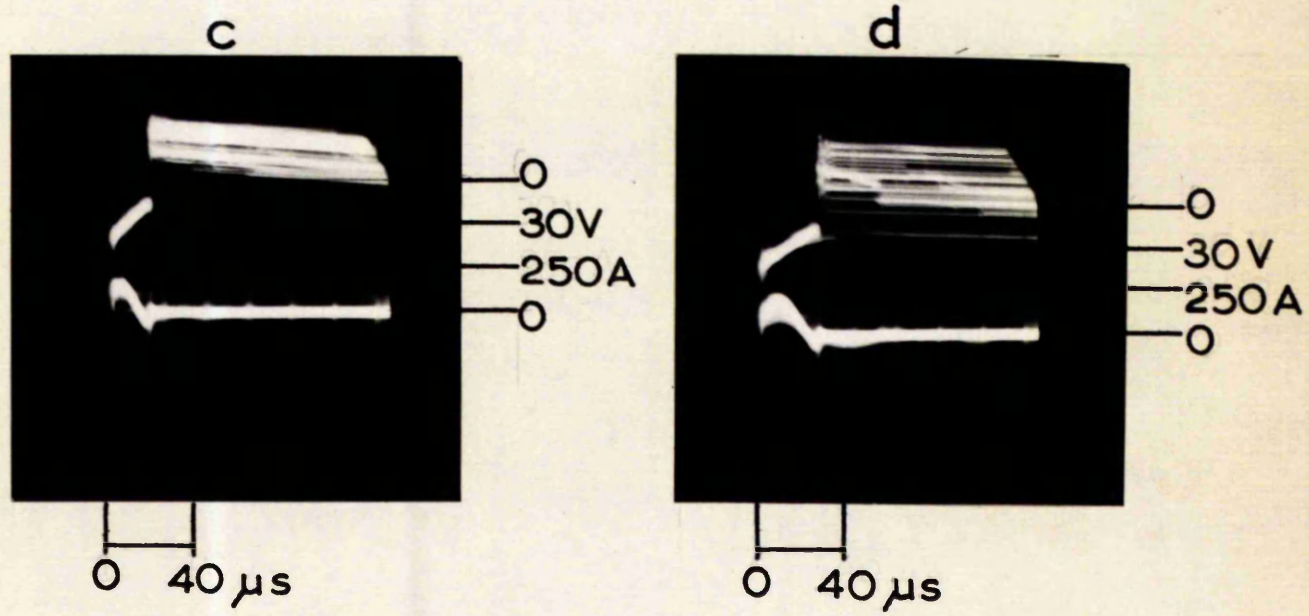

SPARK CURRENTS AND VOLTAGES

Fig. 17 a-d

e

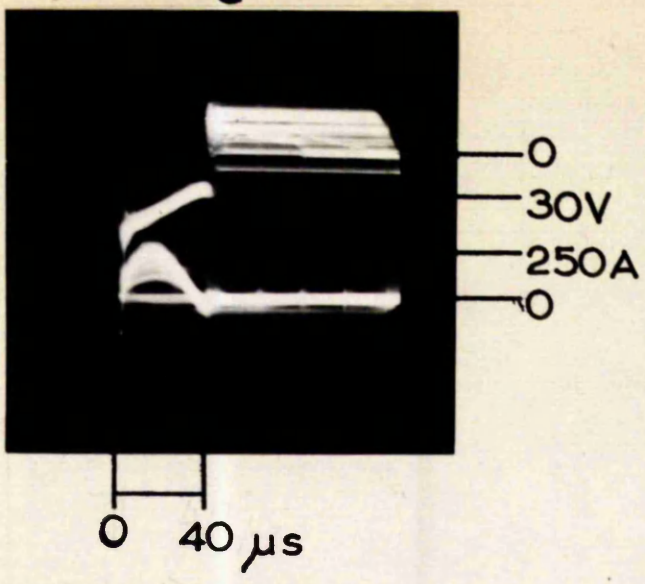

50μF contin.

f

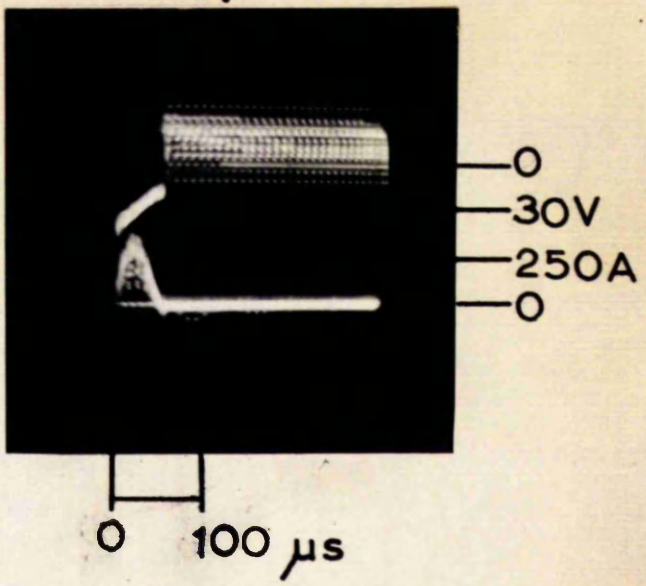

100μF contin.

g

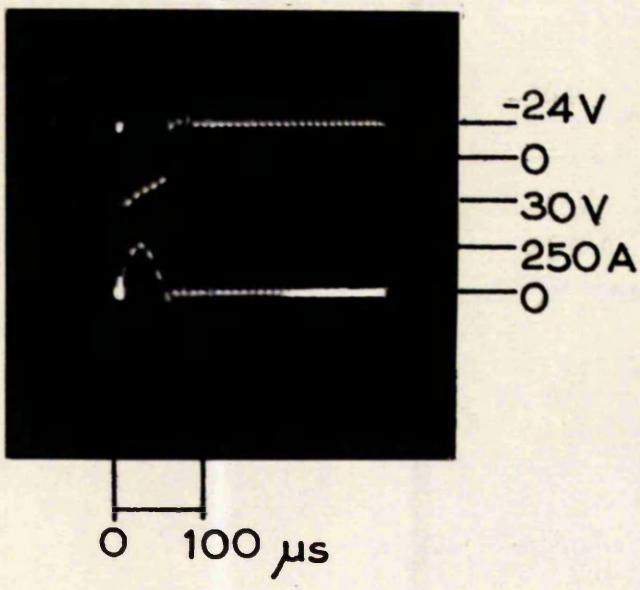

100μF single

h

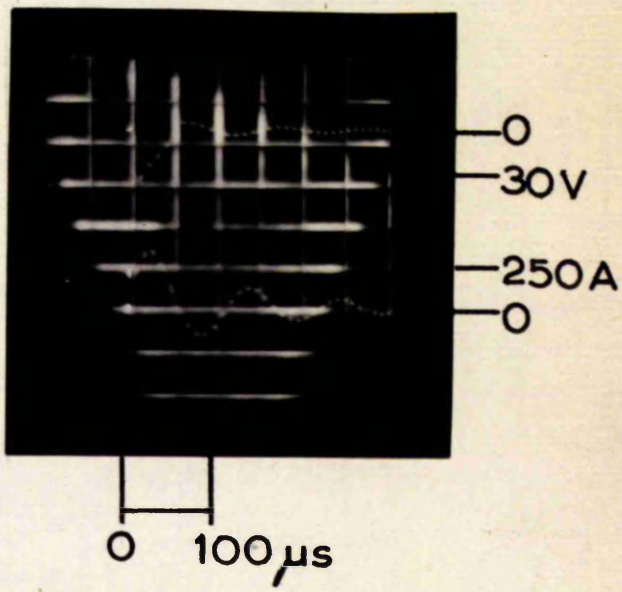

100μF, dropped
100 mm

Fig. 17 e-h

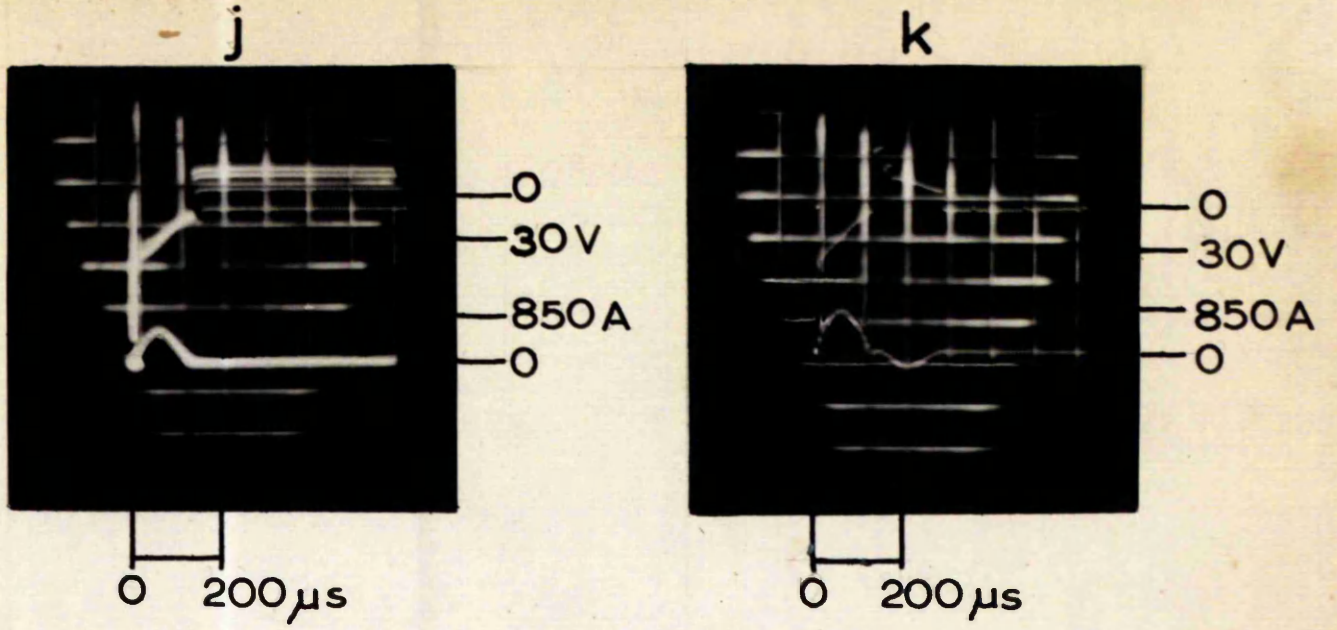

500μF contin.

500μF single

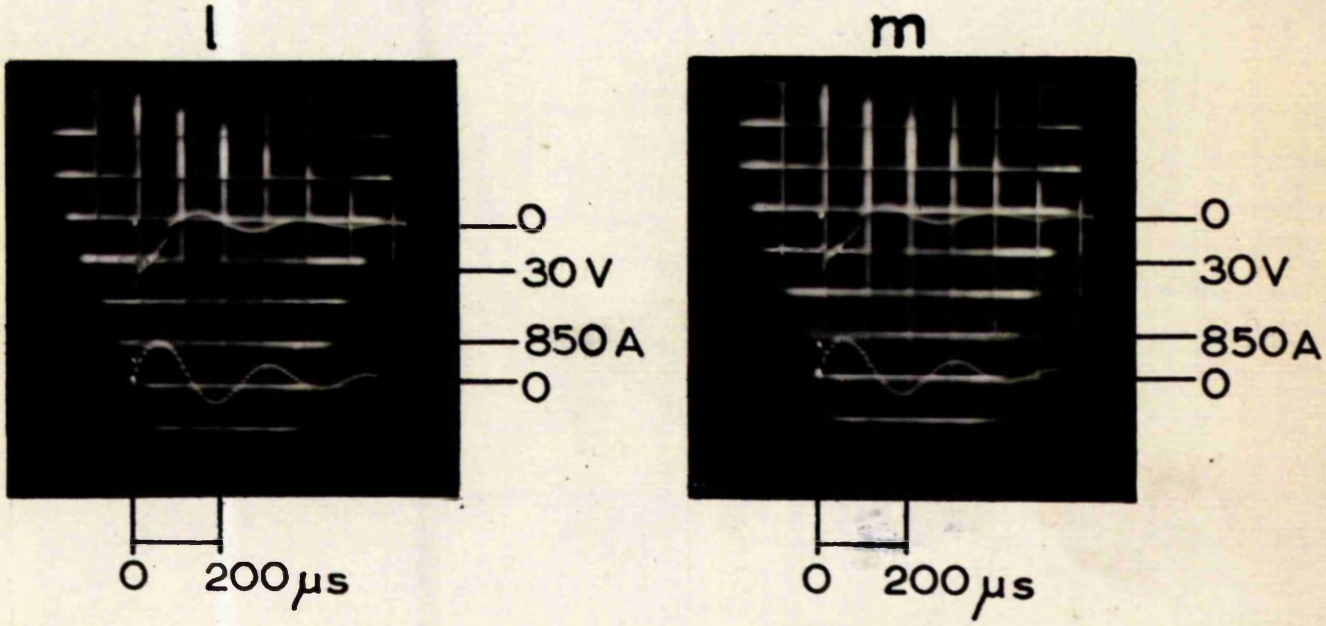

500μF, dropped 2mm

500μF, dropped 100 mm

Fig.17 j - m

CAPACITY μF

0.5 1.5 4.5 12.5

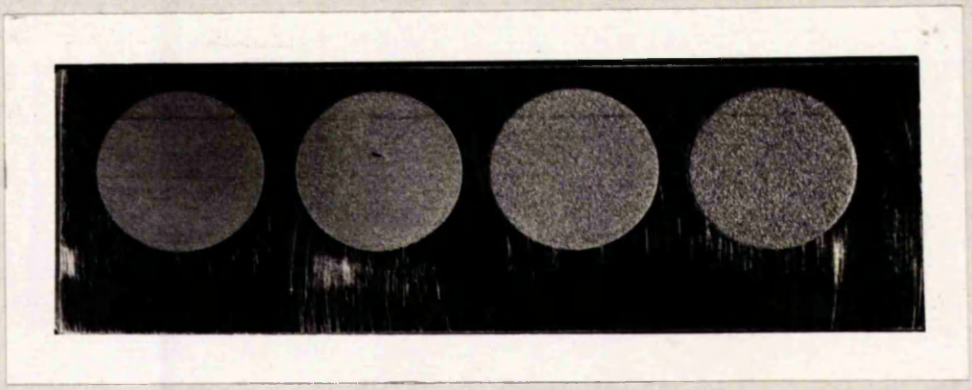

BREAKDOWN VOLTAGE 75-85 V

CAPACITY μF

40 120 250 500

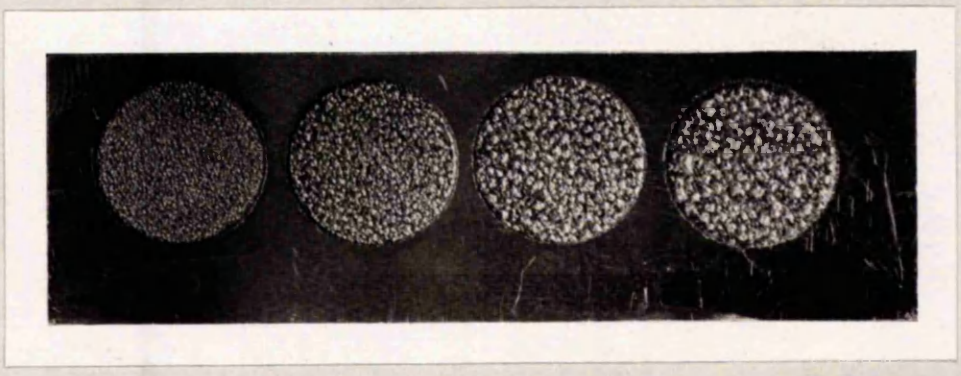

BREAKDOWN VOLTAGE 70-80 V

SURFACES PRODUCED WITH DIFFERENT CAPACITIES (actual size)

Fig. 18

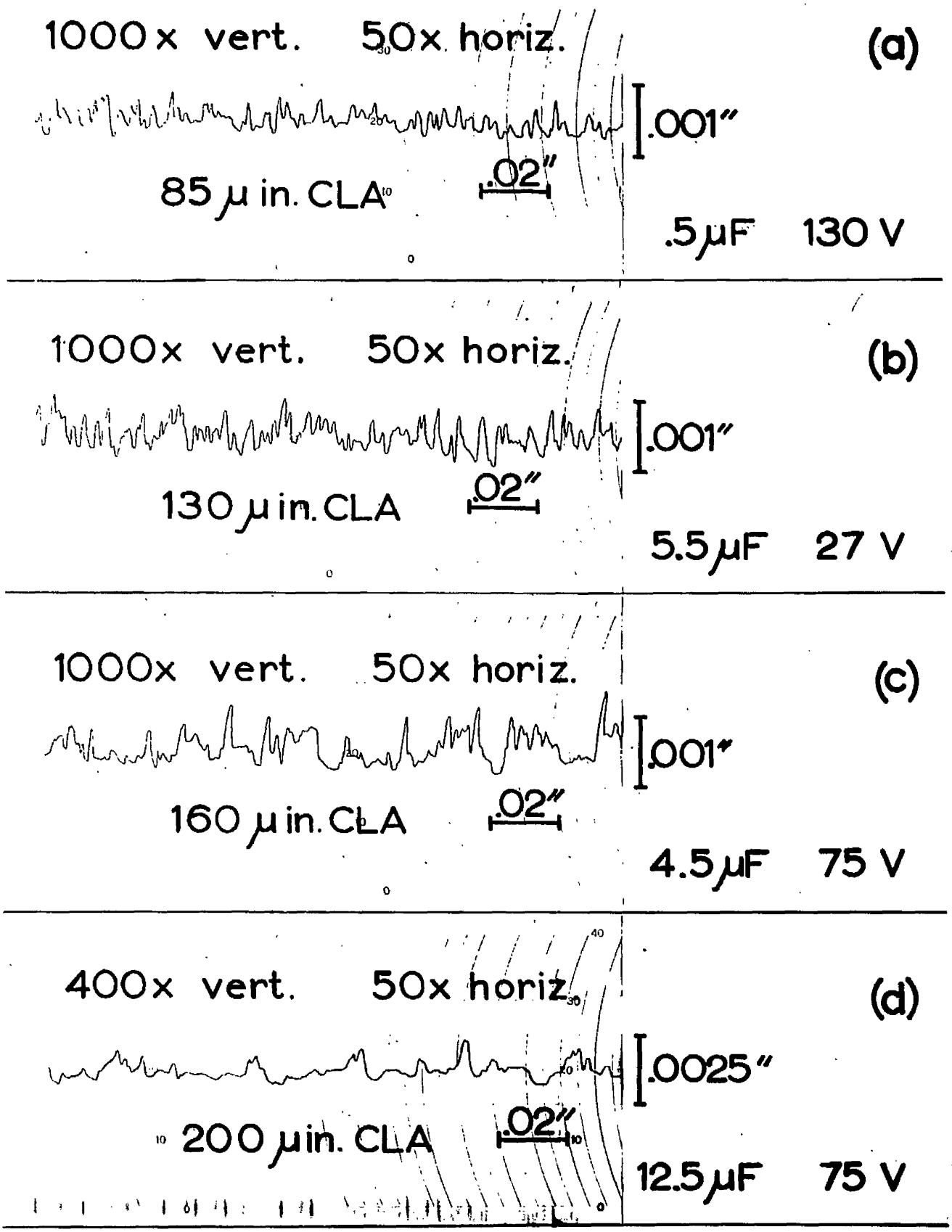

TALYSURF RECORDS OF SPARK ERODED SURFACES (MILD STEEL)

Fig. 19 a-d

400x vert. 50x horiz. (e)

230 µin. CLA

10.5 µF 130V

400x vert. 50x horiz. (f)

350 µin. CLA

40.5 µF 70V

175x vert. 50x horiz. (g)

650 µin. CLA

500 µF 70V

400x vert. 50x horiz. (h)

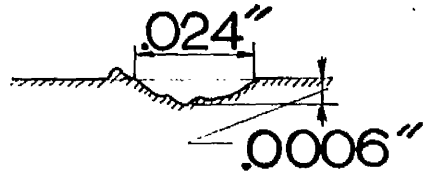

A CRATER SECTION

100 µF 120V

Fig. 19 e-h

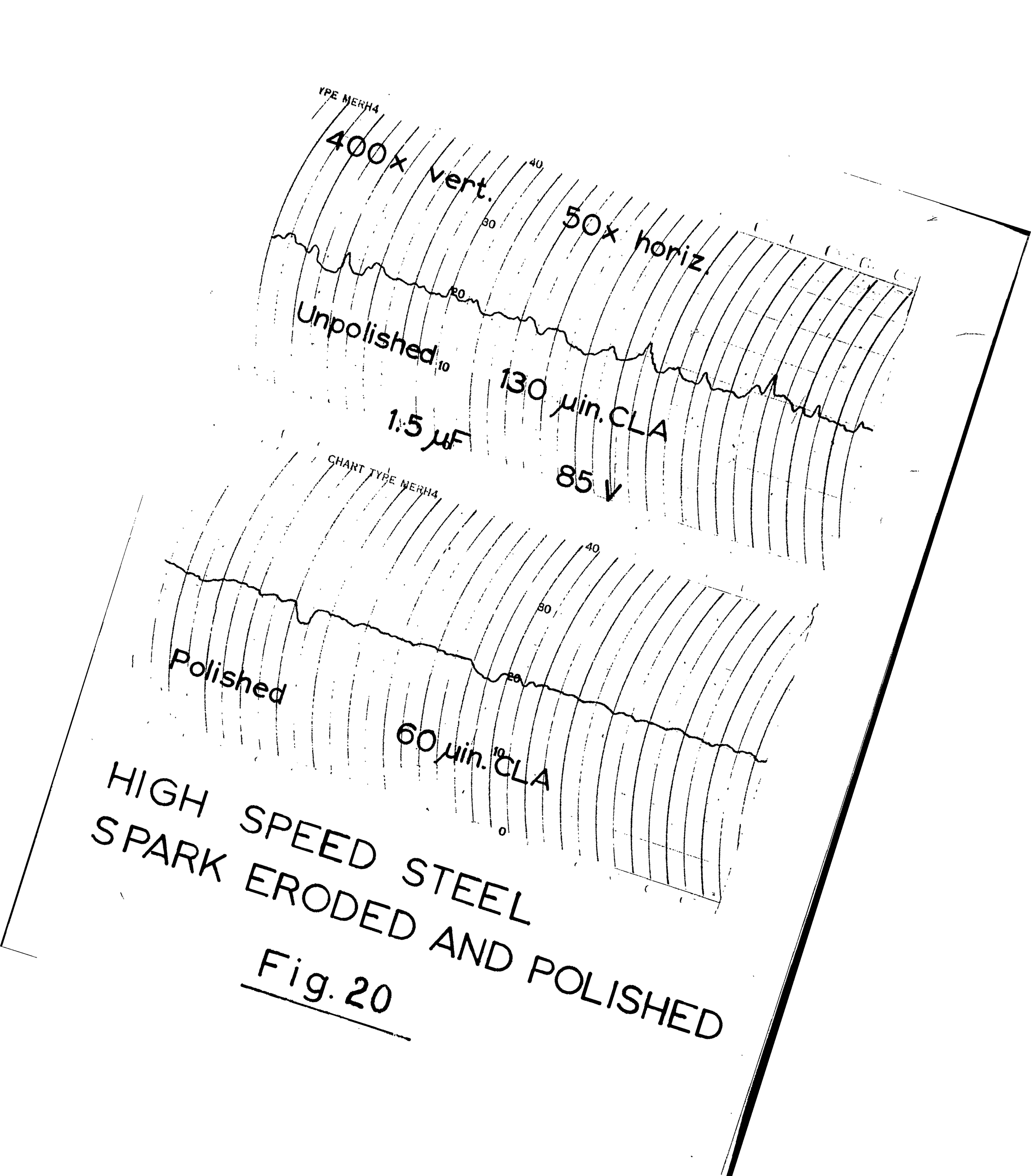

HIGH SPEED STEEL
SPARK ERODED AND POLISHED

Fig. 20

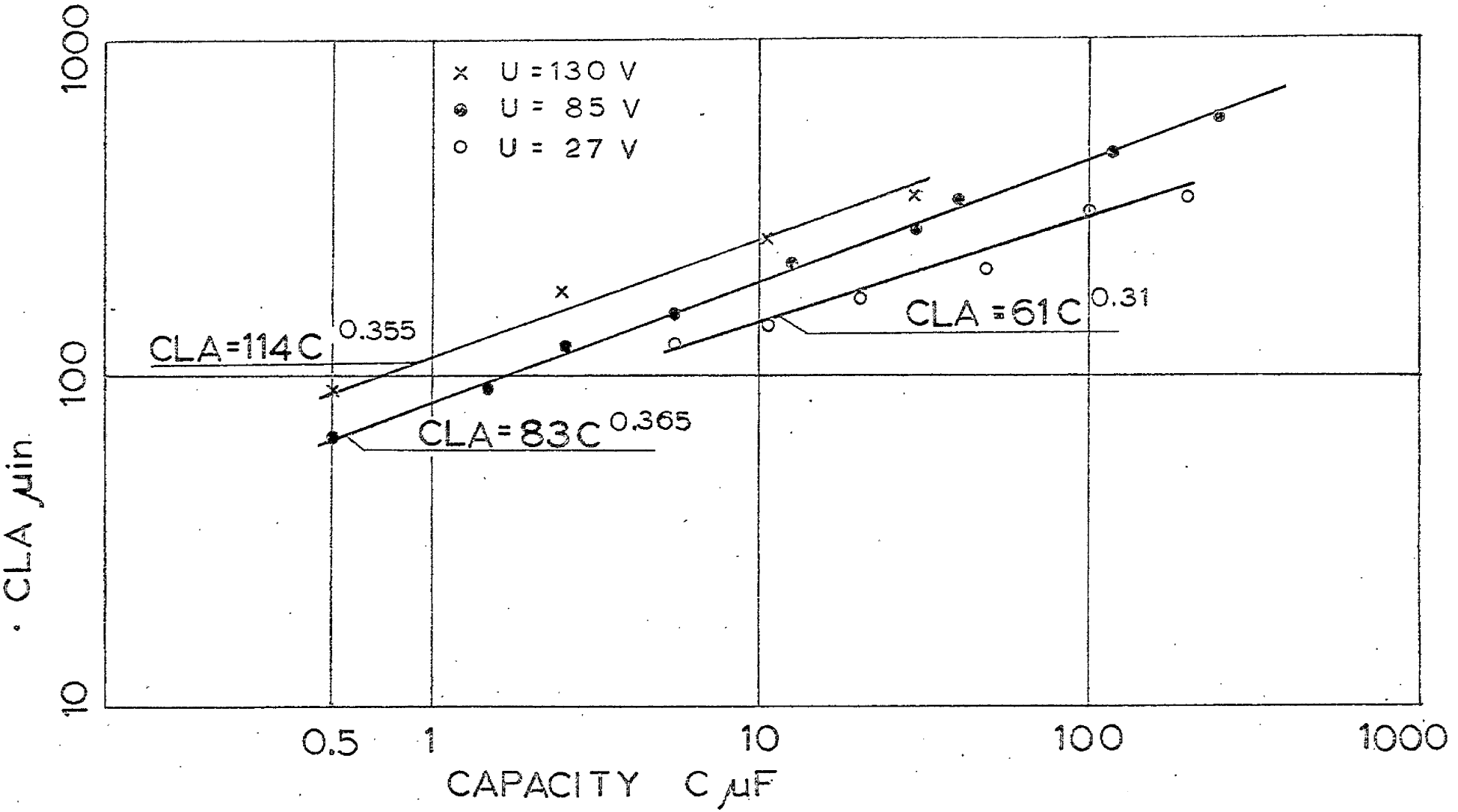

SURFACE FINISH (CLA) - CAPACITY (C) RELATIONSHIP (MILD STEEL)

Fig. 21

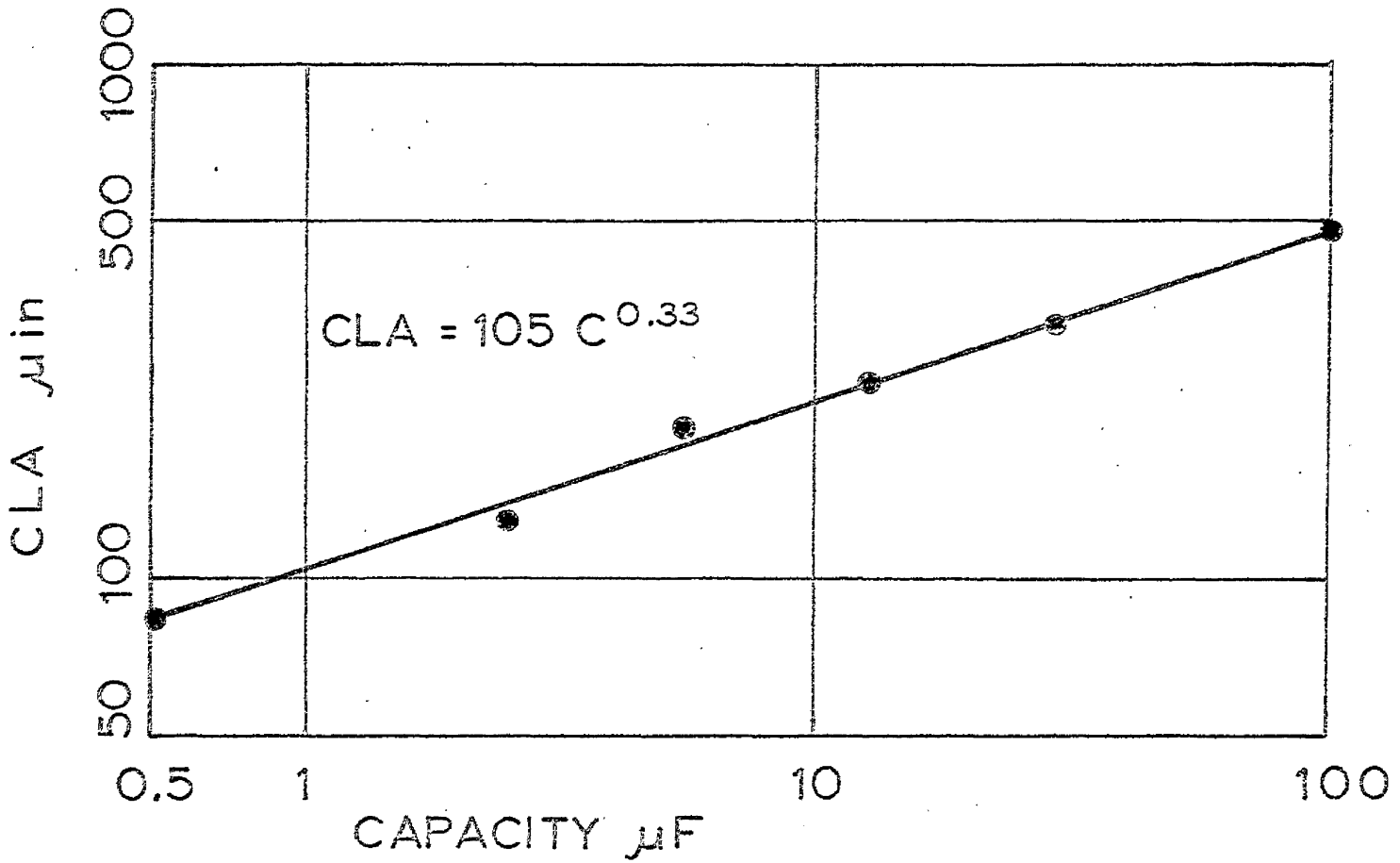

SURFACE-FINISH (CLA) - CAPACITY (C) RELATIONSHIP
(HARDENED STEEL)

Fig. 22

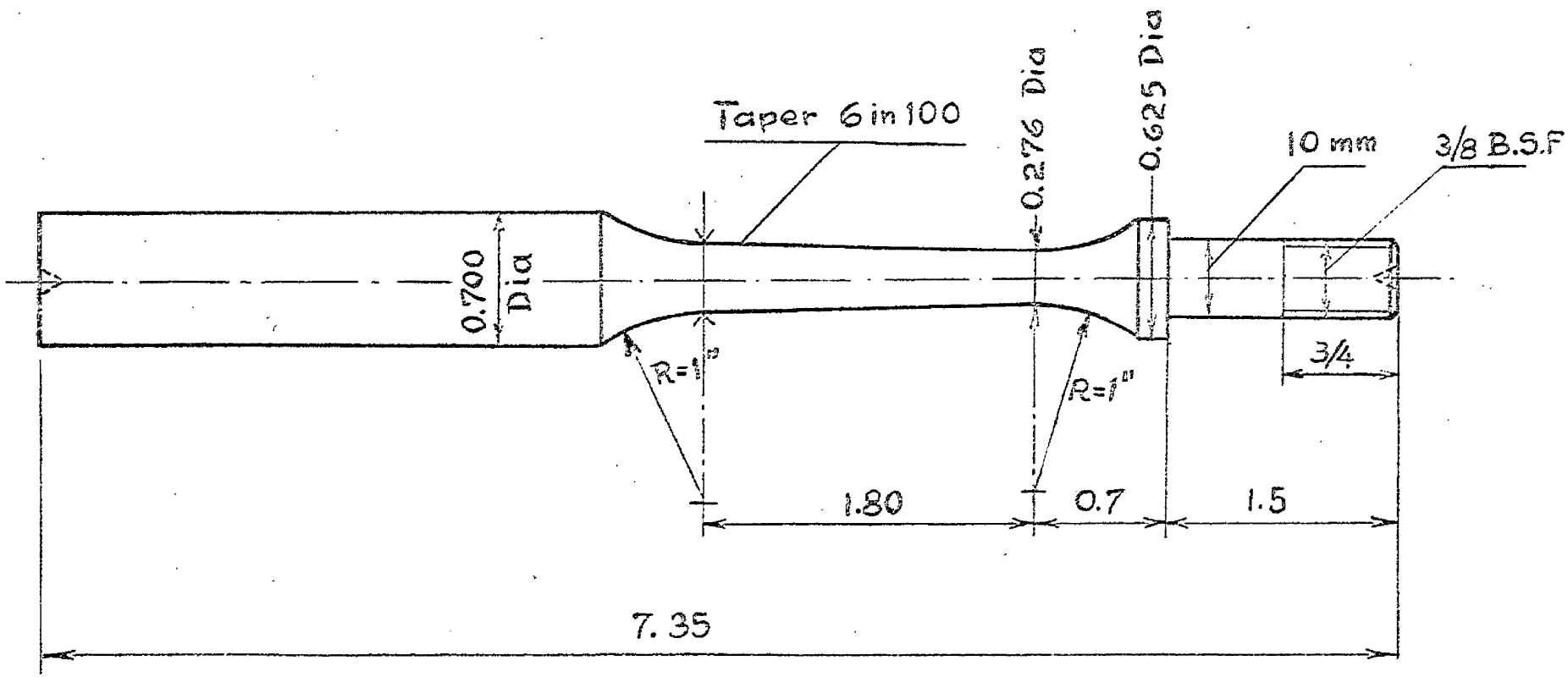

THE FATIGUE SPECIMEN

Fig. 23

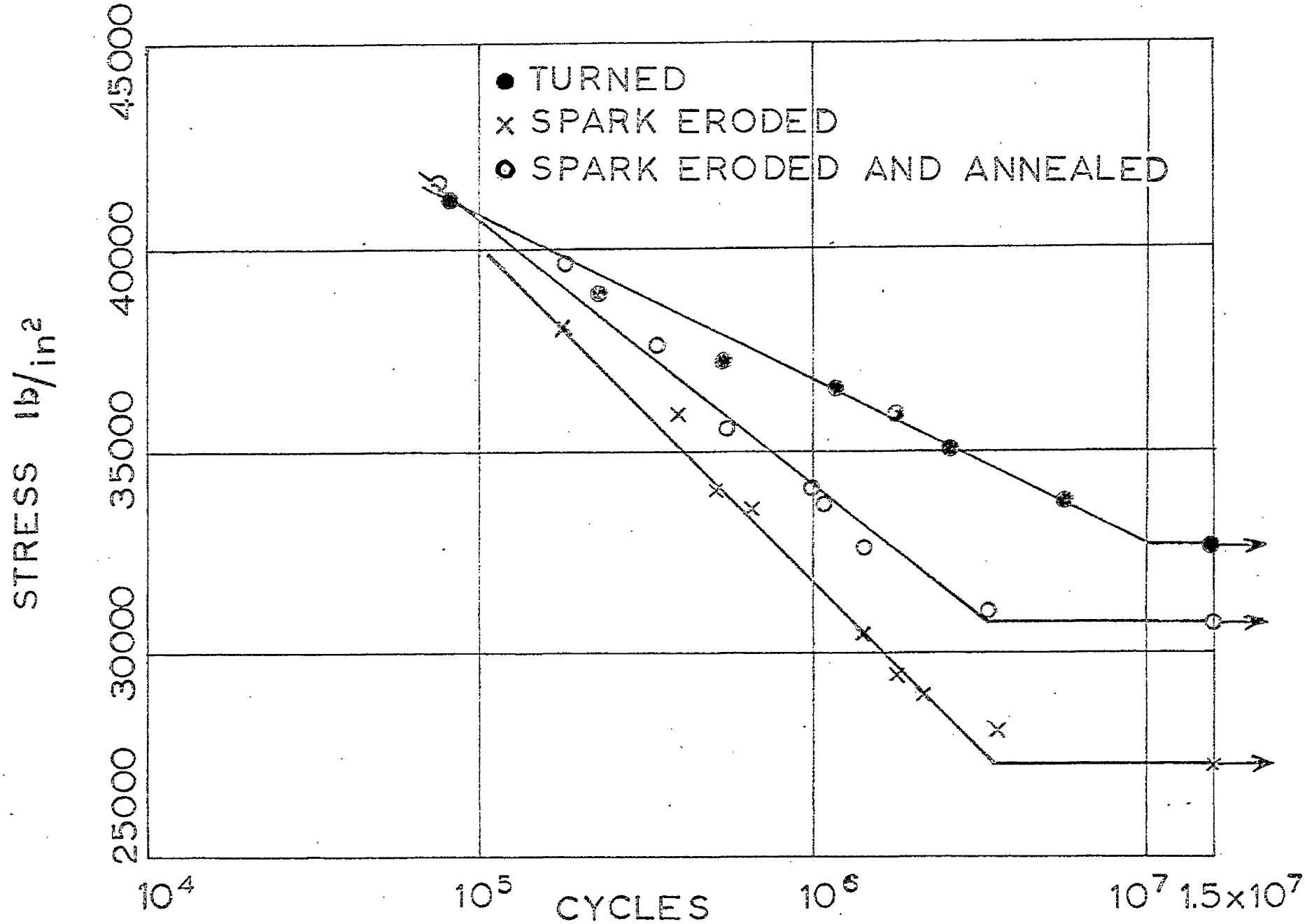

ENDURANCE TESTS ON MILD STEEL

Fig.24

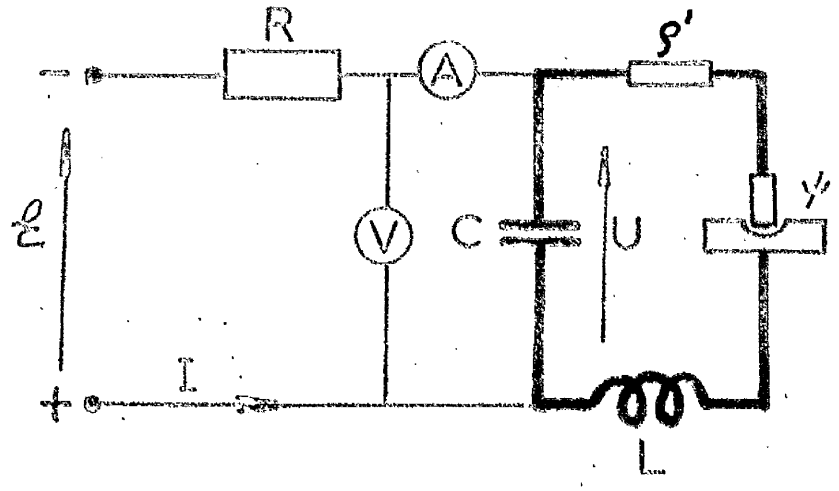

THE BASIC RELAXATION (R-C) CIRCUIT

Fig. 25

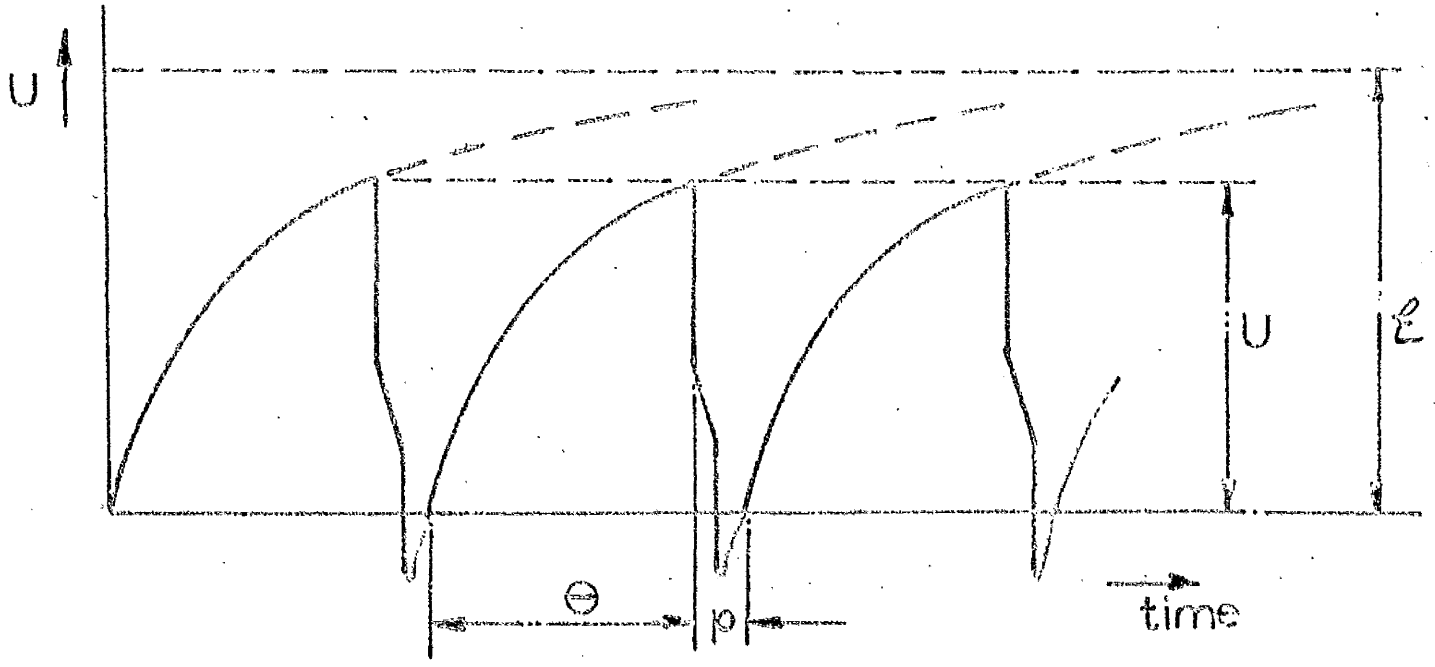

VOLTAGE-TIME CURVE FOR R-C CIRCUIT

Fig. 26

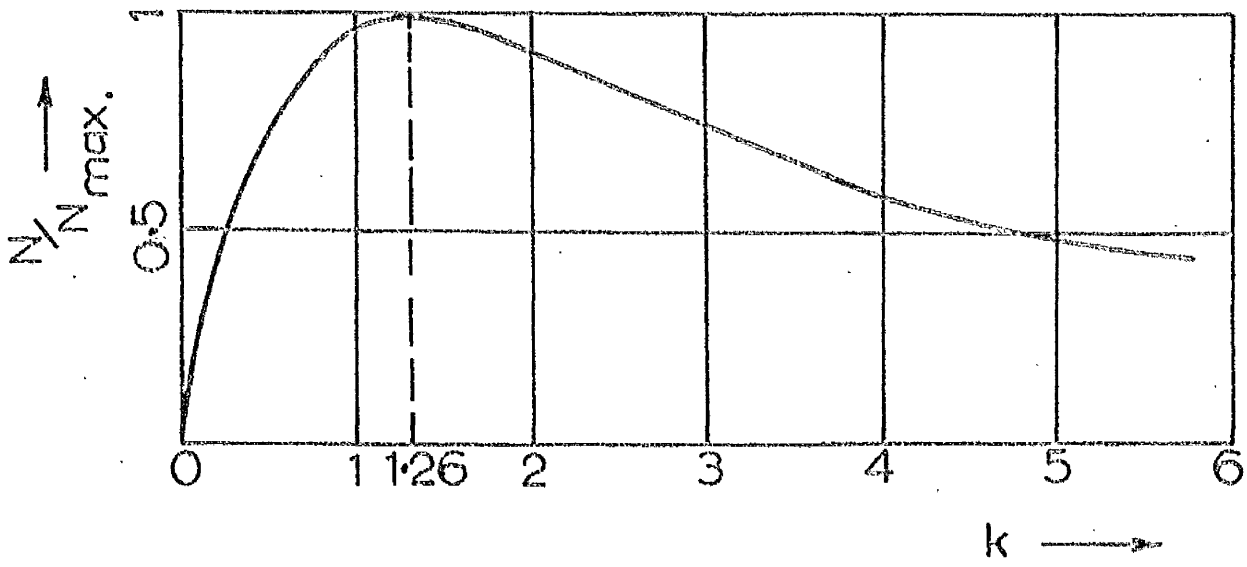

POWER – k CURVE $k = \theta/RC$

Fig. 27

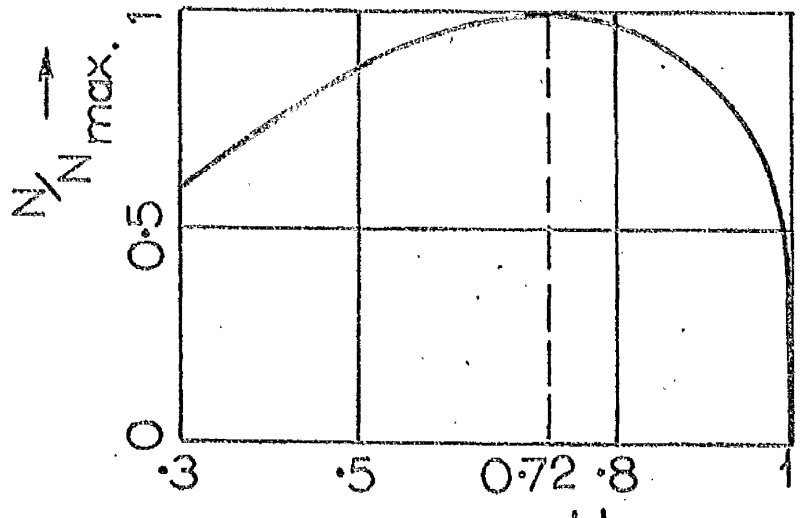

POWER – $U/\mathcal{E}$ or

POWER – $gap/gap_{max.}$ RELATIONSHIP

Fig. 28

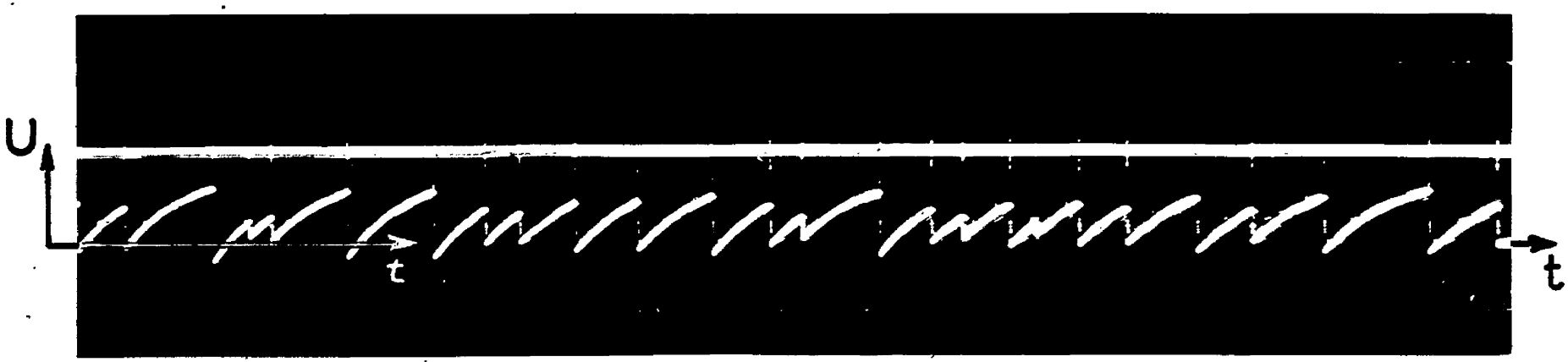

CONTINUOUS „SPARKING" ; VOLTAGE (U) CURVE

Oscillogram made on a moving film

Fig. 29

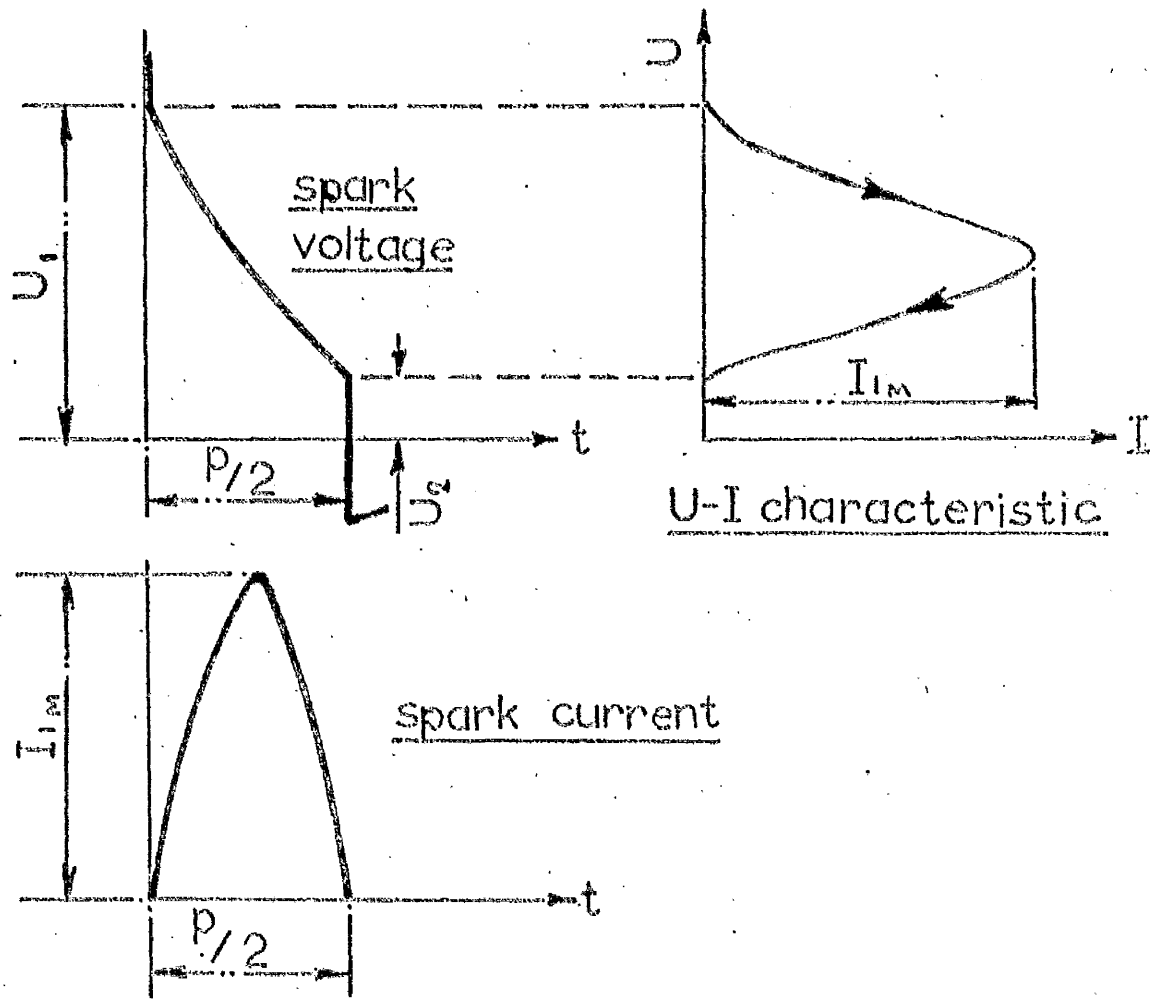

TYPICAL VOLTAGE–CURRENT CHARACTERISTIC OF A SPARK

(First half-wave)

Fig. 30

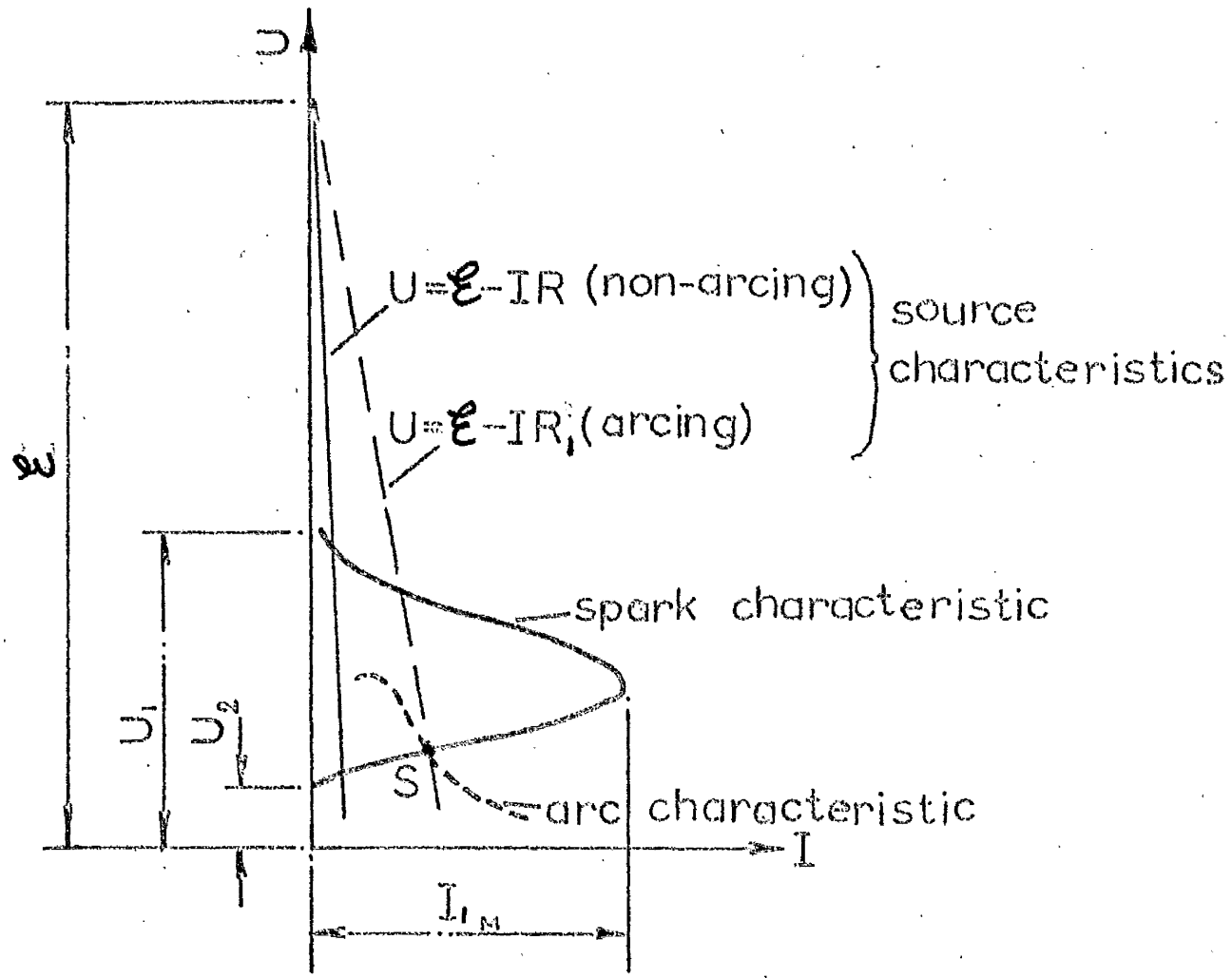

S – Point of a stable arc

ARC, SPARK AND SOURCE CHARACTERISTICS.

Fig. 31

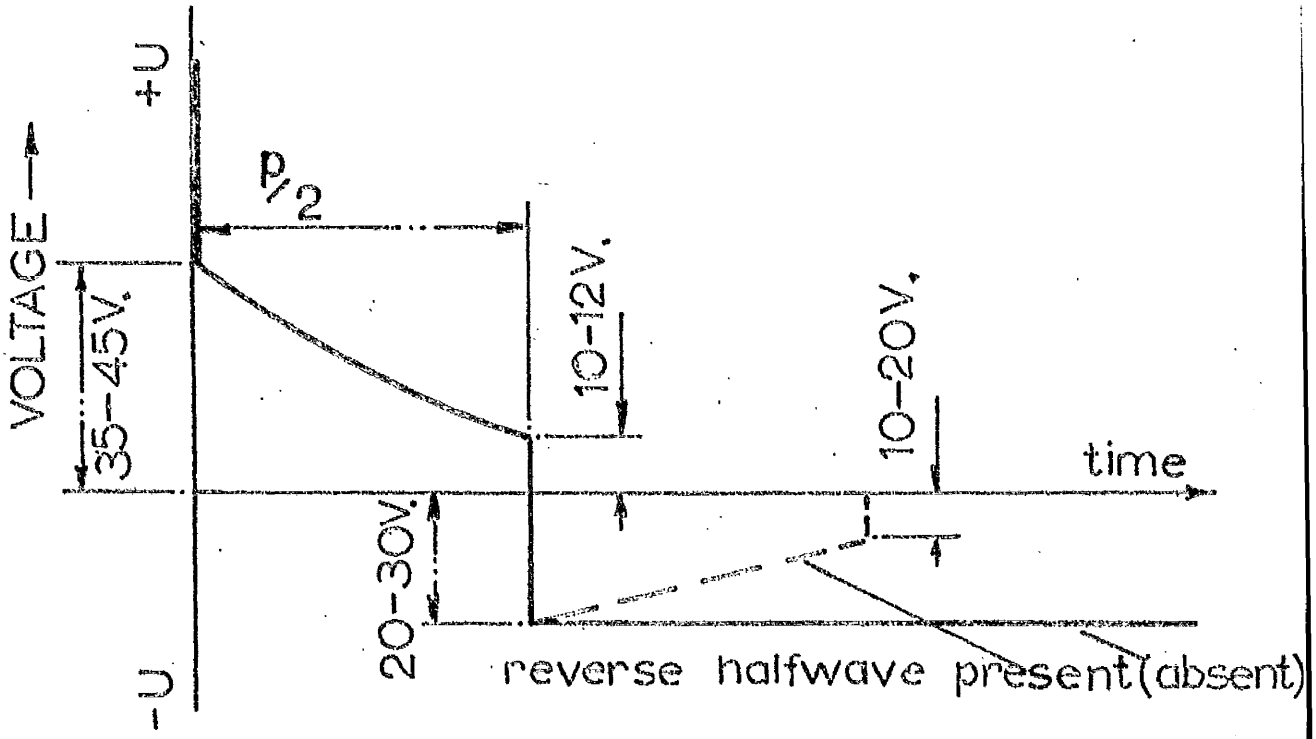

SPARK DISCHARGE: TYPICAL VOLTAGE FORM

Fig. 32

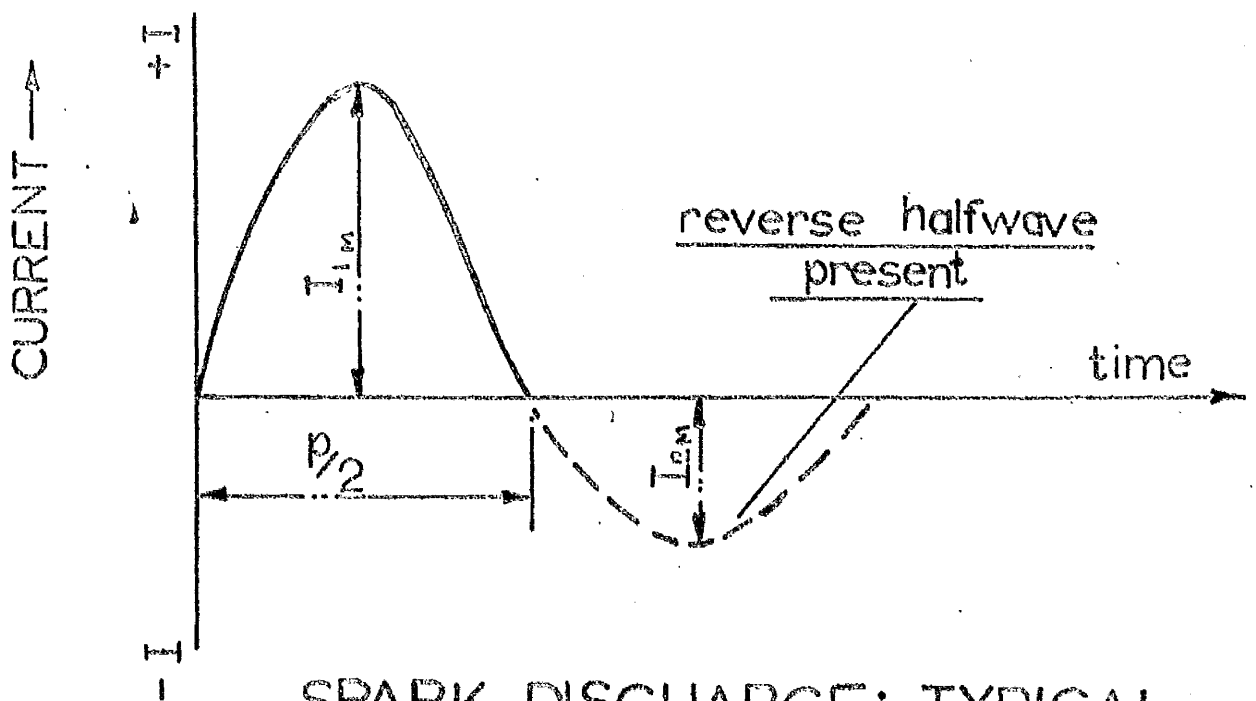

SPARK DISCHARGE: TYPICAL CURRENT FORM

Fig. 33

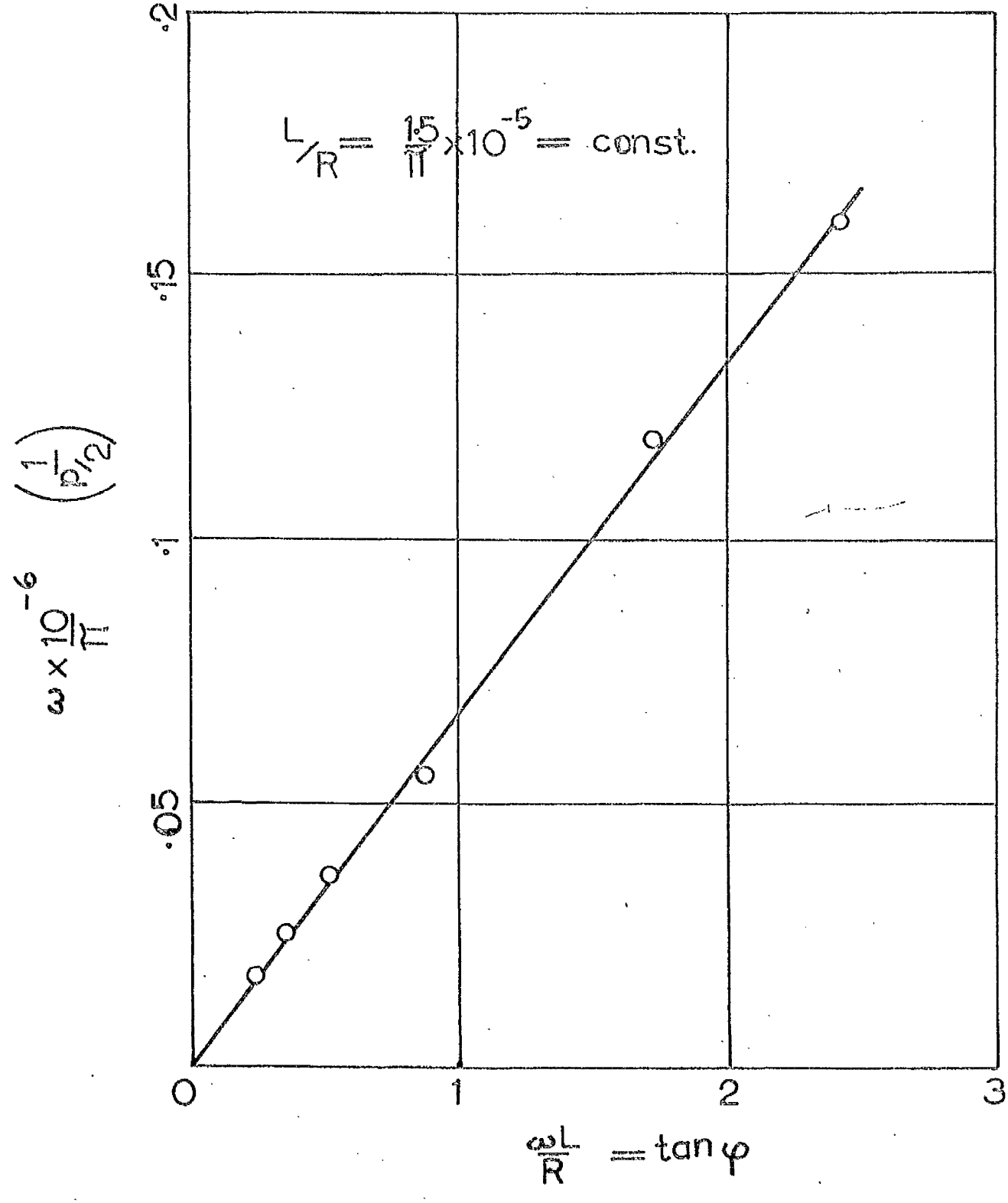

THE LAG φ OF THE CURRENT

Fig. 34

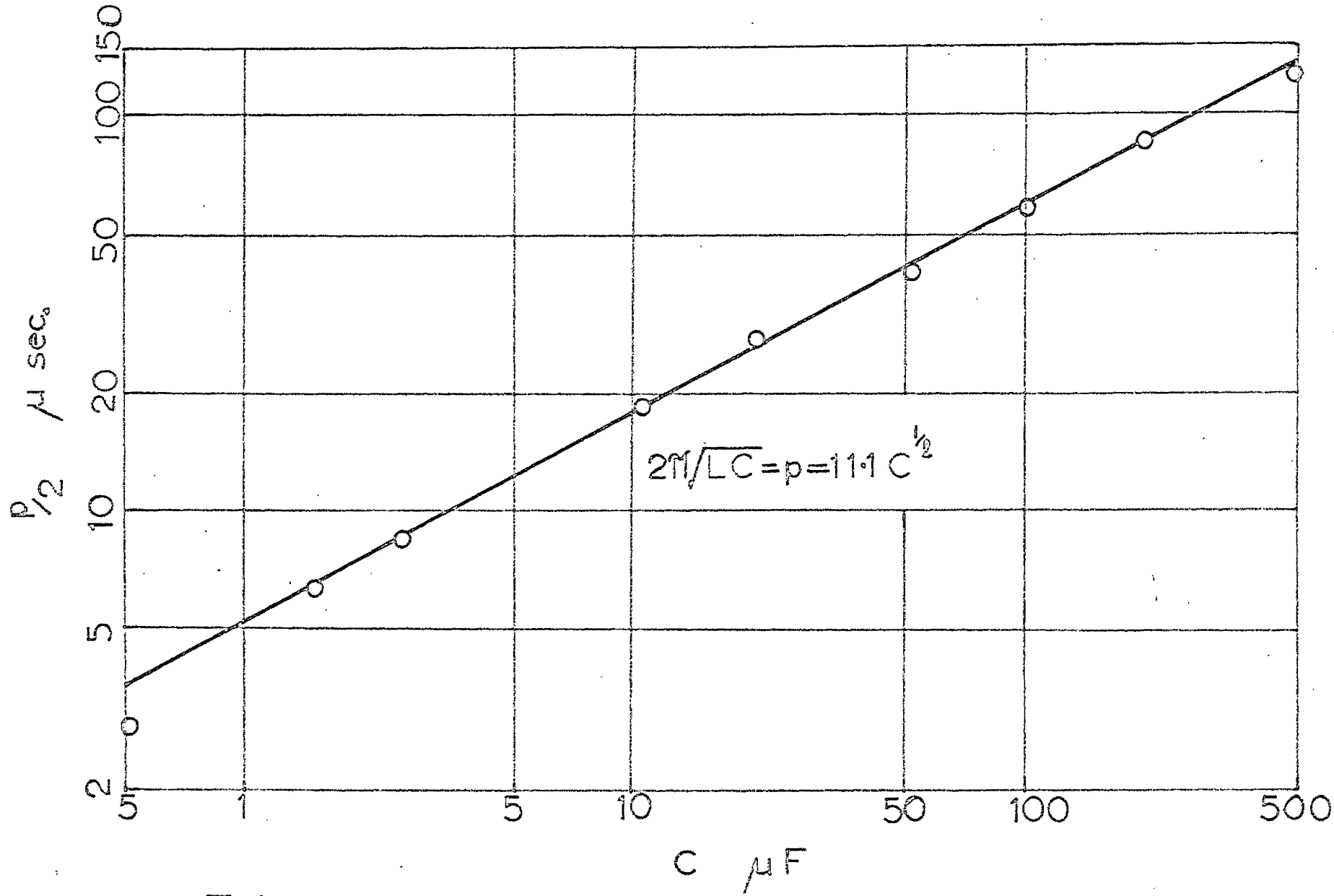

PULSE LENGTH p — CAPACITY C RELATIONSHIP

CALCULATED INDUCTANCE L = 3·1 μH

Fig. 35

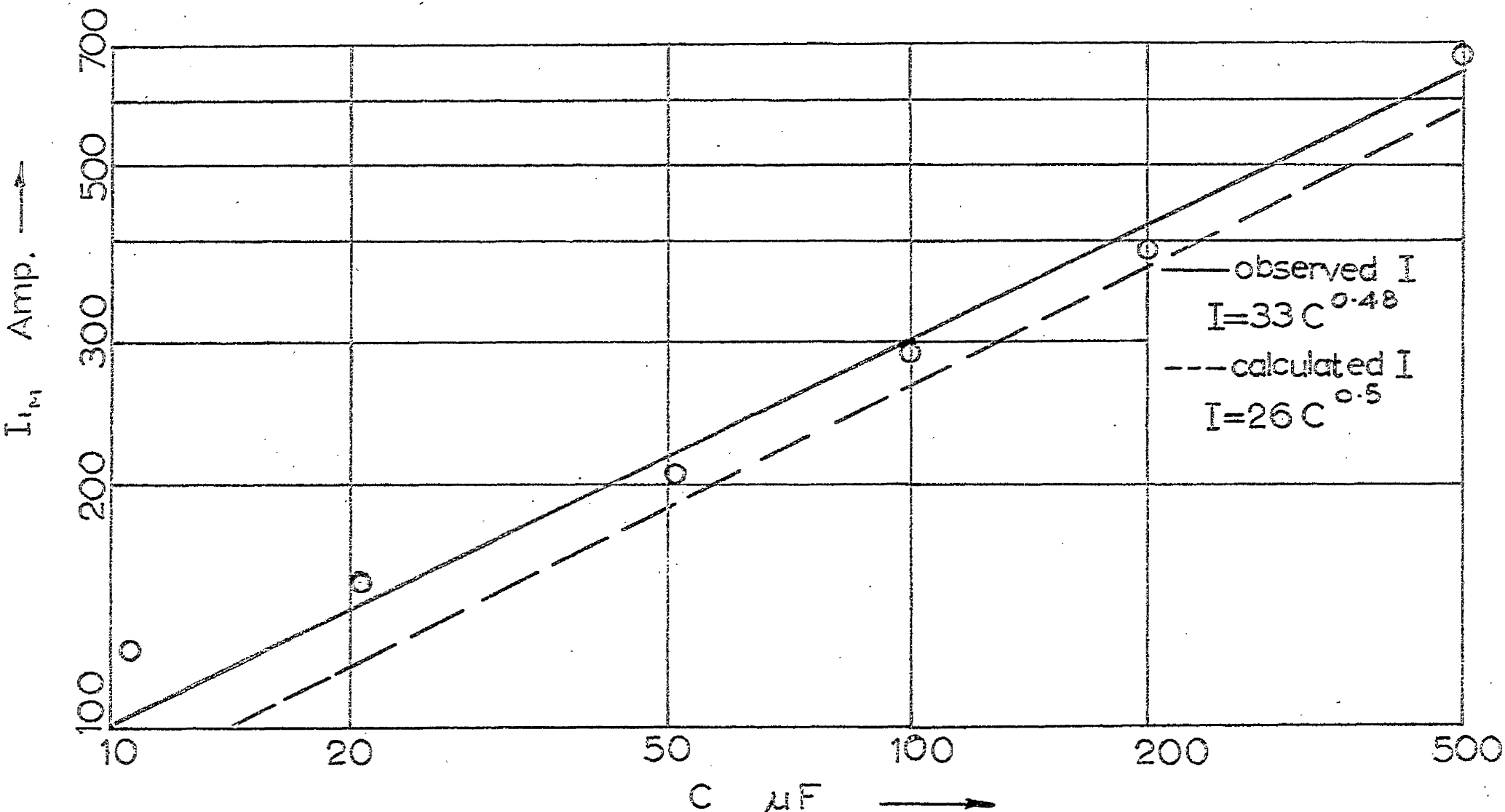

THE CURRENT AMPLITUDE I_{1M} OF THE FIRST HALF-WAVE

Fig. 36

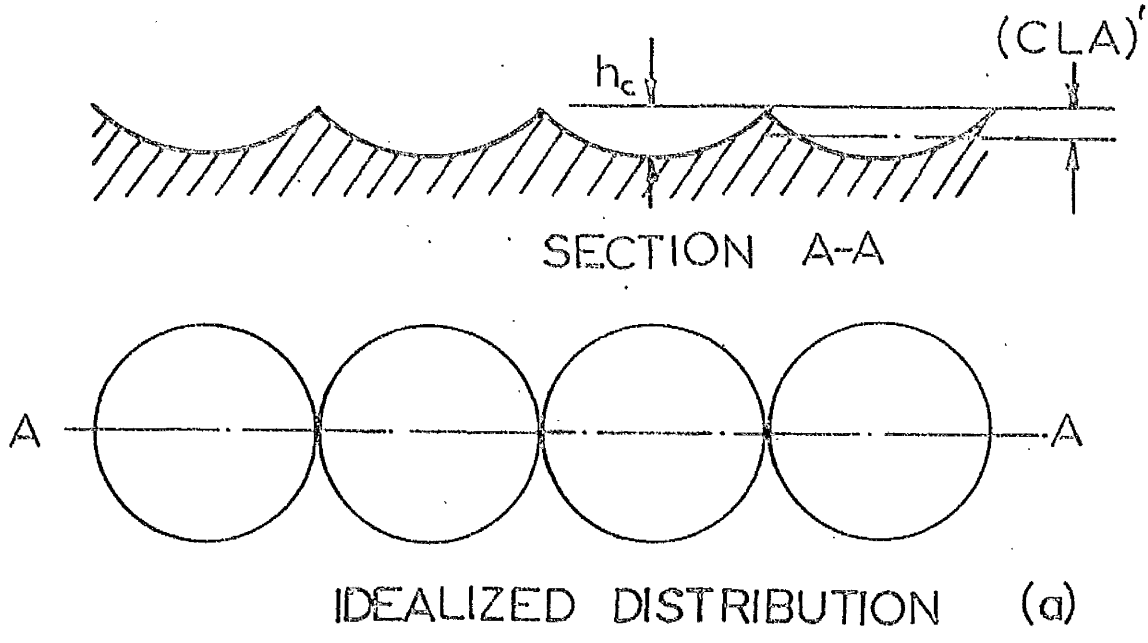

IDEALIZED DISTRIBUTION (a)

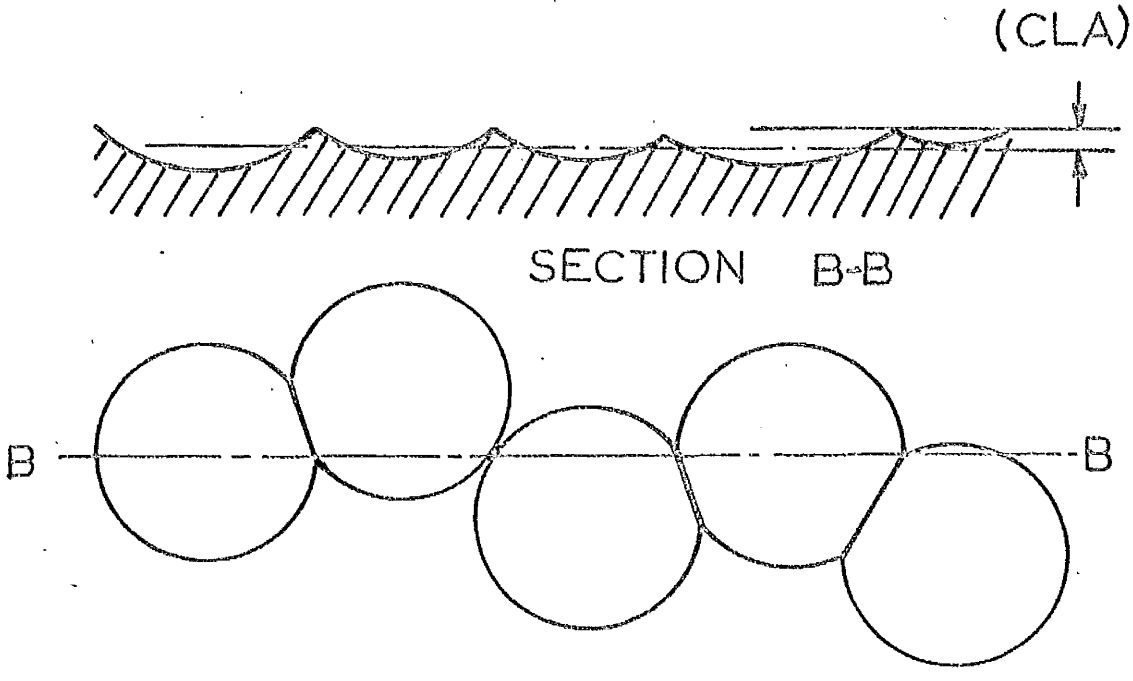

RANDOM DISTRIBUTION (b)

CRATERS AND SURFACE FINISH

Fig. 37

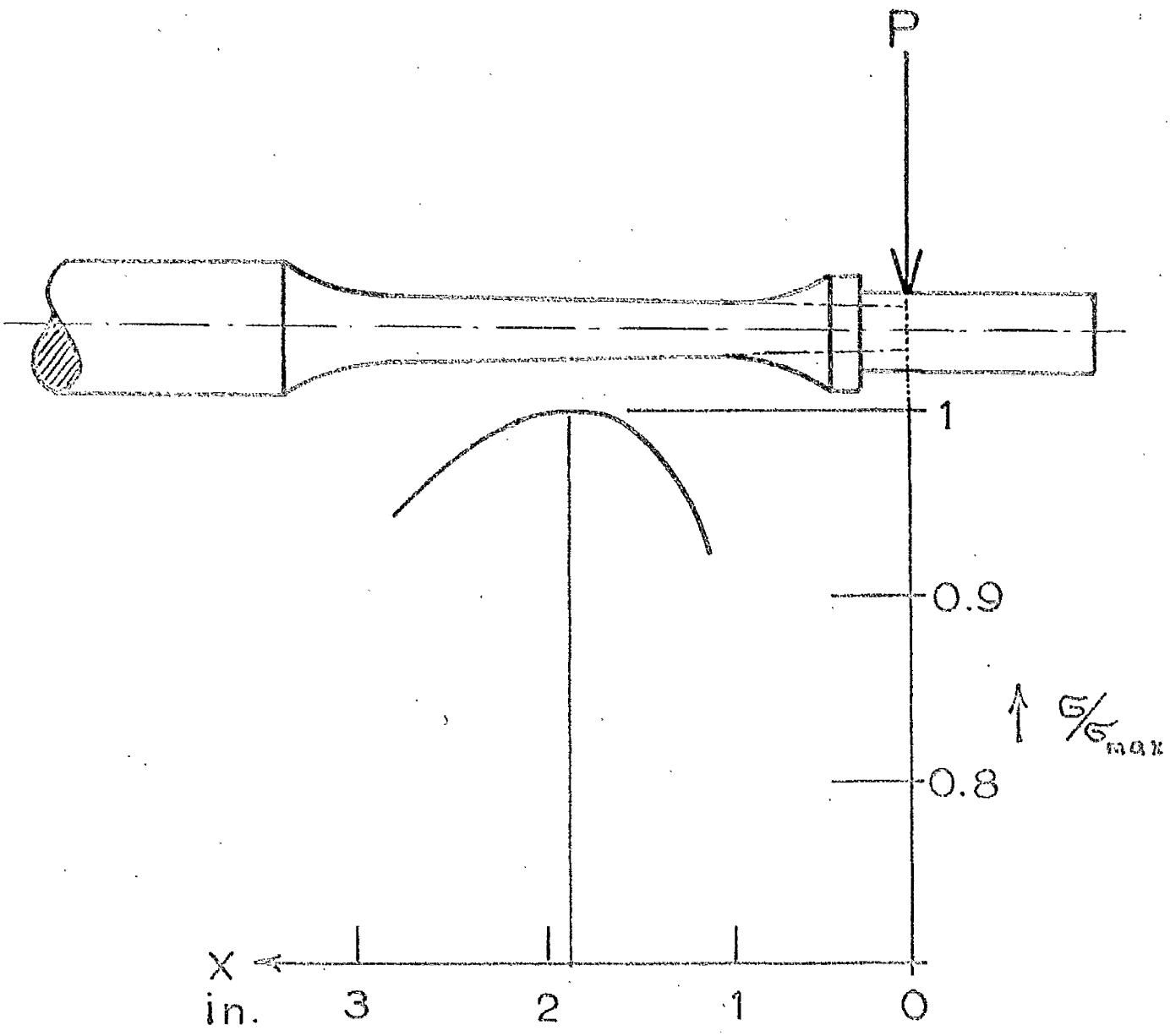

STRESSES IN THE FATIGUE SPECIMEN

Fig. 38

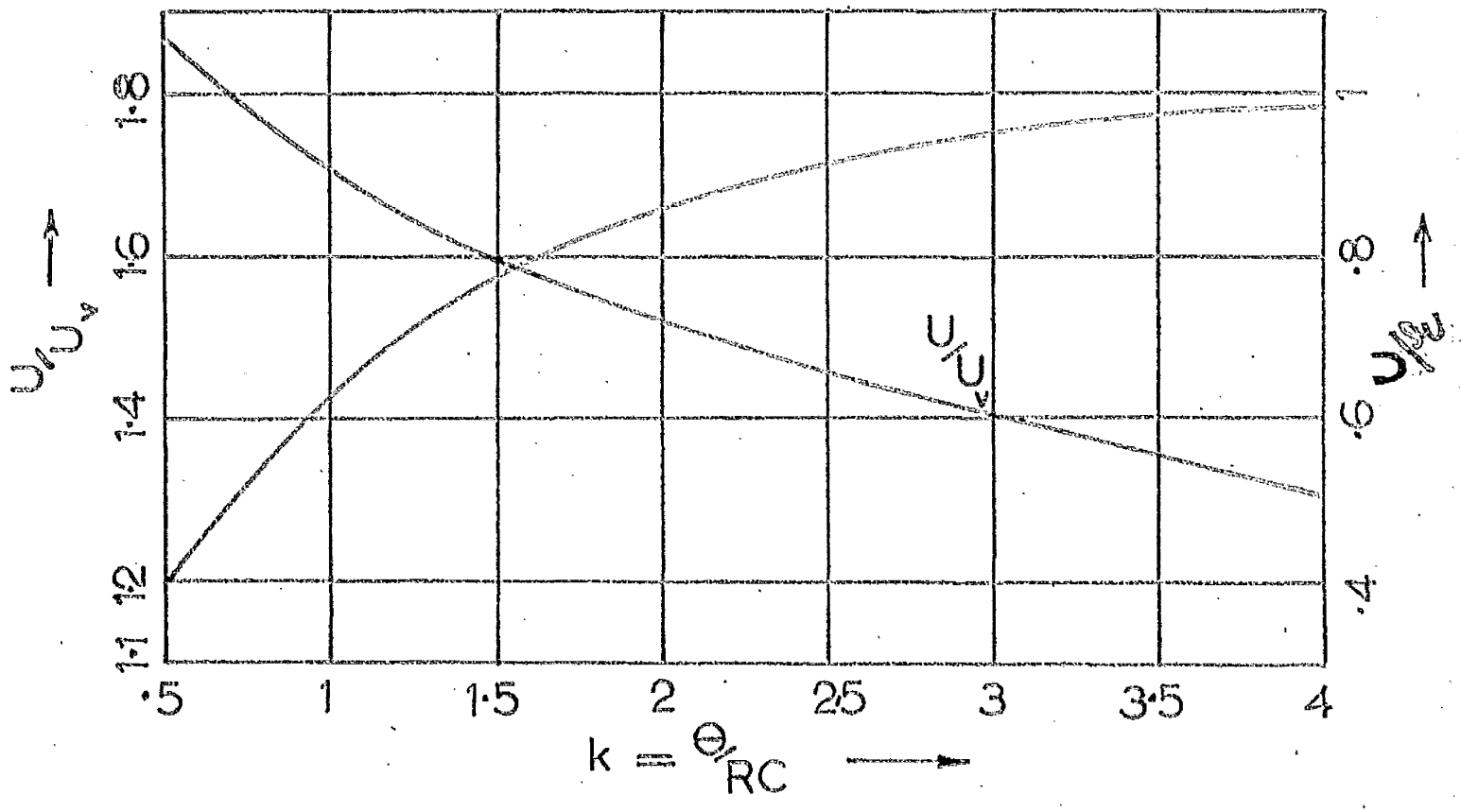

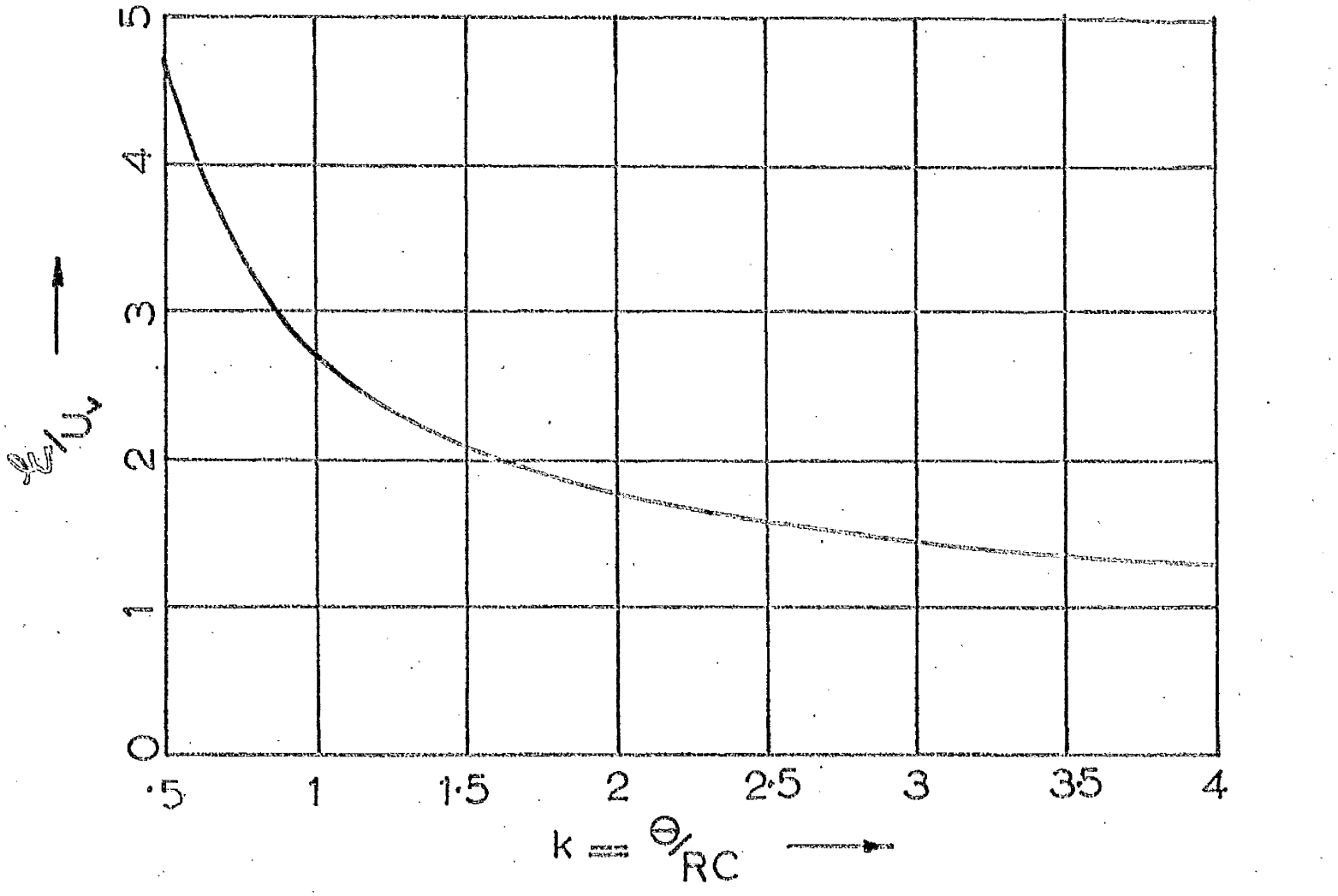

AUXILIARY CURVES FOR VOLTAGE CALCULATIONS

Fig. 39